ANL-19/13

Environmental creep-fatigue and weld creep cracking: a summary of design and fitness-for-service practices

Applied Materials Division

ANL-19/13

Environmental creep-fatigue and weld creep cracking: a summary of design and fitness-for-service practices

Prepared by
M. C. Messner
B. Barua
A. Rovinelli
T.-L. Sham
Applied Materials Division, Argonne National Laboratory

Prepared for the U.S. Nuclear Regulatory Commission
under interagency agreement 31310018F0053
with the U.S. Department of Energy

January 2020

ABSTRACT

This report surveys current creep-fatigue design and fitness-for-service assessment procedures, with a particular focus on environmental effects and creep-fatigue cracking near weldments. Included in this assessment are the American Society of Mechanical Engineers Boiler and Pressure Vessel Code Section III, Division 5, the British R5 standard, the French RCC-MRx design code, the ITER Structural Design Criteria, and the API-579/ASME FFS-1 fitness-for-service rules for petrochemical components. The focus of this review is to identify gaps in the available methods that could prevent the regulator from evaluating future advanced non-light water reactor designs. The report makes recommendations, where appropriate, on actions that could be taken to fill these gaps by either providing adequate assessment procedures for creep-fatigue damage in harsh environments or by identifying strategies vendors could use to mitigate regulatory concerns with creep-fatigue damage in advanced non-light water reactor components.

TABLE OF CONTENTS

LIST OF FIGURES

LIST OF TABLES

1 Introduction

This report surveys current design and fitness-for-service evaluation practices for structures subject to creep-fatigue damage. The purpose of this survey is to identify potential challenges to a regulatory assessment of an advanced reactor design, with a particular focus on the interaction of creep-fatigue damage with the reactor environment and on creep-fatigue cracking near weldments. The report identifies gaps in current practices and makes recommendations on future development work required to address these deficiencies.

The development of creep-fatigue design and fitness-for-service assessment was driven by work on high temperature nuclear reactors in the 1970s. This effort incorporated earlier work on aerospace applications dating back to the 1950s and focusing on high temperature design in jet turbines and for aerodynamic heating. The initial development of design rules was done by American Society of Mechanical Engineers. These rules are now contained in Section III, Division 5 of the ASME Boiler and Pressure Vessel Code. Section 2 traces their history in greater detail. This work eventually focused on the development of a design standard for the Clinch River Breeder Reactor. However, as that plant was never built service experience with the ASME rules is limited to scaled testing done as part of the Clinch River project.

Both the British and the French built and operate commercial high temperature reactors: the gas and advanced gas reactors in the UK and Phenix and Superphenix in France. As such, both countries developed standards for the design and fitness-for-service assessment of advanced non-light water reactor (ANLWR) components in support of their respective reactor designs. Both countries started from the ASME rules, but over time significant differences have developed between these standards and the current rules in ASME Section III, Division 5. This report evaluates the French RCC-MRx and R5 British standards. Technically, the R5 standard is a fitness-for-service methodology, but it can be applied to plant design by starting from an as-built condition, without prior history. As both countries had/have operating plants, these standards are somewhat more comprehensive than the ASME rules, generally covering both design and fitness-for-service and, in the case of RCC-MRx, irradiation damage.

The ITER Structural Design Criteria (ISDC) for fusion reactors are also surveyed here. In their current form these rules closely mirror the French RCC-MRx standard. Uniquely, given the challenges inherent in designing fusion containment structures, these rules only cover creep-fatigue damage in high radiation flux environments. They do not provide rules for structures experiencing low radiation doses.

Finally, the report surveys the American Petroleum Institute API-579/ASME FFS-1 standard for fitness-for-service evaluation as an example of current non-nuclear industry practice. The design of components in non-nuclear power plants and in petrochemical facilities conventionally does not include creep-fatigue criteria, even at temperatures and operating transients where creep-fatigue might be expected to be an issue. However, recent changes in the power generation industry causing existing plants to experience more intermittent service and the development of combined cycle gas plants using heat recovery steam generators has pushed the non-nuclear industries towards incorporating creep-fatigue in their design. For example, ASME is currently sponsoring an effort to include creep-fatigue rules in Section I and Section VIII of the Boiler and Pressure Vessel Code. However, it is unlikely the non-nuclear power and petrochemical industries will

develop entirely new practices. Most likely, they will adopt the current nuclear methods with appropriate modifications.

Creep-fatigue damage has a somewhat longer non-nuclear history for fitness-for-service evaluation. The first version of API 579 was published in 2000 and contains rules for evaluating the initiation of creep-fatigue flaws and the propagation of flaws found by inspection.

The report also attempts to survey the literature on creep-fatigue damage initiation and propagation mechanisms for base metal, in adverse environments, and near and in welds. A mechanistic understanding of creep-fatigue may be of particular importance when considering environmental effects, where general rules covering all the potential mechanisms will be difficult to develop. Unfortunately, despite a great deal of effort, the fundamental cause of creep-fatigue interaction is still unclear, particularly when combined with corrosion or irradiation damage mechanisms. This uncertainty, and the large variety of potential interacting mechanisms, is likely one reason why none of the existing procedures provide comprehensive methods for creep-fatigue in corrosive environments and why methods for accounting for irradiation damage on creep-fatigue are typically padded with large design margins to make up for the degree of uncertainty.

Section 2 of the report covers creep-fatigue damage and flaw initiation in base metal. Section 3 discusses creep-fatigue combined with exposure to radiation or corrosive coolants. Section 4 discusses methods for creep-fatigue flaw evaluation in general as well as specific methods for initiation and propagation near weldments. Each of these sections has a common format. The first subsection surveys the underlying mechanisms that may contribute to creep-fatigue for the specific conditions discussed in the section. The next section surveys existing design and fitness-for-service methods. The final subsection discusses potential gaps and makes recommendations for on how to address those gaps. Section 5 briefly summarizes the more important recommendations discussed in detail earlier in the report.

2 Creep-fatigue design and analysis

2.1 Creep-fatigue mechanisms

2.1.1 General overview

Creep-fatigue is the initiation and subsequent growth of flaws under cyclic load interspersed with hold periods at constant, or slowly varying, load. For the purposes of engineering design and assessment creep-fatigue interaction expresses the experimental observation that a strain-controlled fatigue test with holds will fail in fewer cycles than an equivalent pure fatigue test with the same strain range and at the same temperature but without any hold periods. Similarly, adding up the hold periods in the test to a total time at an equivalent stress produces a lower failure time than when compared to a pure creep test at constant load. Creep-fatigue interaction then describes the detrimental interaction of creep and fatigue failure modes.

Given this definition it is also worth defining pure fatigue and pure creep damage and deformation. Fatigue damage is the initiation and growth of flaws under cyclic load. At least for the purposes of this report, fatigue damage is a time-independent failure mechanism associated with either rapid cycling, without holds, or lower temperature cyclic service where creep is insignificant. It is far beyond the scope of this report to summarize the voluminous literature on fatigue damage initiation and fatigue crack growth. For a general overview of mechanisms see [1] and for a recent review of initiation models see [2]. For the materials of interest to this report, ferritic and ferritic-martensitic steels, austenitic iron-based and nickel-based alloys, fatigue has mostly, but not exclusively, been reported as initiating as a transgranular crack associated with a persistent slip band impinging on a grain boundary.

Similarly, a general overview of creep damage mechanisms is beyond the scope of this report. Reference [3] provides a general overview. For the materials of interest for this report, creep damage is generally assumed to be an intergranular mechanism occurring at grain boundaries and associated with the nucleation, cavitation, and coalescence of cavities [4]. This makes creep damage a distributed mechanism, occurring simultaneously at many locations in the material, whereas fatigue damage nucleates only at a few critical locations.

Given that, by definition, creep-fatigue loading involves creep, which is only a significant deformation and failure mode at high temperatures, creep-fatigue is a high temperature failure mode. Creep-fatigue damage has been recognized as a significant, potentially controlling failure mode for high temperature structures at least since the middle of the 1960's. This work was primarily led by the nuclear industry, in anticipation of planned high temperature commercial reactors, but was also influenced by the aerospace industry's concerns about aerodynamic heating for, at the time, current supersonic aircraft and anticipation of future hypersonic craft (c.f. [5]).

It is difficult to ascertain directly from the open literature how significant of a failure mode it has been in practice for operating high temperature facilities, primarily concentrated in the petrochemical and fossil power generation industries. The conventional design practice for such structures, discussed below, does not account for creep-fatigue. However, there is some indication that creep-fatigue is becoming a concern in these industries. Fossil power generation facilities are operating at increasingly higher temperatures [6] and increasingly must respond to fluctuating load on the electrical grid. Both factors have led to failures attributed to creep-fatigue interaction [7]–[9], for example as ligament cracks between tube bore holes in Cr-Mo steel header pipes. For

natural gas generation, numerous failures have been ascribed to creep-fatigue in modern combined cycle plants, particularly in the heat recovery steam generator [10], [11].

2.1.2 Creep-fatigue mechanisms

The brief description of creep and fatigue damage mechanisms provided above summarizes fatigue damage as transgranular and localized to critical slip bands and describes creep damage as intergranular and distributed widely over many grain boundaries (see Figure 1). The question is then how do these two mechanisms interact to lead to the experimentally-observed decrease in life compared to pure fatigue or pure creep deformation and damage?

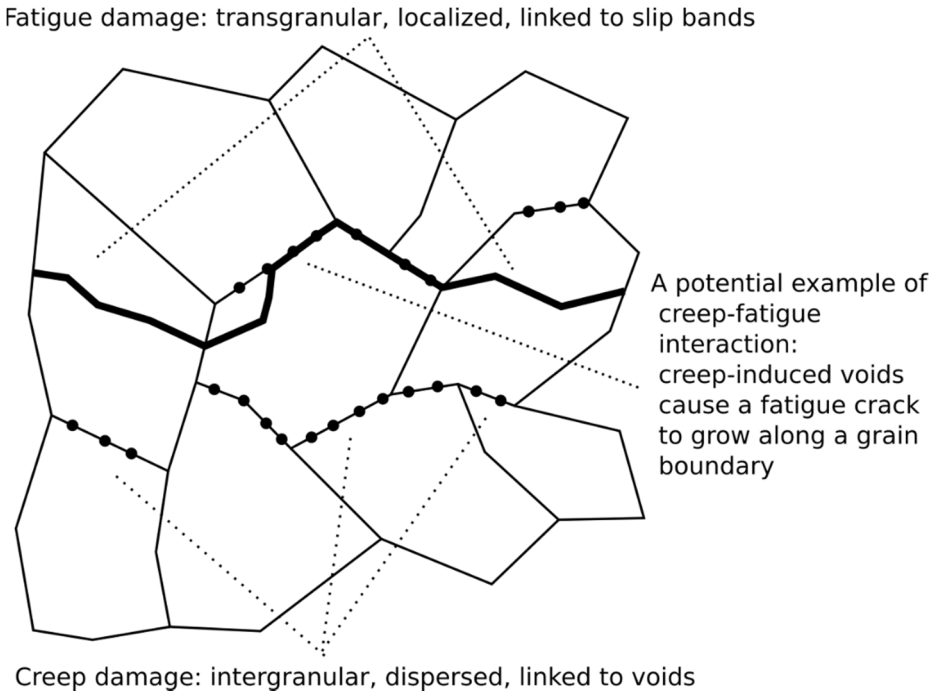

Figure 1 Schematic diagram of creep, fatigue, and creep-fatigue cracking.

There is no definitive answer to that question. The following is a brief overview of some of the theories that have been presented in the technical literature over the past 50 years.

Generally, the experiments described in the literature support the general model described above – increasing creep deformation tends to promote intergranular cracking over transgranular cracking [12]–[16]. Increased creep deformation here means either a higher temperature or a longer hold time. Similarly, increased creep deformation tends to increase the likelihood that the flaw would nucleate on the interior of the specimen and that the time to flaw initiation would be independent of the surface finish, which again supports a model associating creep with intergranular damage. A few studies did report a transition back to transgranular cracking at very high temperatures [17], [18]. These studies provided a complicated explanation linked to competition between wedge cracking and sliding on grain boundaries. Given the limited number of experiments reporting this behavior and the fact that only one study reported the effect for an

alloy of interest (304 stainless steel), the body of evidence seems to support the general association of fatigue and transgranular cracking and creep and intergranular cracking.

Surprisingly few papers provide a mechanism for the cause of creep-fatigue interaction. Those that do provide a micromechanical explanation can be divided into three categories:

1. Creep damage on grain boundaries promotes earlier nucleation of a flaw on the order of the grain size [19]. This flaw then grows under the subsequent fatigue cycling. This theory has been applied to both ferritic and stainless steels.
2. Cracks initiate either through fatigue mechanisms (persistent slip bands) or creep mechanisms (void coalescence or wedge cracking) and material softening effects promote the subsequent growth of flaws, causing detrimental creep-fatigue interaction. There are two subcategories here. The first subcategory hypothesizes that the softening mechanism is creep cavitation. This theory can be applied to cyclic-hardening materials like 316 and 304 stainless steel [20]. The second subcategory attributes the softening mechanism to plastic deformation in low cycle fatigue causing softening through microstructural recovery mechanisms affecting the grain and dislocation structure [21]. This mechanism can only be applied to cyclic softening materials, such as 9-12% Cr ferritic-martensitic steels.
3. Creep deformation "holds open" grain boundaries, promoting diffusion of oxygen along the boundary network, causing internal oxidation, detrimental microstructural changes, and hence creep-fatigue interaction as these microstructural changes promote increased fatigue crack growth. This theory is primarily applied to nickel-based alloys at very high temperatures [12], [16].

We should note a further category of authors that refuse to attribute creep-fatigue interaction to a single mechanism, instead describing several different mechanisms depending on the material, temperature, and type of loading [22], [23]. A final category of papers, primarily focusing on aerospace applications, does not report any creep-fatigue interaction (c.f. [24]). These papers typically examine very short dwell times and therefore creep may simply not have been significant in these tests.

Overall then, the experimental literature shows that there is likely not a single mechanism for creep-fatigue interaction that can be applied to all materials, or even to the relatively limited types of materials likely to be used in high temperature nuclear reactors. To some extent, this fact may explain the prevalence of empirical engineering methods over mechanistic models. The connection to oxidation in nickel-based alloys may be particularly important as current design practices do not account for the effects of environment beyond factors on design fatigue curves aimed at enveloping possible environmental effects.

2.1.3 An overview of creep-fatigue design and assessment

The subsequent sections of this report examine, in detail, current design practice for basic creep-fatigue damage evaluation, creep-fatigue damage evaluation in the presence of detrimental environmental effects, and the evaluation of damage and flaw growth under creep-fatigue loading near welds. This subsection gives a general overview of creep-fatigue design and flaw evaluation

and provides an overview of alternate methods for creep-fatigue evaluation that have not been adopted by the major design and fitness-for-service codes and standards.

We can divide engineering methods for creep-fatigue into two categories: design and construction codes and fitness for service codes. Design and construction codes specify how to design a new structure to withstand creep-fatigue damage over some specified design life, given the expected loading, and further specify construction processes aimed at minimizing the initiation and growth of flaws. This is supplemented by in service inspection methodologies, for example as specified in ASME Section XI that provide, in concert with design and construction rules, added assurance on the structural integrity. Fitness for service methods instead aim to ascertain the remaining life of a component given the current material condition, a characterization of any detected flaws, and some estimate of past and future loading.

We can also group methods into two additional categories: methods for preventing creep-fatigue flaw initiation and methods for predicting creep-fatigue crack growth, given some initial flaw geometry. This report focuses on crack growth near welds, though most methods generally apply to both welds and base material.

In general, fitness-for-service procedures cover both flaw initiation and flaw growth, while design procedures focus on preventing flaw initiation. Fitness-for-service procedures for flaw initiation can be used for design by applying the procedure to virgin material and using the design loads. Fitness-for-service procedures for flaw growth could be used for design by requiring designers to consider a library of prospective design flaws. This methodology is commonly used for the design of low temperature, light water reactors but does not seem to be commonly used for high temperature design. Table 1 lists and categorizes the codes and standards considered in this report according to these criteria.

Code	Type	Initiation?	Flaw evaluation?
ASME Boiler and Pressure Vessel Code Section III, Division 5	Design	Yes	No
ASME Boiler and Pressure Vessel Code Section XI	Fitness	No	Yes (under development)
ASME FFS-1/API-579	Fitness	Yes	Yes
R5	Fitness	Yes	Yes
RCC-MRx	Design	Yes	Yes
ITER criteria	Design	Yes	Yes

Table 1 Summary of design and fitness-for-service rules considered in this report.

There are a several additional high temperature codes and standards that are not covered in this report. ASME B31.1 covers high temperature piping. This report does not consider it because the methodology overlaps with the Boiler and Pressure Vessel Code and is less well developed than the detailed Section III, Division 5 rules. The Japanese Society of Mechanical Engineers, the Japan Atomic Energy Agency and other Japanese professional and governmental agencies maintain codes and standards used to design and maintain the Monju Fast Breeder Reactor and future high temperature reactors in Japan. However, these standards are not widely available outside of Japan. Various European standards cover portions of high temperature design and evaluation, for example

EN 13480 for piping, but there is no comprehensive high temperature design methodology suitable for high temperature nuclear reactors.

Finally, the ASME Boiler and Pressure Vessel Code covers high temperature non-nuclear structures in Section I (Power Boilers) and Section VIII (which covers high temperature petrochemical equipment). Neither of these sections provides rules for creep-fatigue design and so they are not considered in detail in this report. Both use an allowable stress method similar to the "design load check" in Section III, Division 5 but with different tables of allowable stresses. Section VIII Division 2 has a code case (Case 2843) that directly incorporates the elastic analysis methods of the Section III Division 5 subpart HBB[1] rules.

All the creep-fatigue damage initiation methods described in detail in this report fundamentally use a similar method, which could be called linear or bilinear damage interaction. All the methods compute a fatigue damage use fraction, D_f, and a creep damage use fraction, D_c, and then plot the two quantities on a design chart of the type shown schematically in Figure 2. If the point (D_f, D_c) falls inside the diagram the section passes the check; if it falls outside the diagram it fails. These design plots are called damage diagrams, D-diagrams, or creep-fatigue interaction diagrams. Different codes use different diagrams and, in some codes, different materials use different envelopes. If the diagram is of the straight-line type shown in Figure 2 then the creep-fatigue interaction can be called linear as it is expressed by the equation $D_f + D_c < 1$. If the diagram is "kinked," also called out on the figure, then the interaction is called bilinear.

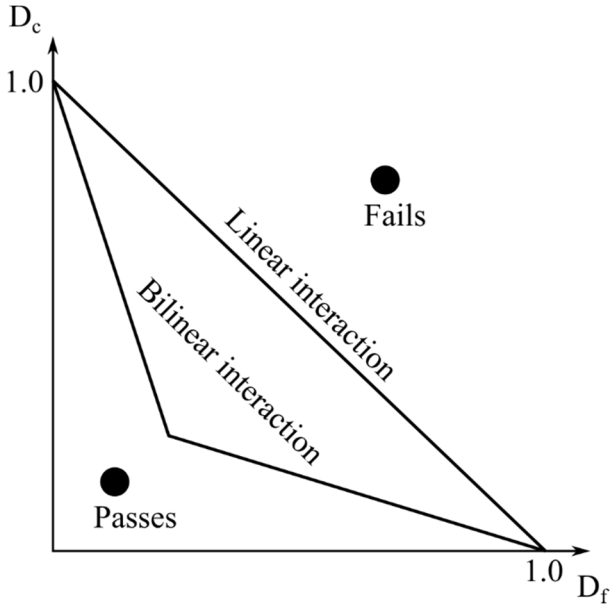

Figure 2 Schematic creep-fatigue interaction diagram illustrating the difference between a linear and bilinear interaction.

[1] We use the notation subpart HBB to reference Section III, Division 5, Subsection HB, Subpart B and so on for other Subparts of the Code throughout the report.

All the standards considered in this report computed fatigue damage using Miner's rule and strain-range based fatigue curves. However, each Code uses a different method of computing creep damage. There are many different rules for calculating creep damage and different studies often assert advantages of certain methods over others (c.f. [18], [25]), but there is no consensus on which method is superior overall.

The design and fitness-for-service methods consider here in detail use variants of three methods: time fraction, ductility exhaustion ([26], [27] among many others), and the Omega approach [28].

In the time fraction approach creep damage is computed as

$$D_c = \int_0^t \frac{dt}{t_r(\sigma)}$$

where $t_r(\sigma)$ is the time-to-rupture corresponding to the stress level at each instant during the stress relaxation profile. The advantage of this approach is that it uses the same database (time to rupture from creep rupture tests) that is used to establish the allowable stresses.

Ductility exhaustion calculates creep damage as

$$D_c = \int_0^t \frac{\dot{\varepsilon}_c(\sigma)}{\varepsilon_R(\sigma)} dt$$

where $\dot{\varepsilon}_c$ is the creep rate and ε_R is the rupture ductility, both of which could depend on stress. Some studies find the ductility exhaustion method to be more accurate than the time fraction approach. However, it does require a database reporting creep rupture ductility as a function of time, stress, and temperature which is not as commonly available as simple rupture time results.

A third method for calculating damage is the MPC Omega approach described in [28]. Here creep damage is given as

$$D_c = \int_0^t \dot{\varepsilon}_{co}(\sigma)\Omega_m(\sigma)dt$$

where $\dot{\varepsilon}_{co}$ describes the initial creep rate and Ω_m describes the rate of damage accumulation. The Omega method was developed so that the Ω parameter, which describes the creep damage accumulated in the material, can be determined from short-term creep tests measuring the creep rate of a sample of material with some prior loading history. Additionally, an extensive database of material parameters exists though MPC Project Omega and is reproduced in API-579/ASME FFS-1. However, the model neglects primary creep in order to develop a one-to-one map between creep strain rate and damage.

The Omega method is one example of a general family of continuum damage mechanics models for creep rupture which originate with the work of Kachanov [29], Rabotnov [30], Hayhurst, and Leckie [31]. These continuum damage approach have not been widely adopted by design codes, perhaps because they are not easily amenable to simple analysis methods but rather require full transient finite element simulations.

In addition to the linear or bilinear damage summation methods adopted by design and fitness-for-service codes, there are several other approaches to representing creep-fatigue interaction that should be mentioned. References [3], [32] provide good general overviews.

Manson and coworkers developed a strain-based approach that divides a generic stress-strain hysteresis loop into components representing all combinations of forward and reversed creep and forward and reversed plasticity, associating a damage with each of the four possible mechanisms [33]. The disadvantage is that detailed, categorized experimental hysteresis loops and associated failure data is required to calibrate the methodology.

Coffin developed an approach based essentially on modifying fatigue curves to account for strain-rate effects. In the average sense of dividing the strain range experienced over a cycle by the total cycle time (including holds) this approach can be applied to creep-fatigue deformation [34]. This approach seems most suitable for slowly varying cycles, rather than conventional ramp-and-hold plant operations. It has been adopted by the concentrating solar power community.

Chaboche and coworkers adopted the Hayhurst-Leckie-Kachanov-Rabotnov creep continuum damage to account for creep-fatigue [35]–[37]. As with the classical continuum creep damage models, their approach is most applicable to fully resolved simulations and hence has not been widely adopted for engineering design or fitness-for-service approaches.

There are numerous other theories. For example Ostergren proposed a method based on the dissipated energy of the hysteresis cycle [38] that seems to work well, at least for some materials. The linear or bilinear damage summation approach seems to have become the dominate method at least in part because of its relative simplicity, allowing for easy evaluation in engineering calculations. We should emphasize that with this approach the creep-fatigue interaction diagram is not a material property, but rather a design aid. A clear demonstration of this fact is found in that the main design codes all posit different creep-fatigue interaction diagrams for the same material. This is because the shape of the diagram is influenced by the methodology used to compute creep (and fatigue) damage.

There is one dominate method for flaw evaluation under creep and creep-fatigue deformation: the C^* (steady state creep) and C_t (time dependent creep) approach for correlating loading to creep crack growth and extended to creep-fatigue growth by linearly adding additional fatigue crack growth based on linear or nonlinear fracture mechanics. This approach is adopted by both R5 and FFS-1 and so is detailed further below. Reference [39] provides an excellent overview and history of the approach.

2.2 Survey of current design practice

2.2.1 ASME Boiler & Pressure Vessel Code

The design and construction rules for nuclear components that will experience elevated temperature loading are in Section III, Division 5 of the American Society of Mechanical Engineers Boiler and Pressure Vessels Code [40]. These Code rules began development as Code Case 1592. This Code Case became Code Case N-47, which later became Section III, Division 1, Subsection NH. Finally, the Code rules were split into their own Section III, Division 5 in the 2011 Addenda.

This report focuses on the current Code rules as of the 2017 edition and does not attempt to extensively trace the history of the Division 5 creep and creep-fatigue design provisions. However, there was a major change in the ASME creep-fatigue design method which occurred around 1990 [41]. The previous rules used modified fatigue curves accounting for creep effects, the current rules use the creep-fatigue interaction diagram described in this report.

The Code provides design rules for two safety classes: Class A, which corresponds to Section III, Division 1, Class 1 and Class CS and Class B, which corresponds to Section III, Division 1, Class 2 and Class 3. The classification of a component is determined through interaction between the owner/operator, reactor vendor/designer, and the regulator through system analysis. As a general rule Class A components will be those in the primary coolant pressure boundary.

Section III, Division 5 covers both metallic and non-metallic (i.e. graphite and SiC/SiC composites) components. This report only considers the rules for metallic components.

Additionally, the Code separates out rules for pressure boundary components, support structures for Class A and B components, and internal structures (also called core supports). Table 2 describes the location of the rules within Division 5. The table also shows where Division 5 rules reference Division 1 rules rather than defining an entirely new design process. In subparts HBA, HCB, HFA, and HGA Division 5 references Division 1 rules with only very small modifications. Subsection HCB references Division 1, Subsection NC with more substantial modifications covering creep buckling and creep effects in piping.

	Low temperatures	High temperatures
Class A	HBA, references Div. 1, NB	HBB
Class B	HCB, references Div. 1, NC	HCB
Class A supports	HFA, references Div. 1, NF	Not applicable
Class B supports	HFA, references Div. 1, NF	Not applicable
Class A core internal	HGA, references Div. 1, NC	HGB
Class B core internal	Not applicable	Not applicable

Table 2. Map of Section III, Division 5 rules. Unnumbered subparts refer to Division 5.

A key distinction in Division 5 is clearly then the division between low temperature and high temperature service. This temperature threshold is provided in HAA-1130-1. The table of temperature cutoffs of permitted materials for low temperature service is reproduced here as Table 3.

Material	Temperature °F (°C)
Carbon steel	700 (370)
Low alloy steel	700 (370)
Martensitic stainless steel	700 (370)
Austenitic stainless steel	800 (425)
Nickel-chromium-iron	800 (425)
Nickel-copper	800 (425)

Table 3. Division 5 temperature thresholds for low and high temperature service.

Division 5 contains two design criteria relevant to creep and creep-rupture. The Code checks the primary stresses against a time-dependent allowable stress. This check covers, among other failure modes, creep rupture under sustained load. Additionally, the Code requires checking Class A components for creep-fatigue failure.

Subpart HCB extends the Division 1, Subsection NC allowable stresses to account for non-negligible creep. Neither Division 5, Subpart HCB nor Division 1, Subsection NC explicitly addresses cyclic service and, therefore, creep-fatigue failure. However, Division 5 does allow a designer to design a component to a higher safety category. This means that the designer could design a Class B component in elevated temperature service to the Class A rules found in Subpart HBB. However, the full scope, and not just a selected portion, of the Class A rules needs to be applied for this option.

The core support rules in Division 5, Subpart HGB are substantially identical to HBB.

As such, this report focuses on the parts of Section III, Division 5, Subpart HBB that guard against creep rupture under sustained loading and creep-fatigue damage in cyclic service. These rules essentially make up the majority of the ASME Code design procedure for all high temperature nuclear components.

Executing a Subpart HBB design requires input from the Design Specification, generally provided by the Owner-Operator. Among other things, this specification defines a series of service loadings, classified into Level A, Level B, Level C, and Level D categories, along with a Design Load.

Ultimately, the classification of transients into the four levels of service loadings is part of the Design Specification and therefore generally the responsibility of the Owner-Operator. However, the general guidance provided by the Code is that Level A corresponds to expected plant operating conditions, Level B corresponds to expected fault conditions that can be recovered from without repair, Level C corresponds to fault conditions that could only be recovered from after the inspection and repair of plant systems, and Level D are fault conditions that cannot be recovered from – a strong earthquake is the canonical example of a Level D service loading. Each of the four categories has different design requirements and therefore different design margins and somewhat different design rules. For example, for a Level D loading the only consideration is the health and safety of the public and plant workers and therefore plant systems can be allowed to fail, provided the primary pressure boundary remains intact.

The Design Loading envelopes the operating conditions described by all the Level A loading conditions and therefore describes the expected operating conditions in the manner of a Section VIII design load.

Each loading (Service and Design) must provide sufficient information to run a thermomechanical analysis to determine the component stress/temperature history. Typically then, a loading condition might be described by a set of thermal and mechanical boundary conditions – typically metal temperatures, pressures, and nozzle and support loads. The thermal analysis could either be done "upstream" from the mechanical designer, in which case the Design Specification would specify metal temperatures, or it could be integrated into the mechanical design, in which the specification might provide fluid temperatures and pressures. These fluid conditions could be translated into metal temperatures using transient thermal analysis.

In general, Division 5 deals with time-dependent failure mechanisms and so the hold times corresponding to each loading must be part of the Design Specification. As such, the thermal analysis must be transient and not simply represent steady-state conditions. The Design Specification must, at a minimum, specify the conditions corresponding to each service load and the number of times the component will experience each particular load over its design life. The specification might also give an expected loading sequence. If it does not, the Code allows the designer to uniformly distribute the service loading cycles over the complete design life.

2.2.1.1 Primary load design: creep rupture under sustained load

The ASME Code considers two creep-fatigue related failure modes: creep failure under sustained loading and creep-fatigue damage under cyclic load. The primary load design criteria guard against creep rupture under sustained applied load.

These checks use the stress determined for the component using an elastic analysis. These elastic stresses must then be classified in order to separate out the primary load. The Code defines the primary load as "Primary stress is any normal stress or shear stress developed by an imposed loading that is necessary to satisfy the laws of equilibrium of external and internal forces and moments" (HBB-3213.8). In the high temperature regime, another way to think about primary load is that the primary load is the stationary stress under steady state creep. Additional stress classes used in the code are local primary (HBB-3213.9), secondary (HBB-3213.10), and peak (HBB-3213.11).

Additionally, the Code requires the designer to linearize stresses, dividing them into membrane and bending contributions. The membrane stress is the average stress across the section of a vessel. The bending stress is then the part of the stress the varies from this average membrane stress. Because the analysis is linear these stress contributions can be superimposed.

For shells and the center of heads the concept of a stress across a section is well-defined. For more complicated 3D geometries, like a nozzle, the conventional procedure is to choose a line through the component from surface to surface and classify stresses along this line.

Stress classification and linearization are really not separate concepts in Section III, Division 5. Instead, the Code provides a table (HBB-3217-1) to aid designers in classifying stresses into the categories of:

1. primary membrane
2. primary bending
3. local primary membrane
4. secondary
5. peak.

Note that local primary stresses are always membrane. Local primary stresses are in effect secondary stresses that must be categorized as primary because if they were not limited they would cause excessive load distribution and distortion elsewhere in the component. These include stresses near nozzles or junctions between heads and shells in vessels.

Secondary stresses are self-limiting. The associated loading can be increased arbitrarily without causing the structure to fail. The classical example is a thermal stress. Consider a vessel section under a through-wall linear temperature gradient. As the magnitude of the gradient increases the stress increases but the vessel, in the ideal case, will never collapse because the loading is self-equilibrating.

Peak stresses are stresses caused by stress concentrations and other local stresses that cause only local distortions. The stresses caused by a notch or hole are a classic example, as are stresses caused by local hot-spots and clad stresses caused by differential thermal expansion. The key

aspect of peak stresses is that they are only significant in the context of fatigue and creep-fatigue design or when considering the propagation of a pre-existing crack.

One helpful way to think about stress classification is to realize that when the Code was developed the only feasible vessel analysis method was through axisymmetric frame theory. The primary load could then be calculated by splitting the vessel at arbitrary points and solving for the stresses for the resulting statically-determinate problem. Axisymmetric frame theory naturally categorizes stresses into membrane and bending stresses through its kinematic assumptions. Additional forces and moments could then be applied at the cuts to bring the discontinuous sections back into equilibrium. The stresses resulting from these continuity forces are the secondary stresses. Finally, this method of analysis cannot account for notches, holes, nozzles, and other local features. As such the perturbation in the stress field from the axisymmetric problem caused by these features had to be calculated separately, for example by using stress concentration factors. These extra stresses are the peak stresses. Local primary membrane stresses are secondary membrane stresses which operating experience, experiments, and analytical models [42] show should be considered as primary in order to maintain a conservative vessel design. Confusion and ambiguity in the stress classification and linearization process results from applying the concept to 3D stress distributions generated through modern finite element analysis. Note that stress classification is not a unique process. Two designers could develop two different, reasonable distributions of primary and secondary stress starting from the same geometry and loading [43].

The designer does stress classification and linearization on each component of the stress tensor individually. Then the Code calculates a stress intensity factor for each type of stress – primary membrane, primary bending, local primary membrane, bending, and peak. The stress intensity factor is twice the maximum shear stress induced by the particular classified stress, in other words the difference between the maximum and minimum principal stresses. This entire process occurs at a single stress classification line or section of a vessel. All the design checks described below must occur for each point along that line in order to find the worst case. For the classical axisymmetric frame analysis, it is immediately clear where this worst point occurs because the stresses are nicely divided into natural membrane and bending contributions. The checks must then be repeated for all sections of the vessel or for a number of stress classification lines at different points in order to ensure the design criteria hold over the entire component.

HBB primary load design considers both a design conditions check and a service conditions check. Checking a structure against the primary design load criteria is essentially analogous to non-nuclear, Section VIII, Division 1 practice. A linear elastic stress analysis of the component, under the Design Loading conditions, provides the (maximum) primary membrane stress intensity. This stress intensity is compared to a time independent allowable stress, S_o, which is based on the material's yield and ultimate strength along with (extrapolated) 100,000 hour creep-rupture strength.

The primary load check for the service conditions considers each loading individually and then also considers the summation of primary-load creep damage for all the service conditions. Essentially, each individual load case must be assessed against a time-dependent allowable stress S_{mt} which in turn is the lesser of a time independent allowable stress, S_m, and a time-dependent allowable stress S_t. S_m is based on the material's yield and ultimate strengths, accounting for property degradation due to thermal aging with reduction factors. S_t includes the time-dependent rupture strength (criteria for both minimum and average material properties) but also additional criteria based on the time to 1% creep strain and the time to the onset of tertiary creep. The service loading checks include factors designed to account for plastic and creep stress redistribution for bending, and so the actual checks consider membrane and bending primary stresses somewhat differently and check S_m and S_t separately.

The assessment procedure for Level A and B loading follows this general approach. Level C increases the time-independent allowable stress. Level D further increases the allowable stress (for example, but using the Code rupture stress S_r instead of S_t) but uses reduced yield and ultimate stresses accounting for thermal aging effects.

The damage summation criteria combines the results from each individual primary load check for each service loading. This summation uses a time-fraction approach. Essentially, for each service loading determine the maximum allowable time for that load, according to the Code S_{mt}, divide the actual time associated with the loading by this maximum allowable time, and sum up these usage fractions for all the service loads.

These primary load checks ensure that the structure will not fail by creep-rupture under prolonged loading. The actual criteria are more stringent than this, consider, for example, the additional criteria incorporated into the time-dependent allowable stress S_t, but at a minimum the primary load criteria guard against long-term stress rupture. Separate criteria in Section III, Division 5 prevent the initiation of a creep-fatigue crack due to cyclic loading.

2.2.1.2 Protection against creep-fatigue initiation using Nonmandatory Appendix HBB-T

Subpart HBB requires "The strains and deformation resulting from the specified operating conditions shall be evaluated. This evaluation shall include the effects of ratcheting, the interaction of creep and fatigue, and the possibility of buckling and structural instability." This mandate then requires that the designer guard against creep-fatigue interaction. Ultimately, the Owner must specify, in the Design Specification, which methods are used to evaluate these secondary load, deformation-controlled limits. The Code provides Nonmandatory Appendix HBB-T as an acceptable design method. The original intent of designating the rules in Appendix HBB-T as nonmandatory was that the methodologies underlying these rules were new at the time of their incorporation and frequent updates were anticipated.

HBB-T provides two options for evaluating creep-fatigue damage: design by elastic analysis and design by inelastic analysis. Additionally, Code Case N-862 provides an additional option using design by elastic-perfectly plastic analysis. Fundamentally, all of these methods share the same underlying technology – an evaluation of creep damage using a time-fraction rule, an evaluation of fatigue damage using Miner's rule and an assessment of creep-fatigue interaction using a creep-fatigue interaction diagram. The basic input to these evaluation procedures are, for each service loading, an equivalent strain range, used to evaluate fatigue damage, and a stress relaxation history, used to evaluate creep damage.

Given some cyclic strain versus time history, the Code defines an equivalent strain range to convert this history into an effective scalar strain (HBB-T-1413). This strain range can then be used to look up an allowable number of cycles to failure from the Code fatigue diagrams. These diagrams are based on strain-controlled fatigue test data at different temperatures. The average fatigue curve determined from these tests are adjusted by dividing the best-fit trendline from the cycles to failure data by a factor of 20 and the corresponding strain ranges by a factor of 2 and taking the minimum of the two resulting curves. The origin of these factors is somewhat opaque, but they are designed to account for not only scatter in the observed fatigue life but also environmental effects. For each cycle, a creep damage fraction is calculated by dividing the number of repetitions of a given cycle type (provided in the design specification) by the allowable number of cycles. A total fatigue damage fraction is then calculated by summing up the fatigue damage fraction from each cycle (Miner's rule).

Given an equivalent, scalar stress relaxation history, HBB-T defines creep damage using a time-fraction rule $D_c = \int_0^{t_h} \frac{dt}{t_r}$, where t_r is the time-to-rupture defined by the Code values of the minimum rupture stress, S_r. These rupture stresses are based on a minimum bound Larson-Miller fit to experimental rupture data, conventionally a constant offset approximation to a 95% lower prediction bound to the experimental data. The Larson-Miller fit may be used to extrapolate the rupture data, but not past a factor of 3 to 5 in time (depending on how stable the material's microstructure is at elevated temperatures) and not below the lowest applied stress in the underlying experimental dataset. In addition to using this lower bound, the Code requires the designer first divide the "actual" stress relaxation profile coming from the analysis by a factor (generally 0.9 for design by elastic analysis and design by EPP and 0.67 for design by inelastic analysis). As rupture times are generally log-linear with stress this requirement greatly adds to the design margin, when computing creep damage. The time-fraction damage for each individual service loading are then summed to produce an overall creep damage fraction.

Now the designer has a fatigue damage, D_f, and a creep damage, D_c, associated with the whole service loading history. The creep-fatigue diagram for the material is used as an acceptance criteria. These diagrams provide an envelope in creep-fatigue damage space. If a particular point (D_f, D_c) falls inside the envelope then the structure passes the HBB-T creep-fatigue design criteria.

The creep-fatigue diagram is constructed from the results of strain-controlled creep-fatigue test data. These tests cycle the material at fixed temperature between a fixed strain range. At either the maximum tensile or compressive strain the test holds the material at fixed strain while the stress relaxes. Sometimes tests are performed with holds on both the tensile and compressive ends of the cycle. These holds will reduce the number of cycles to failure, when compared to a standard fatigue test at the same strain range. Creep-fatigue tests produce a number of cycles to failure, a strain range, and a series of stress relaxation profiles. The strain range can be used to determine a number of cycles to failure for pure fatigue *using a nominal fatigue curve*. A fatigue damage fraction can be calculated for the creep-fatigue test by dividing the actual number of cycles to failure observed in the test by this pure-fatigue number of cycles to failure. A creep damage fraction can be computed from the test stress-relaxation history by calculating creep damage using the time-fraction approach and summing the results for the entire stress-relaxation history. Again, this creep-damage calculation is done using nominal rupture data, not the lower-bound and factored design approach described above. Each creep-fatigue test can therefore be reduced to a single data point (D_f, D_c). The creep-fatigue interaction diagram is produced by plotting the results of numerous creep-fatigue tests and fitting a bilinear trendline. This process generates the diagram using nominal property data and so the diagram, notionally, represents the nominal response of the underlying material to creep-fatigue loading. However, oftentimes the selected trendline more closely follows the lower bound of the available data. The calculation of fatigue and creep damage, described above, therefore contains the design margin in the ASME creep-fatigue approach.

Traditionally, both tension and compression holds are tested and the worst of the two used in constructing the interaction diagram. One diagram is used for all temperatures and so the design diagram tends to conform to the data from the worst tested temperature.

Each of the three methods of design analysis (elastic, EPP, and inelastic) constructs the input data to this general procedure in a different way.

Design by elastic analysis starts from the elastically-calculated strain range for a service cycle. This strain range is modified by factors intended to approximately account for the increase in strain caused by creep and plasticity. This strain range is then used to estimate a stress relaxation profile using the Code isochronous stress-strain curves. The hot tensile curve at the material temperature and at the design strain range is used to produce an initial stress. A stress relaxation history is constructed by the determining the stress at the design strain range and temperature for subsequent times during the hold. For example, the isochronous stress-strain curve value for 10 hours life at the design strain range and temperature provides the stress after 10 hours of stress relaxation and so on down to the cycle hold time. The elastic rules provide methods for combining the effects of multiple load cycles. For fatigue this involves a variant of rainflow counting. For creep, this requires superimposing the service relaxation profiles and using the resulting, bounding relaxation history in the calculation of creep damage.

The methods used to construct the design strain range and relaxation from the base elastic analysis are all conservative. For example, constructing a relaxation history using the isochronous curves is very conservative compared to both integrating a creep-rate equation into a relaxation history and compared to experimental stress relaxation data. This conservatism adds to the design margins contained in the Code stress rupture data, creep damage calculation, and design fatigue diagrams.

The EPP method uses the Code values of rupture stress to directly bound the creep damage experienced by a component. The strain range resulting from this bounding EPP analysis is then used to calculate fatigue damage. In practice, the elastic shakedown requirement of the EPP creep-fatigue method tends to make this method very conservative.

Design by inelastic analysis is conceptually the most straightforward approach. The designer uses a suitable inelastic model to simulate the full transient history of the component to generate a temperature-strain-stress-time history. The Code definition of equivalent strain range converts the strain tensor into fatigue damage. The Code defines an equivalent stress using Huddleston's model [44], which accounts for multiaxial stress effects. Finally, these strain ranges and stress-relaxation profiles can be used to assess the adequacy of the structure using the creep-fatigue interaction diagram.

2.2.1.3 A general assessment of the ASME procedure

Historically, the ASME procedure was developed first among the creep-fatigue design methods described here and many of the subsequent methods described below share similar features with the ASME approach [45]. As such, it is worthwhile to describe the design margin contained in the base ASME approach, now described in Nonmandatory Appendix HBB-T and Code Case N-862 and reflect on the assumptions and limitations inherent in the process.

As implemented in Section III, Division 5 the ASME creep-fatigue design approach ties directly to experimental data to determine the fatigue damage fraction (by reference to experimental fatigue curves), the creep damage fraction (by reference to an experimental creep-rupture curve), and in the construction of the creep-fatigue interaction diagram (by reference to creep-fatigue tests). Given a perfect representation of the components stress-strain-time-temperature history, the margin in the method is in the factors of 2 and 20 used in constructing the design fatigue diagram, the use of a minimum stress to rupture in calculating creep damage, and the use of a factorized, rather than notional, stress relaxation history. Nominal properties are used in the construction of the creep-fatigue interaction diagram, converting the stress tensor into an effective stress, and converting the strain tensor into an effective strain range. The procedures used for combining multiple load cycles are constructed to give a conservative estimate of the effect of superimposing transients.

In addition to the basic conservatism of the assessment method, the design by elastic analysis procedure makes conservative assumptions in calculating the design strain range and relaxation history. The EPP method uses a very conservative bound on the creep damage accumulated over the structure's design life.

In the absence of environmental effects, the ASME approach is thought to be very conservative. Direct operating experience with structures designed to the Code is limited to subscale testing of components in preparation for the Clinch River Breeder Reactor. The overall experience was that the Code rules are somewhat difficult to execute, but the procedure leads to very conservative designs.

2.2.2 RCC-MRx

The Afcen (French Society for Design and Construction Rules for Nuclear Island Components) RCC-MRx design and construction code [46] constitutes a single document that covers in a consistent manner the design and construction of components for high temperature reactors and research reactors and the associated auxiliaries, examination and handling mechanisms and irradiation devices. Although initially developed for Sodium Fast Reactors, Research Reactors, and Fusion Reactors, the methods can also be used for components of other types of nuclear facilities if the different radiation environments are properly accounted for. It was first issued in 2009 from the merging of the RCC-MX code, edition 2008 [47], developed in the context of the research reactor Jules Horowitz Reactor project, and the RCC-MR code, edition 2007 [48], devoted to high temperature reactors and ITER vacuum vessels. The scope of application of the RCC-MRx code design and construction rules exclusively covers mechanical components – considered to be important in terms of nuclear safety and operability, – having a leak-tightness, partitioning, guidance and retaining or supporting role, and – containing fluids such as vessels, pumps, valves, piping, bellows, box structures or heat exchangers and their supports.

The RCC-MRx code proposes three quality classes in the design and construction rules: N1Rx, N2Rx, and N3Rx. They correspond from 1 to 3 to a decreasing levels of assurance of ability to withstand different types of mechanical damages to which the component might be exposed as result of loading corresponding to specific operating conditions. The Prime Contractor, the Contractor and the Manufacturers shall draw up, as part of the contract, the list of mechanical components and supports to be designed and constructed in compliance with this Code and specifying the required Code Class, service loading considerations, and the level of criteria to be met. The level criteria are categorized in to Level A, Level C, and Level D categories. For normal operation including normal operation incidents, start-up and shut down the minimum level criteria is Level A. Level C corresponds to the emergency conditions with very low probability of occurrence, while Level D corresponds to fault conditions that are highly improbable but whose consequences on components are studied among others for safety reasons. Note that, the ASME code introduces a Level B into the design of pressure retaining enclosures by introducing a certain tolerance into the design internal pressure value. This provision does not figure in RCC-MRx code.

To introduce design and construction rule sets such as those contained in new Standards NF EN 13445 (pressure vessels) and NF EN 13480 (pipes), the usual RCC code format was modified in RCC-MRx by creating three sections (see Table 4). The design rules were adapted to cover the mechanical resistance of structures close to neutron sources that can also operate in significant

thermal creep conditions. The code provides a broader choice of materials than the steels used in Pressurized Water Reactors (PWR) and Sodium Fast breeder Reactors (SFR) such as alloys of aluminum and zirconium which can meet requirements for neutron transparent materials of research or irradiation reactors (RR). The design rules are divided into general rules for design by analysis and component specific design rules for particular components – shells and vessels, supports, pumps, valves, and piping. The code also provides design rules for examination, handling, or drive mechanisms and irradiation devices in separate subsections. The general design by analysis rules are the same for all classes except class N3Rx for which those are not provided in the code. Rules for bolts, bolted assemblies, and welded joints are also covered within general design by analysis rules.

	Titles (acronyms)
Section I	General provisions (RDG)
Section II	Addition requirements and special instructions (REC)
Section III • Tome 1 – Subsection A – Subsection B – Subsection C – Subsection D – Subsection K – Subsections L – Subsections Z • Tome 2 • Tome 3 • Tome 4 • Tome 5 • Tome 6	Rules of nuclear installation mechanical components • Design and Construction rules – General provision for Section III (RA) – Class N1Rx reactor components, its auxiliary systems and supports (RB) – Class N2Rx reactor components, its auxiliary systems and supports (RC) – Class N3Rx reactor components, its auxiliary systems and supports (RD) – Examination, handling or drive mechanism (RK) – Irradiation devices (RL) – Technical appendices (A1, …) ➢ A3: properties groups for base metal ➢ A9: properties groups for welded joints ➢ A16: guide for prevention of rupture, leak before break analysis and defect assessment ➢ Other technical appendices • Parts and product procurement specifications (RM) • Destructive tests and non-destructive examination methods (RMC) • Welding (RS) • Manufacturing operations other than welding (RF) • Probability phase rules (RPP)

Table 4 Table of content of RCC-MRx code

The RCC-MRx code allows three methods of analysis – elastic analysis, inelastic analysis, and experimental analysis. Elastic analysis is carried out on the assumption that the behavior of the material is elastic and linear, that the displacements are small and there is no initial or residual stress. Elastic analysis should be the most commonly used method, the other methods of analysis should be used when it is not possible to check certain criteria associated with elastic analysis. Experimental analysis consists in subjecting models representing the component or some of its elements to loadings in order to determine the deformation and stresses or margins with regard to the damage under study. Depending on the type of damages, different inelastic analysis methods are proposed in the code – elastoplastic or limit analysis under monotonic loading, elastoplastic analysis under cyclic loading if creep is negligible, and elasto-visco-plastic analysis under cyclic loading when creep is significant. Limit analysis is performed by considering an elastic perfectly-plastic material model while material hardening is considered in elastoplastic analysis. For elasto-

visco-plastic analysis, a creep law representing material creep behavior must be included into the material model.

The general analysis rules are provided in Chapter RB 3200. Rules are drafted with due regard for the corresponding chapter of the RCC-MR code in order to introduce additional rules into it to cover where irradiation is significant. In addition to the negligible creep test in the RCC-MR which, if met, allows the effects of creep to be disregarded, a negligible irradiation test is provided in RCC-MRx. This test makes it possible to disregard the effects of irradiation if the fluence received by the component is below a value specified for the material concerned at the service temperature. The structure of RB 3200 is described in Table 5. In this section, rules for negligible irradiation are discussed. Rules in the case of significant irradiation are discussed in Section below.

	Negligible creep	Significant creep
Negligible irradiation	RB 3251.1 (Type P damages) RB 3261.1 (Type S damages) Identical to RCC-MR	RB 3252.1 (Type P damages) RB 3262.1 (Type S damages) Identical to RCC-MR
Significant irradiation	RB 3251.2 (Type P damages) RB 3261.2 (Type S damages) New rules	RB 3252.2 (Type P damages) RB 3262.2 (Type S damages) New rules

Table 5 Structure of RB 3200.

2.2.2.1 Negligible Creep Test

The code provides two test methods to determine whether the effect of creep and the corresponding additional analysis can be neglected. Test 1 is defined with two conditions. The first condition checks whether the maximum temperature during the total operating period is less than the negligible creep temperature of material. Here it is necessary to consider the maximum temperature of the structure inside the thickness. The use of maximum local temperature is because the negligible creep test covers both Type P (related to means stresses and strains in the thickness) and Type S damages (taking care of local stresses and strains) [49]. The through thickness mean temperature could be sufficient to describe the effect of creep for the former one, while the maximum local temperature is required for the latter.

If the first condition is not met in Test 1, the code requires the total operating period, including all loading levels, to be broken into N intervals of times. For each time interval, the maximum time, T_i during which the material may remain at the maximum temperature reached during t_i without creep is obtained from the negligible creep curve. Then, the effect of creep can be neglected if $\sum_i^N \left(\frac{t_i}{T_i}\right) \leq 1$.

If both conditions in Test 1 cannot be satisfied for total operating period, Test 2 can be used which is to check whether any of the conditions in Test 1 is met after ignoring Level D loadings.

The rules for negligible creep are applied if the negligible creep test is satisfied. However, if the primary membrane plus bending stress intensity exceeds the time independent allowable stress, S_m

for a condition for which the maximum temperature is higher than the material negligible creep temperature, then all rules for significant creep must be applied.

Since the focus of this report is creep-fatigue design, we limit our discussion to rules under significant creep condition.

2.2.2.2 Rules for Prevention of Type P Damages under significant creep – negligible irradiation condition

Type P damages have the same meaning as in ASME code – P means Primary. For ductile and hardening materials, these damages are caused by primary loads – e.g. constant pressure, force – not by displacement controlled loads – e.g. temperature gradients. As with the ASME Code only primary loads are considered when designing the structure against long-term sustained loading. Again, as with the ASME Code the designer is responsible for classifying stresses [49]. Type P damages could lead to the burst or collapse of the structure if they are not limited. The code divides Type P damages into two parts – immediate excessive deformation and plastic instability due to plastic strains and time-dependent excessive deformation and plastic instability due to creep strains. Both immediate and time-dependent parts are covered in Level A and Level C criteria while Level D criteria covers only immediate part of Type P damages.

If an elastic analysis is used the designers are required to classify and linearize stresses in order to determine primary membrane, primary bending, local primary membrane stresses. Other two categories are secondary and peak stresses that are not used in rules for preventing Type P damages. The RCC-MRx code uses same definitions for all stress categories as those in the ASME code. Detailed descriptions of stress classification and linearization are provided in Section 2.1.1. The code then uses either maximum shear theory or octahedral shear theory to determine various stress intensities and ranges.

To prevent the immediate Type P damages, Level A criteria to be verified are:

$\overline{P_m} \leq S_m(\theta_m)$

$\overline{P_L} \leq 1.5\ S_m(\theta_m)$; in local non overlapping areas

$\overline{P_L} \leq 1.1\ S_m(\theta_m)$; in local overlapping areas

$\overline{P_L + P_b} \leq 1.5\ S_m(\theta_m)$

where, $\overline{P_m}$ is general primary membrane stress intensity, $\overline{P_L}$ is local primary membrane stress intensity, $\overline{P_L + P_b}$ is primary membrane plus bending stress intensity, θ_m is the mean temperature in the thickness of the supporting line segment used to determine stress intensity, and S_m is the allowable stress which is time independent but a function of temperature. Note that, all the stress intensity values are determined by a linear elastic stress analysis of the component. The explanation for multiplying allowable stress with 1.5 in the case of primary bending and local stresses is that these kind of stresses cannot lead to necking and rupture but they can produce large strains and must be limited. However, the limitation is not so severe compared to the limitation of the general primary membrane stress. The values of S_m are the smallest of the followings:

2/3 times the yield strength at 20°C

0.9 (austenitic stainless steels and nickel alloy) or 2/3 (other materials) times the yield strength at θ_m

1/3 times the tensile strength at 20°C

1/3 (austenitic stainless steels and nickel alloy) or 1/2.7 (other materials) times the tensile strength at θ_m.

In the case of Level C and Level D criteria, the S_m values are replaced by the lesser of 1.35 S_m and yield strength at θ_m and the lesser of 2.4 S_m and minimum rupture strength at θ_m, respectively.

For time-dependent Type P damage check, in the case of elastic analysis, the code introduces creep usage fraction, U($\bar{\sigma}$) which is used to estimate total creep damage for overall service time of the component. To determine creep usage fraction, the total service time is first broken down to N intervals. For each time interval, t_j the maximum operating temperature and maximum stress intensity are calculated to determine maximum allowable time, T_j on the basis of time-dependent allowable stress, S_t. The cumulative creep usage fraction is $U = \sum_j^N \left(\frac{t_j}{T_j}\right)$. For a given temperature, θ and application time, t, the value of S_t is equal to the smaller of the following quantities:

2/3 of the minimum rupture stress, S_r (θ, t)

80% of the minimum stress leading to the appearance of tertiary creep

the stress inducing total strain (elastic + plastic + creep) of 1%

To prevent time-dependent Type P damages, all loadings related to level A and C criteria must meet

$U_{A,C}(\Omega.\overline{P_m}) \leq 1$

$U_{A,C}(\overline{P_m + \Phi.P_b}) \leq 1$

where, Ω is a correction factor to account for local primary membrane stress and cannot be less than 1. Φ is a coefficient which takes into account the less damaging effect of the bending stress.

The check for Level D criteria, all loadings related to Level A, C, and D must meet

$W_{A,C,D}(1.35\ \Omega.\overline{P_m}) \leq 1$

where W is the cumulative creep rupture usage fraction determined similarly as creep usage fraction but using minimum rupture stress, S_r instead of S_t.

If elastoplastic analysis is performed, Type P damages for Level A criteria are checked under loadings obtained by multiplying the loading concerned by 1.5 and 2.5 for excessive deformation and plastic instability, respectively. In case of Level C criteria, the multiplication coefficients are 1.2 and 2. Check for excessive deformation not required in Level D criteria and plastic instability is checked by a multiplication coefficient of 1.35. The elastoplastic analysis is performed under monotonic loading and the mathematic model of the material behavior is based on von Mises plasticity criterion, plastic flow rule, and an isotropic hardening rule.

If limit analysis is used, the code provides following two rules.

$S_o \leq S_m(\theta_{max})$

where $S_o = (\frac{C}{C_L}).\ R_L$; C is the mechanical or thermal load and C_L is the collapse load obtained for an elastic perfectly-plastic material with a yield strength R_L.

and

$U_{A,C}(\Omega'.S_o) \leq 1$; for Level A and C criteria

$W_{A,C,D}(1.35\ \Omega'.S_o) \leq 1$; for Level D criteria

where Ω' = creep correction factor due to plasticity.

2.2.2.3 Rules for Prevention of Type S Damages under significant creep – negligible irradiation condition

Type S damages are those which can only result from repeated application of loadings. These damages are progressive deformation or ratcheting and creep-fatigue. The code provides separate rules for preventing both ratcheting and creep-fatigue damages. However, the ratcheting rules must be satisfied before applying creep-fatigue rules. Thus, rules for preventing ratcheting are also discussed here along with rules to prevent creep-fatigue damage. All the rules for Type S damages are checked only for Level A criteria.

The RCC-MRx code proposes the famous conservative $3S_m$ design rule as an alternative rule for structures in the domain of negligible creep. However, in the case of significant creep, the code recommends the concept of effective primary stress through the use of an efficiency diagram validated for austenitic steel in the significant creep domain. Since 2002 [50], the efficiency diagram rules have been extended to structures with secondary membrane stresses (e.g. cylinders subjected to axial thermal gradients varying with time and in space) and to the case of an overload of short duration (e.g. a level A seismic load). The efficiency diagram allows the calculation of the relative variation of secondary stress in relation to the primary stress considered. Two types of relative variations called secondary ratios – one in relation to the primary membrane stress and

another related to the sum of primary stresses – are determined for use in the efficiency diagram. There are several methods to determine these secondary ratios depending on the presence of secondary membrane stress and overload of short duration. Using the secondary ratios and the efficiency diagram the effective primary membrane stress intensity and the effective primary stress intensity of the sum of primary stresses corrected by a creep factor are determined. To prevent ratcheting the code limits the effective primary membrane stress intensity to 1.3 times S_m and the effective total primary stress intensity to 1.3 times $1.5S_m$. Again, the bending stresses are less prone to create a damage compared to membrane stress, thus a 1.5 coefficient is applied to S_m. After confirming the limits on effective primary stress intensities the code applies following limits to strain at all points of the structure.

- Plastic strain + associated creep strain at 1.25 times the effective primary membrane stress intensity should not exceed 1%
- Plastic strain + associated creep strain at 1.25 times the effective total primary stress intensity should not excide 2%

The plastic strain is determined from average tensile stress-strain curves and the creep deformation is determined from creep strain rules provided in material properties.

Once ratcheting rules are satisfied, creep-fatigue rules can be checked. Rules to prevent creep-fatigue damage in RCC-MRx code are analogues to those in ASME code. As in the ASME code, the RCC-MRx code also uses creep-fatigue interaction diagram to limit the creep-fatigue damage. For a structure to pass the creep-fatigue design criteria, the representative points $[V(\overline{\Delta\varepsilon}), W(\sigma)]$ must fall within the allowable envelop in creep-fatigue interaction diagram at all points of the structure. Here, $V(\overline{\Delta\varepsilon})$ is the fatigue usage fraction and $W(\sigma)$ is the creep rupture usage fraction.

To determine the fatigue usage fraction, the strain cycles corresponding to the operating period are classified into M types of cycles. The fatigue usage fraction for the type of strain cycle j is equal to the ratio of the number of strain cycles n_j to the maximum allowable cycles N_j. The cumulative fatigue usage fraction is the sum of the fatigue usage fractions calculated for all types of strain cycles. The maximum allowable cycles Nj is determined from the fatigue curve using the estimated real strain range, $\overline{\Delta\varepsilon}$ for cycle j. Similar to ASME code, the RCC-MRx code also factors the nominal fatigue curve by a factor of 2 on strain range and 20 on the number of cycles to failure. The real strain range, $\overline{\Delta\varepsilon}$ includes the strain range found from elastic analysis; the plastic increase in strain due to primary stress range, plastic redistribution and triaxiality; and the strain increase due to creep. RCC-MR recommends the use of the equivalent strain variation as defined by the von Mises criterion. Since the analysis is performed assuming elastic behavior, correction is made by taking into account for plasticity, creep, and triaxiality. The creep rupture usage fraction is determined as $W(\sigma) = \sum_k W(\frac{\sigma_k}{0.9}, \theta)$ using S_r values. Here, σ_k is determined based on primary stress intensity and secondary stress range during time interval k.

The ratcheting and creep-fatigue rules discussed above are applicable when an elastic analysis method is used. If an elasto-visco-plastic analysis is used, to prevent ratcheting the code limits the greatest positive principal strain of the mean strain tensor along the supporting line segment to material specific maximum allowable strain. The maximum allowable strain is usually 1% for most of the materials. The code also limits the greatest positive principle strain of the tensor equal to the sum of the mean strain and bending strain to twice the maximum allowable strain. Creep-fatigue

rules for elasto-visco-plastic analysis are same as those for elastic analysis, except the maximum strain range to calculate fatigue usage fraction and stress to determine creep rupture usage fraction are directly calculated from the analysis results after a stabilized state is reached. The elasto-visco-plastic analysis may need to run for several loading cycles to reach to a stabilized state.

2.2.3 ITER design criteria

ISDC design criteria [51] were developed specifically for in-vessel component of a Tokamak fusion reactor, specifically ITER. The in-vessel components of ITER are irradiated by high energy neutrons which affect material properties, most importantly ductility and fracture toughness. Thus ISDC design code was developed based on material behavior under irradiation. The code provides design rules for both low temperature and high temperature. The high temperature rules are for structures that experience creep. The code checks the applicability of high temperature rules by a negligible creep test. The code does not distinguish between different component classes, however the approach taken in the ISDC is to evaluate the structures using rules that are equivalent to the design by analysis rules of ASME Class A components. The code categorized criteria level into A, C, and D – similar to those in RCC-MRx code. The general objectives of these criteria are: negligible damage in Level A; significant local distortion may happen and inspection may be required in Level B; and large general distortion may happen but keeping the pressure boundary intact with no loss of safety margin in Label D. Level A criteria covers normal and upset loading conditions, while Level C and D cover emergency and faulted loading conditions, respectively.

Because of the expected operating conditions, rules are only provided for high temperature components that experience significant radiation. These rules are therefore detailed in Section 3.

2.2.4 R5

2.2.4.1 Overview

The R5 code [52] is a comprehensive manual for assessing continued operations of components and structures subject to high temperature conditions. The R5 Code by default using a reference stress approach and shakedown analysis. However, the assessment procedures available in R5 do not preclude the use of a full inelastic analysis.

The modes of failure considered in R5 are:

1. Excessive plastic deformation due to overload
2. Incremental structure collapse due to the applied load history
3. Excessive creep deformation and/or stress rupture
4. Crack initiation through creep-fatigue damage
5. The growth of flaws due to creep and creep fatigue
6. Failure of dissimilar metal welds due to creep and creep-fatigue

There are a few general limitations for the use of R5 procedures. It does not consider: unstable structures that may be subject to creep buckling, severe dynamic loading, short time fracture (this is covered in the R6 standard) and the effects of corrosion. The choice to not include creep-buckling has been made R5 was originally developed to design and maintain the gas-cooled reactors in the UK, most of the components have larger wall thickness than liquid metal reactors or molten salt reactors due to the higher system pressure, and creep buckling is of lesser concern. Severe dynamic loading (i.e. earthquake loading) has not been included. The interaction between corrosion and other mode of failure at high temperature is still under consideration.

The general steps required to apply any of the procedures described in R5 are:

1. Identify the temperature and load history of the structure under consideration, determine the current service seen by the structure and define the additional required service life
2. Perform an elastic finite element analysis
3. Perform load classification and linearization from finite element results
4. Assess if creep plays a significant role
5. Decide if inherent flaws play a crucial role in the residual life estimation, and therefore need to be considered
6. If a dissimilar weld is present, determine its integrity by using the procedures available in R5 Volume 6
7. If flaws are not considered or the structure is flaw free, then use Volume 2/3 to assess structural integrity and crack initiation. If crack initiation is detected from the Volume 2/3 procedures then the propagation stage is evaluated by using Volumes 4/5 and 7. If flaws are present in the structure than directly use Volumes 4/5 and 7

When dealing with crack-like flaws and fatigue damage R5 always divides the time history of a crack like flaws into two steps: incubation and growth. The incubation is the time required for a crack like flaw to reach a predetermined size a_i. The value of a_i is generally set to the maximum non-detectable flaw size during inspection and is therefore methodology dependent. A value of $a_i = 0.2\ mm$ is suggested if no other information is available. The determination of the incubation time t_i is then performed using strain range-based fatigue endurance curve as follow:

$$ln(N_i) = ln(N_l) - 0.86N_l^{-0.28}$$

where N_i is the number of cycles required for incubating a defect of size a_i. N_l is the fatigue endurance determined from the fatigue strain range curve. The incubation time $t_i$is computed from N_i knowing the relationship between the two. The incubation time is used to discount a portion of the service life from the fatigue damage in the procedure. It should be noted that if a crack is present considering a zero incubation time always lead to conservative results.

In general, R5 is mostly concerned about assessing if a structure can sustain systematic service loads (and small variations to them) without the need for repair during the planned future service time. For this reason, one of the main assumption is the quasi shakedown behavior of the structure

or component of interest. This assumption is partially removed when performing crack growth assessments.

R5 classifies primary and secondary loads consistently with the ASME code. The purpose of classifying and limiting primary, secondary and peak stress and adding design margin can be summarized as follow:

- The limit on the primary stress is used to ensure that the structure operates in elastic regime and to prevent ductile burst pressure overload or plastic collapse
- The limit on the primary plus secondary stress aims to prevent incremental inelastic deformations leading to a structure collapse and to validate the use of elastic analysis for crack growth assessment
- The limit on the peak stress is intended to guard against fatigue failure

A general concern for rules based on elastic analysis is the treatment of the elastic follow-up because it contributes to enhanced creep damage. R5 includes the effects of the elastic follow-up by means of the elastic follow up factor Z. The follow up factor Z is used to assess the creep fatigue damage and creep crack growth. It should be noted that the value of Z depends on the mechanism of interest and that the methods used for determining Z are empirical and based on judgment and experience.

Safety margins are not generally included in R5 procedures, instead sensitivity analysis of the input parameters is required to assess the robustness of the evaluation. There are exceptions. In Volume 2/3 a safety factor is imposed on the yield stress for the determination of the plastic collapse, minimum rupture properties are scaled by a 1.3 factor, and the two are sometimes combined in a pessimistic manner to evaluate a conservative life or damage estimates.

As mentioned before, R5 relies on a reference stress concept to reduce the conservativism of elastic analysis while still using simplified estimation technique. Another advantage of using a reference stress method is the ability to incorporate complex material data without the use of a full inelastic analysis. In Volume 2/3 the reference stress σ_{ref} is computed using a limit load analysis and increased by a factor to define a rupture reference stress σ_{ref}^{R}. The rupture reference stress is used to evaluate bulk creep damage and deformation caused by primary loads. For cyclic loading a shakedown reference stress σ_{ref}^{S} is defined to account for stress redistribution. This shakedown reference stress can be interpreted as the reference stress at the beginning of dwell when shakedown is achieved and it is used to assess surface creep damage and enhanced bulk creep damage arising from fatigue loading. In volumes 4/5 and 7 the reference stress is modified to account for the presence of defects. The reference stress is then used to compute the C^* parameter, from which crack-growth can be estimated.

Time dependent damage is evaluated in R5 by considering independently three factors and combing them in a linear fashion. The three factors are: creep rupture due to necking instability, time independent mechanical fatigue, and local failure due to ductility exhaustion. In R5, the separation between creep rupture and local failure is justified by invoking the length-scale difference of the two phenomena. The three different factors are defined as follows:

1. The creep usage factor is based on life fraction rule and is defined as

$$U = \int \frac{dt}{t_f\left(\sigma_{ref}^R, T_{ref}\right)}$$

where t_f is the allowable time to failure as function of the reference stress and temperature.

2. The fatigue damage factor is assessed using Miner's Rule

$$D_f = \sum_{j=1}^{J} \frac{n_j}{N_{0j}}$$

where the index j represents a cycle type, n_j represent the number of applied cycles and N_{0j} is the corresponding fatigue endurance.

3. The creep damage factor related to ductility exhaustion is defined as:

$$d_c = \int_0^{t_h} \frac{\dot{\bar{\varepsilon}}_c}{\bar{\varepsilon}_f(\dot{\bar{\varepsilon}}_c)} dt$$

where t_h is the dwell time, $\dot{\bar{\varepsilon}}_c$ is the instantaneous equivalent creep rate and $\bar{\varepsilon}_f$ is the corresponding multiaxial creep ductility.

2.2.4.2 Volume 2/3: Crack initiation procedure for defect-free structures

R5 utilizes simplified inelastic analysis to guarantee the integrity of a structure. The procedure relies on shakedown analysis to identify the parameters used in creep fatigue damage calculations and guards against the following failure mechanisms: excessive plastic deformation, creep rupture, ratcheting, crack initiation due to creep fatigue damage and creep deformations enhanced by cyclic loading.

The procedure described in R5 is summarized below:

First identify the complete load history of the component and resolve it into well-defined cycles either by event or service loading. If well-defined cyclic event cannot be easily identified than one should use the rainflow procedure, or similar methods, to derive cycle types and numbers. Then, a finite element elastic stress analysis of the component shall be performed for each cycle type. Critical location shall be recorded (there might be more than one critical location). Welds can be neglected in this finite element analysis.

At each critical location:

- Compute the equivalent von Mises stress, elastic strain and associated ranges for each point in time.
- Identify a stress classification line including the critical location and compute the equivalent primary membrane, primary local membrane, primary bending, secondary and peak stresses, P_m, P_L, P_B,Q and F, respectively.
- Demonstrate sufficient protection against plastic collapse, which means that the following inequalities must be satisfied:
    - $P_m \leq 0.67\, S'_y$
    - $P_L + P_B \leq S'_y$
    - $\Delta(P_L + P_B + Q) \leq 2.0 S'_y$ for ferritic steel
    - $\Delta(P_L + P_B + Q) \leq 2.7 S'_y$ for austenitic steel

where S'_y is in general the 0.2% proof stress S_y. For materials with creep exponent smaller than 2 then $S'_y = 3nS_y/2(n+1)$, where n is the creep exponent
If margins are adequate one proceeds to the next step otherwise full inelastic analysis shall be performed

- Evaluate if creep is significant. This means checking the following inequalities:

$$\sum_{j=1}^{J} n_j \left[\frac{t}{t_m(T_{ref})}\right]_j \leq 1$$

where t is the dwell time, t_m is the allowable time from the insignificant creep curves and T_{ref} is maximum temperature at the critical local for a certain cycle. If this criterion is not met one needs to compute the creep usage factor U which is a function of the allowable time to failure t_f at the given rupture reference stress σ^R_{ref}:

$$U = \sum_{j=1}^{J} n_j \left[\frac{t}{t_f(\sigma^R_{ref}, T_{ref})}\right]_j$$

If $U < 1$ then the analysis can continue, otherwise one needs to perform a more detailed analysis.

- The next step is to check if the structure is in global shakedown. This requires computing the size of the region of cyclic plasticity by means of a yields stress S_y scaled by a parameter K_s (typical value of K_s are between 0.7 and 1, however if justified K_s can be larger than one). The parameter K_s measures the ability of a material to develop steady cyclic behavior. All regions along the stress classification line exhibiting an equivalent elastic stress larger than $S_y K_s$ are considered plastic. The total length of plastic zone along the classification line shall not exceed 20% of the wall thickness and a continuous elastic core should be present for at least 80% of the wall thickness. If this is satisfied a detailed shake down analysis is not required and one proceeds directly to check if the effects of cyclic loading are significant via the following criteria (see Volume 2/3 Section 6.2.2 for more detail):
    - The most severe cyclic equivalent elastic stress range is within the elastic range of the material, e.g. $\Delta\bar{\sigma}_{el,max} \leq \left(K_s S_y\right)_c + \left(K_s S_y\right)_{nc}$. The subscript c and nc denote the creep and non-creep end of the cycle
    - The total fatigue damage $D_f = \sum_{j=1}^{J} \frac{n_j}{N_{0j}} < 5\%$ where N_0 is the fatigue endurance given the calculated elastic strain range associated to $\Delta\bar{\sigma}_{el,max}$
    - The creep behavior is unperturbed by cyclic loading: $\Delta\bar{\sigma}_{el,max} \leq \sigma_{SS} + \left(K_s S_y\right)_{nc}$, where $\sigma_{SS} = \sigma^R_{ref}$ is the steady state creep stress. Note that if all loads are secondary $\sigma_{SS} = 0$.

If the above inequalities are all satisfied then one proceeds to compute the creep damage

$$D_c = \sum_{j=1}^{J} n_j \left[\frac{t_h}{t_r(\sigma_{ss})}\right]_j$$

where t_h is dwell time, σ_{SS} is the steady state primary equivalent stress and t_r is the time to rupture as function of σ_{SS}.

The assessment is performed computing the total damage $D = D_c + D_f$. If $D < 1$ and the crack initiation will be avoided and the component is assessed for future service, otherwise the procedure for crack propagation describe in Volume 4/5 shall be used to assess the structure/component suitability. Note this implies that R5 uses a linear interaction diagram. To gain confidence in the assessment R5 strongly suggests performing a sensitivity analysis on the input parameters.

2.2.4.2.1 Refined shakedown assessment

If the simple global shakedown criterion discussed above is not satisfied, e.g. the size of the plastic zone along every stress classification line is not limited, one needs to demonstrate that the structure will not collapse under incremental loading in another way. To achieve this a more detailed shakedown analysis can be performed. R5 provide a simple superposition method to postprocess finite element elastic results to check if a residual stress field can be used to satisfy shakedown. The core concept is to find an equilibrated residual stress field $\hat{\rho}(x)$ such that when added to the linear elastic stress field $\hat{\sigma}_{el}(t,x)$ generates a shakedown stress field $\hat{\sigma}_s(t,x) = \hat{\rho}(x) + \hat{\sigma}_{el}(t,x)$. The shakedown stress field $\hat{\sigma}_s(t,x)$ must then be used to compute the size of plastic zone as described previously.

2.2.4.2.2 Additional steps for significant creep or significant cyclic effect

If creep effects are significant additional checks are required to avoid crack initiation and to guard against cyclically enhanced creep. For globally shaking down structure subject to creep there are two important factors to consider: the start of dwell stress σ_0 and the elastic follow up factor, Z.

If peak stresses have been included in the shakedown calculations then $\sigma_0 = \sigma_{ref}^s$ otherwise the value of the start of dwell stress σ_0 must be updated to better represent the start of the dwell stress state. This can be achieved by identifying the maximum elastic stress range $\Delta\bar{\sigma}_{el,max}$ and subtracting from it the modified non-creep yield $\left(K_s S_y'\right)_{nc}$:

$$\sigma_0 = \max\left(0, \Delta\bar{\sigma}_{el,max} - \left(K_s S_y'\right)_{nc}\right)$$

note that the max function is used to ensure that the start of dwell stress is a non-negative quantity.

For selecting an elastic follow up factor Z, R5 provides several options: i) completely disregarding relaxation (e.g. $Z = \infty$), ii) use a value of $Z = 3$ if some conditions about temperature and stress level are satisfied everywhere in the structure, or iii) perform a monotonic elastic creep computation. With Z computed the equivalent stress relaxation drop $\Delta\sigma_{rD}$ is available and the total equivalent strain range $\Delta\bar{\varepsilon}_t$ can be evaluated. The total equivalent strain range $\Delta\bar{\varepsilon}_t$ is defined as the sum of the strain increment due to creep and the strain increment due to plastic deformations. The total equivalent strain range $\Delta\bar{\varepsilon}_t$ will be used for assessing the creep-fatigue damage. To guard against excessive creep deformation the creep usage factor W need to be evaluated. A shakedown reference stress and a reference temperature should be used to evaluate W. Because the concern about excessive creep deformation is on the structure as whole the reference stress of interest is related to the stress exhibited by the core of the structure. For this reason, R5 provides different methodologies to compute a core reference stress that should be used for this evaluation. The reference is then selected to be the computed cores stress. The reference temperature is selected as

the shakedown temperature computed in the residual stress procedure. The creep usage factor W is then evaluated utilizing a life fraction approach:

$$W = \sum_{j=1}^{J} n_j \left[\frac{t}{t_f\left(\sigma_{ref}^{s}, T_{ref}^{s}\right)} \right]_j$$

where t_f is the allowable time to failure read from the appropriate rupture stress curve (e.g. S_R vs time). If the creep usage factor $W < 1$, then no further analysis is required and the creep damage per cycle can be computed as

$$d_c = \int_0^{t_h} \frac{\dot{\bar{\varepsilon}}_c}{\bar{\varepsilon}_f(\dot{\bar{\varepsilon}}_c)} dt$$

where $\dot{\bar{\varepsilon}}_c$ is the instantaneous equivalent creep rate. To accurately compute the creep damage R5 suggests using inelastic finite element simulations. If this is not possible a pessimistic value of d_c can be computed assuming that the most extreme stress state during dwell applies at all times and that the creep ductility is independent from the strain rate and equal to a lower shelf ductility. Note that if this approximation is used the elastic follow up factor will be used in the calculation. R5 also permits adding the creep damage due to the transition before shakedown. Guidance about this issue is given in Volume 2/3 Appendix A3.

The total creep damage D_c is then computed as follow:

$$D_c = \sum_{j=1}^{J} n_j d_{cj}$$

The fatigue damage is calculated using the fatigue endurance N_0 obtained as a function of the strain range $\Delta\bar{\varepsilon}_t$ obtained in this section. The fatigue damage is computed as:

$$D_f = \sum_{j=1}^{J} \frac{n_j}{N_{0j}}$$

2.2.5 API-579/ASME FFS-1

API 579-1, also known as ASME FFS-1, regulates how a Fitness-For-Service (FFS) assessment should be performed on components and equipment degrading during service. An equipment is defined as an assembly of components.

An Assessment is used to calculate if a component is suitable for continuing operations or if it should be repaired or retired.

In general, FFS-1 provides three different Assessments levels:

- Level 1 provides conservative screening criteria, requires the least amount of data and is performed by using mostly pen -and-paper calculations

- Level 2 is less conservative than Level 1, but it requires more complicated calculations and more information about the past and planned operating conditions for a component/equipment
- Level 3 provides the most detailed evaluation and is usually the least conservative. A Level 3 assessment may require FEA analysis and or additional experimental data to characterize the state of the component of interest.

FFS-1 also provides guidance on which Assessment Level can or shall be used to evaluate the suitability of the component depending on the type of service condition and the current state of the component. For instance, for components operating in the creep-regime exhibiting a crack like flaw only Level 3 assessments can be used.

Level 1 and Level 2 Assessments can be used only to predict rupture life if and only if the component does not exhibit crack-like or volumetric flaws. For all other cases a Level 3 should be performed.

For all Assessments Level the following data should be available:

- Original Equipment Design Data
- Maintenance and Operating History

Chapter 10 in FFS-1 provides procedures for how a component subject to creep-regime shall be evaluated for continued operations.

2.2.5.1 Creep damage

2.2.5.1.1 Data Requirements

The data required for a FFS evaluation are:

- Original component and equipment data. These data may include manufacturer's data report, fabrication drawings with enough detail to permit the calculation of the maximum allowable working pressure (MAWP), inspection records, material test reports, etc. For more detail see FFS-1 paragraph 2.3.1.
- A progressive record of maintenance and operational history including: the actual operating envelope consisting of pressure and temperature including upset conditions, documentation of any significant changes in service conditions, the date of installation and a summary of all alterations and repairs, records of all hydrotests performed as part of any repairs, results of prior in-service examinations including wall thickness measurements, records of all internal repairs, etc. For more detail see FFS-1 paragraph 2.3.2.

2.2.5.1.2 Level 1 Assessment

A Level 1 Assessment can be performed only if:

- The original design criteria the component has been designed to a recognized code or standard
- The component has not been subject to thermal shocks or any other event resulting in significant permanent shape changes, including corrosion and erosion.

- The material meets or exceeds the respective minimum hardness and carbon content (see FFS-1 Table 10.1 for more detail).
- The component does not contain:
    - A local thin area (LTA) or groove-like flaw,
    - Pitting damage,
    - Blister, hydrogen induced cracking (HIC), or stress-oriented hydrogen induced cracking (SOHIC) damage,
    - A dent or dent-gouge combination,
    - Any imperfection exceeding the original design code tolerances,
    - A crack-like flaw, or
    - Microstructural abnormality such as graphitization, sigma phase formation, carburization or hydrogen attack.

The Level 1 Assessment procedure relies on the computation of a total creep damage parameter D_c^{total} but it is not always required. The total computed accumulated creep damage D_c^{total} is compared to a reference value $D_c^{ref} = 0.25$. If $D_c^{total} < D_c^{ref}$ the component is suitable for continued operation. The calculation of the total creep damage D_c^{total} is different depending on if the component is subject to a single or multiple design and operating condition. Required assessment information are the nominal load, the maximum operating temperature and the component construction material. Note that in both cases the effect of wall-thinning shall be included, if present.

- Single design and operating conditions
    a. Determine the total service time t_{sc} that shall include past and futured planned operations. The nominal stress calculation shall include the effect of wall thinning.
    b. Use screening curves provided in Chapter 10 to identify the maximum permissible time for operation and compare it to the total service time. If total service time is smaller than or equal to the maximum permissible time for operation, then the component is suitable for continued operations; otherwise, proceed to step c
    c. Determine the creep damage rate R_c using the appropriate damage rate curves provided in Chapter 10. The appropriate damage curve is selected based on the nominal conditions. Compute the creep damage and the associated damage $D_c^{total} = t_{se} R_c$.
    d. Compare D_c^{total} with D_c^{ref}
- Multiple design and operating conditions
    a. Determine the number of operating conditions J
    b. For each operating condition j, identify the nominal load, the maximum operating temperature and exposure time t_{se}^j, must be identified. Again, the effect of wall thinning shall be included.
    c. For each operating condition, determine the creep damage rate R_c^j using the appropriate damage rate curves provided in Chapter 10. The appropriate damage curve is selected based on the nominal conditions. Compute the creep damage as $D_c^j = t_{se}^j R_c^j$.
    d. Compute the total creep damage $D_c^{total} = \sum_{j=1}^{J} D_c^j$
    e. Compare D_c^{total} with D_c^{ref}

In practice, for multiple operating conditions the total damage is computed as the sum of all the damages generated from each condition.

In both cases, if $D_c^{total} \leq D_c^{ref}$ the component is deemed suitable for continued service. If not, one can either change the future inspection time, tune planned operating conditions or rerate the component using Assessment Level 2 or 3

2.2.5.1.3 Level 2 Assessment

A Level 2 assessment can be performed if:

- The original design criteria the component has been designed to a recognized code or standard
- A history of the operating conditions and documentation of future operating conditions for the component are available.
- No more than 50 cycles have been applied to the components. Note this includes startups, shutdowns.
- The component does not contain:
    - An LTA or groove-like flaw,
    - Pitting damage,
    - Blister, HIC, or SOHIC damage,
    - Any imperfection exceeding the original design code tolerances,
    - A dent or dent-gouge combination,
    - A crack-like flaw, or
    - Microstructural abnormality such as graphitization, sigma phase formation, carburization or hydrogen attack.

The Level 2 Assessment is the same as applying Procedure 1 for creep rupture life outlined in the Level 3 assessment. For a Level 2 Assessment the temperature should be considered uniform for the component at each specific timestep.

2.2.5.1.4 Level 3 Assessment

A Level 3 Assessment can be used when the Level 1 or 2 Assessment fails or they cannot be applied because of the presence of flaws. It should be noted that this assessment level is the only one allowing creep-fatigue interaction to be considered.

Four different kind of level 3 assessments can be performed. The choice of the assessment depends on the problem of interest:

- Creep rupture: determine creep rupture the life of a component without flaws.
- Creep-crack growth: is applicable to components with crack like flaws operating in creep regime (discussed in the subsequent section on flaw evaluation.)
- Creep-fatigue interaction.
- Creep-fatigue assessment of dissimilar weld joints: it is applicable to 2.25Cr-1Mo and 2.25Cr-1Mo-V ferritic steel structure welded with a stainless steel or a nickel-based filler metal. This procedure is applicable for structure operating in the creep regime and subject to cyclic operations, but is not applicable if a crack is present (discussed in the subsequent section on weldments.)

The two creep-rupture life procedures described in FFS-1's paragraphs 10.5.2.3 and 10.5.2.4 can be utilized to evaluate the rupture life of a component operating in the creep range using the results from a stress analysis. This assessment evaluates stresses and strains through the wall thickness based on the best available estimate of the actual operating conditions. For the case in which an inelastic analysis has been performed a material model accounting for creep or time hardening is required. Plasticity should also be included in the material model if the computed stresses exceed the yield strength of the material at the operating temperature.

These assessments provide a systematic approach for evaluating the creep damage experienced by the component for each operating cycle. The total creep damage is the sum of all creep damages computed for all cycles.

Inelastic accumulated strain limit	Weld and HAZ	Base metal
Anywhere in the structure	2.5%	5%
when considering only primary bending and membrane stress	1.25%	2.5%
when considering only primary membrane stress	0.5%	1.25%

Table 6. Limit of accumulated inelastic strain for base metal, weldments and heat affected zone (HAZ). Different strain limits are used for base metal or welds. Different strain limits are allowed depending on stress combination type considered.

There are two procedures:

- Procedure 1: The first procedure (see FFS-1 paragraph 10.5.2.3) is based on the total accumulated creep damage D_c^{total} throughout the component service life and inelastic strain limits. The total accumulated creep damage is evaluated by computing stresses and using material data from either the MPC Omega Project or Larson-Miller parameters (both are provided in FFS-1). Stresses at discrete times during the load history may be computed via elastic analysis, or inelastic analysis considering the effects of creep relaxation. The use of this procedure implies the identification of a load histogram including the past and future operating conditions and it is suitable for cyclic loading. If required, the entire load history should be divided into cycles. Each cycle must be subdivided. For each cycle m the procedure's steps are the following:
    - Determine the total cycle time ${}^{m}t$ and divide into N time steps. The time steps should be small enough to capture all relevant changes in operating conditions. Note that the analysis should be performed accordingly to the actual sequence of operating conditions. If the component is subject to corrosion and/or erosion the time-steps should be small enough to capture this.
    - Determine the temperate ${}^{n}T$ and the stress state ${}^{n}\sigma_{ij}$ for the time increment ${}^{n}t$. Note that the stresses can be computed by numerical or closed form solution for simple geometries.
    - Check if the component has adequate protection against plastic collapse. The margin against plastic collapse is determined by doing a stress classification and linearization analysis and by checking the following inequalities:
        i. ${}^{n}\sigma_{ref}^{p} \leq \sigma_{ys}$
        ii. ${}^{n}\sigma_{ref}^{p} \leq 0.75\ \sigma_{ys}$ for austenitic steel

where the reference stress is computed as ${}^{n}\sigma_{ref}^{p} = \frac{{}^{n}P_b + \left({}^{n}P_b^2 + 9\,{}^{n}P_L^2\right)^{0.5}}{3}$, P_b and P_L are the primary bending and local membrane stress for the n^{th} increment, respectively, and σ_{ys} is the yield strength at the reference temperature ${}^{n}T$.

- Determine the principal stresses ${}^{n}\sigma_1$, ${}^{n}\sigma_2$ and ${}^{n}\sigma_3$ and the effective stress ${}^{n}\sigma_e$. The effective stress is:

$${}^{n}\sigma_e = \sqrt{\frac{\left({}^{n}\sigma_1 - {}^{n}\sigma_2\right)^2 + \left({}^{n}\sigma_3 - {}^{n}\sigma_2\right)^2 + \left({}^{n}\sigma_1 - {}^{n}\sigma_3\right)^2}{2}}$$

- Determine the remaining life for the computed equivalent stress level and temperature for n^{th} increment and define it as ${}^{n}L$. The calculation the remaining life depends if material data used are from MPC Project Omega or from the Larson-Miller parameter (LMP):
    i. When MPC Project Omega Data are used the time to rupture is given as ${}^{n}L = \frac{1}{\dot{\varepsilon}_{co}\Omega_m}$, where $\dot{\varepsilon}_{co}$ is the initial creep rate at the beginning of the sub step being evaluated based on stress state and temperature and Ω_m is the multiaxial damage parameter (see paragraph 10.5.2.3.g.1 for more details).
    ii. For LMP the time to rupture is given by $\log_{10}[{}^{n}L] = \frac{1000\,LMP\left({}^{n}S_{eff}\right)}{T_{refa} + {}^{n}T} - C_{LMP}$, where $LMP\left({}^{n}S_{eff}\right)$ is the Larson Miller parameter at a given effective stress ${}^{n}S_{eff}$ and C_{LMP} are the Larson-Miller constant.

  It should be noted that for both cases the parameter of both equations are constants. For this reason, smaller the sub step time higher the accuracy obtained by the remaining life calculation. Additional margins are introduced in the remaining life when using material data based on the ${}^{n}L$ parameter. If the source of material data is the MPC Project Omega database, the value of $\dot{\varepsilon}_{co}$ and Ω_m can be adjusted by using the creep adjustment factor $\Delta_{\Omega}^{\mathrm{sr}}$ (linearly affects the minimum time to rupture and range between -0.5 and +0.5) and the creep ductility factor $\Delta_{\Omega}^{\mathrm{cd}}$(linearly affects the expected time to rupture range between -0.3 and +0.3) respectively. If creep rupture data are given in terms of Larson-Miller parameter then the minimum or average time to rupture may be used.

- Determine the used life fraction as $D_c^N = \frac{{}^{n}t}{{}^{n}L}$.

The total creep damage for cycle m is therefore computed as ${}^{m}_{c}D = \sum_{n=1}^{N} D_c^N$ and the total creep damage for the entire load histogram is computed as $D_c^{total} = \sum_{m=1}^{M} {}^{m}_{c}D$. If $D_c^{total} \leq 1$ the component is suitable for continued operations, from a creep damage perspective. If the component satisfies both the creep damage and inelastic strain limit criterion the component is suitable for continued operation, otherwise the component shall be rerated, repaired or retired.

- Procedure 2 (see FFS-1 paragraph 10.5.2.4) is defined in terms of integral equations and is better suited for implementation in numerical software. This procedure considers ratcheting and shakedowns at all points in the structure as means to guarantee global structural integrity. The operation time histogram shall be defined in the same manner as in Procedure 1. This procedure provides three options for assessing structural integrity:

a. Elastic analysis for which the following limit $P_L + P_b + Q \leq (S_h + S_{yc})$ shall be satisfied where Q is the secondary stress, S_h is the maximum allowable stress at the maximum temperature within the cycle being considered and S_{yc} is the minimum yield strength for the cycle under consideration. In other words, for both S_h and S_{yc} pessimistic values are used.
b. A simplified inelastic analysis is used to demonstrate elastic shakedown at all points in the structure. For this option a conservative load histogram should be used (e.g. for each sub-step n use the most extreme loading condition). At least two complete cycles shall be considered. A minimum hold time of at least one year must also be included to establish the effects of creep relaxation.
c. A complete inelastic analysis is used to account for time dependent material properties and the complete load history, including transients. The purpose is to demonstrate structural shakedown or steady ratcheting. In either case the strain limits in Table 6 of FFS-1 shall be satisfied.

For options a and b a simplified histogram may be used. Option c requires a complete inelastic analysis of a load histogram. For stabilized cycles an elastic-perfectly-plastic model is used to produce conservative results. Furthermore, shakedown is not required because a limit on total accumulated inelastic strain is used (this is similar to ASME Section III, Division 5, paragraph HBB-T1310). The strain rate to be used in the inelastic analysis, i.e. a creep model shall be determined using the following equation (see FFS-1 paragraph 10.5.2.4.c for more details):

$$\dot{\varepsilon}_c = \frac{\dot{\varepsilon}_{oc}}{1 - D_c}$$

where $\dot{\varepsilon}_{oc}$ is the initial creep rate evaluate at the beginning of time period being evaluated based on stress and temperature. The creep model for the inelastic analysis is determined by equations 10.30 through 10.42 in FFS-1 paragraph 10.5.2.4. This model is based on MPC Project Omega Data.

It should be noted that the provided strain rate model does not include the effect of primary creep. In general, primary creep is irrelevant when calculation is performed utilizing design data. Furthermore, the Omega model accounts for accelerated creep rates and creep relaxation when high stresses are present. This is a conservative approach compared to letting primary creep relax without damage.

Furthermore, inelastic analysis is required to assess the creep life for regions of the component experiencing extreme conditions of stress and temperature which may lead to inelastic behavior of the component. It is the responsibility of the analysist to select such locations and to ensure that the worst-case scenarios have been analyzed. The life due to creep damage is defined as the time for which the accumulated creep damage $D_c = 1$. The remaining life is defined as the creep life minus the time in actual operation.
At local discontinuities the use of inelastic analysis account for creep damage and creep-fatigue interaction. The use of a local shakedown requirement guarantees that accumulated inelastic strains are small everywhere in the structure. Results of the inelastic analysis must satisfy the following criteria.

1) The creep damage D_c must be smaller than unity everywhere in the structure

2) The equivalent accumulated inelastic strain should not exceed the following limits (see Table 6):

- 5% anywhere in the structure
- 2.5% when considering only primary bending and membrane stress
- 1% when considering only primary membrane stress

2.2.5.2 Fatigue damage

FFS-1 provides rules to assess the fatigue damage and the remaining fatigue life in chapter 14. For creep-fatigue conditions only Level 2 and Level 3 Assessments can be used because Level 1 assessments do not provide a fatigue damage analysis. Note that only Level 3 Assessments are described in detail as they produce the most accurate fatigue damage estimate. For detail about Level 2 Assessments see FFS-1 section 14.4.3.

There are three methods for a Level 2 fatigue assessments:

1) Method A – Fatigue Assessment Using Elastic Stress Analysis and Equivalent Stresses. The computed effective total equivalent stress amplitude obtained from a linear elastic stress analysis and experimental data from smooth bar fatigue curve are used to evaluate fatigue damage and remaining life.
   The effective equivalent stress range is then computed and scaled by a fatigue penalty factor $K_{e,k}$ whose value can be computed as a function of the stress or strain range.
2) Method B – An elastic-plastic analysis is required to determine the appropriate equivalent strain. This method computes the fatigue life based on an equivalent strain range determined from numerical calculations and compares the results using experimentally determined strain range and life.
3) Method C – Assess the life of welds using an equivalent stress obtained from elastic analysis. This method utilizes the computed equivalent structural stress ranges and compares them with weld and joints fatigue curves. The equivalent structural stress range parameter is defined as the structural stress range scaled by the product of three different factors: a power of the structural correction factor $f_{M,k}$, a power of the means stress correction factor I and a power of the equivalent structural stress effective thickness t_{ess}.

Note that a fatigue assessment entails a secondary ratcheting check. Two methods are provided:

1) Elastic Stress Analysis – The protection against ratcheting is evaluated using an elastic analysis with conservative assumptions to approximate the effects of steady-state and cyclic loading conditions. The conservatism comes from using the highest value of equivalent stress range $\Delta S_{n,k}$ throughout the thickness and by limiting it with the maximum allowable primary plus secondary stress range S_{PS}.

2) Elastic-Plastic Stress Analysis – It is used to determine the structural shakedown and to evaluate the accumulated plastic strain. This assumes the use of an elastic-perfectly plastic material model and the use of minimum specified yield strength at a temperature. The acceptance criteria for the Assessment are: there is no plastic action in the structure, or there exists an elastic core in primary-

load-bearing boundary of the component, or there is no permanent change in the overall dimension of the component under cyclic loading.

Level 3 fatigue assessments leverage a critical plane approach in combination with a multiaxial strain-life equation, and incorporating a mean stress correction, to evaluate the allowable fatigue life for the given loading history. The aim of the critical plane approach is to identify the cutting plane exhibiting the maximum fatigue damage. Fatigue damage is computed using a strain/life equation. The critical plane approach shows improved correlation with fatigue test results and its post processing complexity is therefore justified, given that it reduces the degree of conservativism.

The results from an elastic stress or elastic-plastic stress analysis may be used. The methodology is different and depends on kind of stress analysis performed:

- Elastic stress analysis and critical plane approach:
    - Determine the loading history and future planned operations. Because this is a fatigue analysis all significant events should be included.
    - Perform an elastic stress analysis of the component record the stress distribution for point of the loading history. Because this is an elastic analysis the order of events is not significant and simulations can be performed independently for each time in the loading histogram. The sequence of events can be reconstructed during post processing.
    - Correct the resulting stress and strains for plasticity using the Neuber correction model. The Neuber correction model used in the FFS-1 plastic correction procedure incorporatse isotropic and multiple back stress kinematic hardening. For more detail on the correction see Section 14C.2.2.2 in FFS-1.
    - Using the Neuber corrected stress and strains compute the maximum shear and normal strain for a candidate critical plane for all times in histogram.
    - Using the elastic (uncorrected) stresses and strain determine the corresponding stress and strain ranges using the cycle counting technique described in paragraph 14C.4.2. Define the total number of stress ranges as M.
    - For each cyclic stress range k:
        - For the selected candidate plane calculate the maximum shear and associated normal strain range, $\Delta\gamma_{max,k}$ and $\Delta\varepsilon_N$ using the Neuber corrected strains.
        - Calculate the admissible number of reversal $N_{f,k}$ by means of the brown miller equation
        $$\frac{\Delta\gamma_{max,k}}{2}+\frac{\Delta\varepsilon_N}{2}=1.65\left(\frac{\sigma'_{f,k}-\sigma_{N-mean,k}}{E_{ya,k}}\right)\left(2N_{f,k}\right)^{b_k}+1.5\varepsilon'_{f,k}\left(2N_{f,k}\right)^{c_k}$$
        where $\sigma'_{f,k}$, $\varepsilon'_{f,k}$, b_k and $c_k$are equations parameter determined for the reference temperature of the k^{th} cycle type. This equation directly considers the effect of Poisson's ratio, elastoplastic strains and means normal stress.
        - Compute the fatigue damage as:
        $$D_{f,k}=\frac{n_k}{2\left(\frac{N_{f,k}}{f_{ND}}\right)} \quad with\ f_{ND}\geq 1$$

where n_k is the number of applied cycles of type k and f_{ND} is the fatigue knockdown factor. The fatigue knockdown factor accounts surface finish, geometry and other effects that might reduce fatigue life. Table 14.8 in FFS-1 gives values for the fatigue knockdown factor.

- Compute the total fatigue damage as the sum of the damages computed for each cycle:

$$D_f = \sum_{k=1}^{M} D_{f,k}$$

- Repeat the all procedure for the next candidate critical plane.
- Once all candidate critical planes have been evaluated determine the maximum fatigue damage as the maximum damage accumulated over all the critical planes $D_{f,amx}$. The component is suitable for continuing operation if

$$D_{f,max} \leq 1$$

- Elastic-plastic stress analysis and critical plane approach: the procedure is the same outlined for the Elastic stress analysis except that Neuber stress and strain correction is not used.

2.2.5.3 Creep-fatigue interaction

Creep-fatigue interaction evaluation in FFS-1 is described in paragraph 10.5.3. Creep damage and fatigue damage are evaluated separately. For evaluating creep damage, use the creep rupture life assessment described above and determine the creep damage (e.g. $D_c = \sum_{m=1}^{M} {}^{m}_{c}D$). For evaluating the fatigue damage per cycle, a damage fraction approach is used (e.g. $D_f = \sum_{m=1}^{M} \frac{{}^{m}n}{{}^{m}N}$), where n is the number of actual cycles and N is the number of allowable cycles for the condition defined by the histogram for cycle type m. Once creep and fatigue damage are computed, FFS-1 provides a creep-fatigue interaction diagram to check whether the combined creep and fatigue damages exceed the limits. Besides satisfying the creep-fatigue damage requirement FFS-1 additionally requires a limit on the maximum accumulated inelastic strain accordingly to Table 6.

2.3 Recommendations

2.3.1 Scope of this report

The authors are aware of parallel efforts by ASME on assessing and identifying gaps in the Section III, Division 5 rules for the design of high temperature nuclear components. Therefore, this report does not duplicate these efforts for the creep-fatigue design rules. The following recommendations might be viewed as improvements to existing creep-fatigue methods, as the current ASME methods are generally over-conservative. However, they do address areas where the current ASME methods, stripped of design margin, could fail to predict the actual life of a component conservatively, particularly for structures with long service lives. For very long service lives experimental data does not exist to directly validate the design method predictions and so it is possible, if unlikely, that the design methods including margin could eventually fail to be conservative.

2.3.2 Assessing creep and creep-fatigue damage methods

Most newer codes and standards adopt a ductility exhaustion approach to calculate creep damage, whereas the ASME code relies on the older time-fraction approach. Given identical databases the two methods do produce different predictions of a structure's rupture life. There is some indication in the literature that the time fraction approach produces longer predicted rupture lives than the ductility exhaustion approaches for low levels of applied load (i.e. components with long design lives). This does not mean predictions using the time-fraction approach will be non-conservative, but it is a potential concern.

The creep damage calculation in the ASME methodology could easily be replaced with any other method of computing damage. However, as described above, the creep-fatigue interaction diagrams would need to be recomputed which would require a much more substantial effort.

A short study could assess the adequacy of the time fraction approach for the long design lives and multiaxial stress states more representative of in service components in future advanced reactors. This study would necessarily be comparative rather than determinative – it could compare the predictions of the time fraction approach to other methods for computing creep damage, but as all methods will be extrapolating from shorter term data it could not directly determine which methods may be non-conservative.

However, knowing for which design lives and/or stress states existing methods make diverging predictions could be valuable for the regulator in setting limits on initial licensing periods or thresholds for requiring a higher scrutiny of a structure subject to creep-fatigue loading. Additionally, such a study could be used as a vehicle for providing the NRC a suite of different models for creep-fatigue evaluation that could be used to make decisions on particular component designs. For example, if all the models provide consistent predictions than the uncertainty in the extrapolated creep-fatigue life is likely low. On other hand, if the predictions of the models diverge than there could be considerable uncertainty in the extrapolated component life.

A similar effort could be undertaken to give regulators a suite of options for creep-fatigue damage evaluation, beyond the linear or bilinear interaction approaches adopted by the current design codes. This suite of models could be used in a similar way to the creep damage model described above. At least some of the alternative models can be calibrated with the same data that underlies the ASME creep-fatigue interaction diagram and so additional testing would not be required.

2.3.3 Notch effects

Nearly all creep-fatigue design procedures are calibrated to uniaxial creep-fatigue test results. The ASME Code is no exception. The effects of multiaxial stress states are incorporated into the design procedure using an effective stress that is supposed to index a multiaxial stress state to an equivalent uniaxial stress. Equivalency, in this case, ideally, means that the two hypothetical stress states will result in the same creep-fatigue life.

The effective stress used in the ASME code for creep-fatigue analysis varies. For design by elastic analysis it is in effect the Tresca stress, because the design by elastic analysis rules use stress intensities. For the EPP method it is in effect the von Mises stress because the bounding creep damage calculation using perfect plasticity and a pseudoyield stress uses a von Mises yield surface. The design by inelastic analysis method explicitly uses the Huddleston [44] stress to account for multiaxiality. Of these three only the Huddleston stress has any direct experimental validation.

Again, ultimately the only way to directly validate the code approaches is to conduct specialized creep-fatigue tests on geometries with controlled stress states. Only example would be a pressurized tube under combined axial load. Another example could be tension-torsion experiments. As with most of high temperature design, such experiments would be complicated by time effects. For example, experiments have established that the effect of stress multiaxiality on creep rupture changes with the applied stress level and hence the design life [53].

However, analysis studies could be used to clarify the issue. One possibility is to evaluate a series of components with a geometry contrived to span a variety of stress states – for example bars with increasing sharp notches – using several creep-fatigue methods to determine the scatter in life predictions and to ascertain any trends in the methods' predictions as the stress state changes. Such studies could be used to gain confidence in the existing methods, if the stress state does not greatly affect the scatter in predicted lives, or to identify which methods may have particular difficulties handling notch effects, for example if one method begins to diverge from the others for particular stress states.

2.3.4 Assessment of margin

The ASME creep-fatigue design approach is likely highly conservative, particularly for structures with relatively short design lives. However, the margin in the current design code approaches was not set probabilistically, but rather through engineering experience. This means, for example, that a probability of premature failure cannot be associated with a particular component, set of loadings, and design life. Furthermore, though it is expected that this hypothetical probability will be very low it will also certainly increase as the design life required of the component increases. Part of this increase in probability will be caused by long-term unknown effects that cannot be directly assessed from existing experimental data – several of effects of this type are highlighted in this section. However, part of the increase will be due simply to a reduced confidence in extrapolating stress rupture data out to longer design lives. This statistical effect could be quantified.

Furthermore, the overall fixed design margin implied by the code approaches for creep-fatigue could be determined as a function of temperature and design life by a consistent comparison to inelastic damage analysis. The general approach could be:

1. Select some inelastic damage model for creep fatigue to represent the true material response. This model must reasonable capture the relevant phenomenon, but not exactly capture the experimental response of any particular material.
2. Use this material model to simulate a set of experiments sufficient to construct creep-fatigue design information following the current code approach.
3. For a series of different components, loadings, and design lives perform two life evaluations: one with the code design approach using the design curves developed from synthetic experiments that will be consistent with the inelastic model and one with the inelastic model directly. The difference in predicted life between the two analyses is the design margin for the code approach for that particular component, design life, and sequence of loadings. The process can be repeated to build up a more complete picture of how the inherent margin in the code changes as a function of design life, temperature, loading, etc.

Combining the statistical uncertainty of extrapolating short-term data and the fixed design margin in the code approaches could give regulators a better understanding of risk in high temperature structural design. This combination could be made by introducing appropriate data scatter in step two of the process described above, tuning the scatter to that found in actual, experimental measurements of the relevant material properties.

The probabilities generated through this approach could only be a lower bound because of general uncertainty associated with long-term creep-fatigue damage (notch effects, changes in creep-fatigue interaction, etc.). However, this method could give regulators a tool for examining single-event scenarios as a function of design life and uncertainties in transient temperature loadings and also a tool for assessing the likelihood of multiple-event scenarios where more than one component fails in a narrow timeframe.

3 Creep-fatigue in adverse environments

3.1 Creep-fatigue mechanisms in corrosive coolants

The fatigue resistance of metals can be significantly affected by the corrosive environment. Hostile liquid or aggressive gaseous environment, most frequently in the presence of damaging impurities, can cause degradation in the fatigue life of structural metallic materials while undergoing cyclic loading through interactions of the chemical and mechanical processes at the crack tip. The phenomena of cracking under the combined action of cyclic loading and a corrosive environment is commonly called corrosion fatigue [54], [55]. Cracks during corrosion fatigue can be initiated at the surface intergranularly or transgranularly [55]. In the case of former, intergranular corrosion provides initiation sites for fatigue cracks which could then grow transgranularly. On the other hand, the initiation can be transgranular when slip intersects the surface and fresh slip steps contact the surface which results in dissolution of atoms. Many small cracks are generated in this process which eventually coalesce and grow. The crack growth rate is sometimes enhanced by hydrogen generated from reactions between environmental species and the newly cracked material at the tip. The generated hydrogen diffuses into the highly stressed region at the crack tip and causes additional damage and increases the crack growth rate.

Corrosion assisted crack can also propagate under sustained loading called stress corrosion cracking (SCC) [56]. The stress required to cause stress corrosion cracking is small, usually smaller than yield stress, and tensile in nature. Residual stresses can also cause stress corrosion cracking. While corrosion fatigue is cycle dependent, SCC is time dependent. However, a recent work [57] on martensitic stainless steel in chloride environment shows that low amplitude cyclic loading, below ΔK_{TH} (i.e. ripple loads), can enable the SSC below K_{ISCC} via mechanical rupturing of the crack tip film and enhancement of the hydrogen embrittlement-based SCC mechanism.

Corrosive environment can also reduce creep rupture strength of metal. Several studies on the high temperature corrosion-creep interaction for different metal-salt systems can be found in [58], [59], [68], [60]–[67] for aircraft, marine, and land-based gas turbine applications. Most of these studies show that molten salt does not significantly affect the secondary or minimum creep rate. However, it does adversely affect the tertiary region which results in consequent reduction in creep rupture life. Molten salt penetrates along the grain boundaries and coalesces with creep cavities, resulting in lower creep rupture life.

Very few studies [12], [69]–[71] have attempted to investigate the impact of corrosive environment on creep-fatigue behavior of structural alloys. Moreover, almost all of these studies basically compared experimental results carried out in air, vacuum, or some inert environment which are not relevant environments for future high temperature reactors.

Overall, there is a paucity of data on creep-fatigue, creep, and fatigue on materials exposed to realistic high temperature reactor coolants. This is reflected in the current design practice (see below), which do not attempt to account for the effect of corrosion on creep-fatigue life.

3.2 Creep-fatigue mechanisms under irradiation damage

When exposed to fast-flux neutron irradiations nuclear reactor metals may exhibit many phenomena such as irradiation hardening and loss of ductility, void and bubble swelling, irradiation creep, irradiation growth, and helium embrittlement. Fundamentals to all these neutron-

induced phenomena are the basic damage production through two different processes: the creation, diffusion, and interaction of point defects such as vacancies and interstitial atoms resulting from collisions with high energy neutrons; and the chemical and isotropic alteration of atoms via transmutations. Detailed discussions of the damage processes are beyond the scope of this report. Several chapters in [72] provide detailed reviews of radiation-induced microstructural changes, radiation damage formation, and radiation-induced segregation in metals. Brief descriptions of the radiation related phenomena are provided here.

Irradiation hardening is the increase in strength of metal under irradiation. The microscopic components such as voids, bubbles, precipitates, dislocation loops etc. produced by irradiation act as obstacles to the movement of dislocations and therefore increase the strength of metal. This increase in strength usually saturates at low irradiation level. This saturation level depends on metal composition and temperature and interestingly does not depend on heat treatment such as annealing, cold-work etc. For example, the yield strength of 20% cold-worked 316 stainless steel and annealed 316 stainless steel converse to the same saturation level when irradiated under same dpa rate and temperature [73]. A concurrent process to strength hardening under irradiation is the loss of ductility.

Void swelling is the progressive accumulation of vacancies whereas bubble swelling is the accumulation gas such as helium produced during irradiation. Both void and bubble swelling lead to macroscopic increase in volume. In most nuclear system swelling is the most important contributor to dimensional instability. In the absence of stress field or constraint, swelling distributes its strains isotopically. When constrained or spatially varying, however, swelling can lead to high stresses and activate irradiation creep which then redistributes the strain anisotopically.

Irradiation creep is the response of the dislocation microstructures to the local stress state. Irradiation creep is widely held to be non-damaging and is not limited by ductility. However, irradiation creep strains can affect the distribution of stresses and can influence other damage mechanisms such as fatigue and thermal creep. In the 1970s, swelling and irradiation creep were used to be considered as two separate processes but now it is known that both are interrelated and interactive processes [74].

Irradiation growth is a volume-conservative anisotropic distribution of strains without the presence of stress and introduces severe distortion. At high temperature, helium can accumulate at grain boundaries through diffusion or dragging by dislocations and may cause grain boundary embrittlement [75]. Some of the parameters that affect all the irradiation-induced phenomena are neutron fluence or dpa (displacements per atoms), dpa rate, temperature, stress, and lattice structure and composition of metal.

All the above mentioned irradiation-induced phenomena influence the creep-fatigue behavior of materials. Very few studies focus on creep-fatigue interaction under irradiation, most of the studies found in literature either focus on the effect of irradiation on the creep rupture strength or on the fatigue strength. Thus the effect of irradiation on creep and fatigue damages are first discussed separately and then the effect on combined creep-fatigue damage is discussed. Note that, this discussion only provides some general overview and some important findings on the effect of irradiation on creep and fatigue damages for some of the nuclear reactor alloys but does not cover

every aspect of it. The intention is to provide some insight that may help decide the approach to developing assessment rules for components that experience significant irradiation.

Under irradiation at high temperature metals experience irradiation creep as well as thermal creep. It is well accepted that irradiation creep is inherently a non-damaging process on the microstructural level [74]. However, there are other irradiation induced processes that do limit the deformation of structures. Such processes are elemental segregation, irradiation-induced precipitation leading to embrittlement, and the formation and growth of helium bubbles on grain boundaries [76]. The last mechanism is the most important. Details of the bubble growth mechanism through the transport of He from grain interiors to grain boundaries and failure due to this mechanism can be found in [77].

Grossbeck et. al [76] investigated the effect of irradiation on creep rupture life of austenitic stainless steel alloy 1.4970 at 700°C and found remarkable reduction in lives for in-reactor specimens. They also noticed a change of stress dependence of the creep-rupture strength. A better explanation of this change can be provided by comparing the creep rupture life of in-reactor and post-irradiation specimen. Several studies [78], [79] reported lower creep rupture life for in-reactor specimens when compared to specimens tested after irradiation though the post-irradiation specimens have higher helium concentration. This is because the presence of tensile stress during irradiation enhances the growth of bubbles, some of which might grow as voids by vacancy absorption, cause the specimen to fail earlier than the post-irradiated samples.

Ukai et al. [80] performed in-reactor creep rupture tests on 20% CW modified 316 stainless steel to determine the effect of irradiation through comparison with creep rupture experiments in air and sodium. The in-reactor creep rupture lives were shorter than those tested in air and sodium. Interestingly, in-reactor creep appeared to show earlier onset of tertiary stage and was significantly accelerated. The resultant larger creep strain does not support the failure mechanism associated with helium embrittlement. It was instead attributed to the earlier recovery of dislocation structure introduced by cold-working. Investigations on the effect of irradiation on creep rupture properties for some of the Ni-based alloys and ferritic-martensitic steels can be found in [81]–[84]. In all cases irradiation adversely affects the creep rupture properties of these metals.

In general, fatigue life of nuclear metal alloys such as austenitic steels, ferritic-martensitic steels, and nickel-based alloys is reduced due to the irradiation-induced defect clusters. However, the extend of the effect can vary significantly depending on the composition, irradiation conditions, and temperature. Kharitonov [85] carried out a review of the low cycle fatigue data up to 1984 and provided a comprehensive review of the effect of irradiation on fatigue life of 316 and 304. The fatigue life of 316 stainless steel was found to be strongly affected by irradiation compared to that of 304 stainless steel. The life of 316 stainless steel was decreased by a factor of 2.5 to 10 with increasing temperature whereas that was decrease by a factor of 1.5 to 2.5 for 304 stainless steel. A possible explanation for the greater reduction of fatigue life for 316 stainless steel, as provided in [85], is the higher concentration of gaseous products, specially helium and hydrogen, from transmutation of 316 stainless steel than 304 stainless steel. The main contribution of these gases comes from nickel whose content in 316 stainless steel is 13.6% and in 304 stainless steel is 9.5%. Same explanation is also true for Incoloy 800 whose fatigue life was reduced by a factor of 5 to

35 due to the large nickel content of 32% [85]. For Erofer97, a ferritic-martensitic steel, at high temperature (>450°C) irradiation seemed not to affect the low cycle fatigue behavior [86].

Irradiation-induced hardening also plays an important role on fatigue life. As reported in [87], fatigue life of solution annealed 316L stainless steel did not decrease due to irradiation when the applied strain range is low. The explanation provided is that at low strain range the deformation may become almost entirely elastic due to irradiation-induced hardening which results in a delayed crack initiation. In most of the studies the effect of irradiation on fatigue life was determined from fatigue experiments on post-irradiated samples which may not be the actual representation of the material behavior under irradiation. For example, as shown in [88] for ferritic-martensitic steel, the fatigue lives of samples tested during irradiation were found shorter compared to the post-irradiated sample, while it is reported the other way around in [89] Simultaneous irradiation and fatigue can develop a different microstructure and lead to different material response which is not considered in post-irradiation experiments.

There are only a few studies that investigated creep-fatigue under irradiation. Scholz and coworkers [90], [91] performed fatigue and creep-fatigue experiments on cold worked and anneal 316L stainless steel during an irradiation with 19 MeV at 400°C. Tests were conducted in torsion mode on hour glass specimens. They imposed hold-time at two positions – maximum and mean – of the loading cycles. The former was to induce creep under irradiation while the latter was to study the effect of cyclic loading on irradiation hardening. While they compared fatigue life of irradiated specimens with unirradiated specimens, they did not compare the creep-fatigue life between irradiated and unirradiated conditions. Thus, the effect of irradiation on creep-fatigue life cannot be determined. Brinkman and coworkers [92], [93] investigated creep-fatigue interaction in irradiated and unirradiated solution annealed 316 and 304 stainless steels based on available data in literature. They found significant reduction in creep-fatigue life under irradiation. However, due to lack of data no recommendation was made on estimating creep-fatigue damage for design purposes.

Overall, there is much more information available in the literature on the effect of irradiation on creep and fatigue life, albeit very few studies that examine creep-fatigue interaction explicitly. However, based on this information several of the design codes have formulated rules for accounting for radiation effects on structural life.

3.3 Survey of current design practice

3.3.1 ASME Section III, Division 5

The design rules contained in Section III, Division 5 explicitly do not consider the effect of environmental conditions on creep-fatigue damage. The only explicit consideration of corrosion contained in the Subpart HBB design rules is in HBB-3121, which requires a corrosion allowance accounting for the expected gross loss of section for a component (or region of a component) over the design service life in the expected operating conditions. The only explicit mention of radiation damage is in HBB-3124 which warns the designer of the detrimental effect of fast neutron radiation on material properties and suggests not placing structural discontinuities in high radiation areas.

HBB-Y-4200 notes that the design material properties in the Code may be degraded by long exposure to irradiation or corrosive coolants. This paragraph explicitly places this issues (with the exception of thermal aging) outside the ASME code but requires that the Owner/Operator account for environmental effects in some way and justify these decisions to the regulator. This provision refers to Nonmandatory Appendix W to Section III, which details possible environmental effects, general construction methods for mitigating the effect of the environment,

Appendix W takes a catalog approach, giving some brief general guidance about mitigating environmental effects and then listing a large variety of possible detrimental environmental mechanisms. For each mechanism, the appendix provides a general overview followed by specific design, construction, and inspection recommendations. Most of the mechanisms in the appendix apply to low temperature lightwater reactors, though there is a brief section (W-4400) covering high temperature effects. While this appendix provides useful general guidance, it does not provide design or fitness-for-service methods accounting for corrosion or irradiation damage.

3.3.2 RCC-MRx

As mentioned above, the RCC-MRx code was developed to cover the mechanical resistance of structures close to neutron sources, thus detailed design rules are provided for irradiation damages. Rules were developed on the basis of standard nuclear installations where irradiation damages occur due to neutron flux and therefore these rules do not cover for damages due to other types of irradiation – e.g. proton irradiation, irradiation producing large amount of helium etc. The code does not provide detailed design rules for damages due to corrosion, erosion, and wear. However, a provision is provided to consider these environmental effects. Effect of thermal ageing is addressed in the code by a negligible thermal ageing test and by adding higher margin on some of the design allowables if thermal ageing is significant.

The provision for corrosion, erosion, and wear is discussed first. If a component is subjected to in-service thinning, a certain additional thickness shall be added to the minimum thickness determined on the basis of the design rules. This addition thickness shall compensate for thinning during the specified service life of the component. Then the code requires the designers to check the correct behavior of the structure in its original condition and in the condition resulting from total or partial consumption of the corrosion allowances.

The code provides a test to check whether the thermal ageing is negligible. If this test is not passed, thermal ageing effect should be considered for checking the design for Type P damages. The design rules are still the same but with applying additional safety margin. The code provides a thermal ageing factor. For elastic analysis, the time-independent allowable stress, yield strength, and minimum rupture strength are multiplied by this factor; while for elastoplastic analysis, load is divided by this factor. The thermal ageing coefficient is material dependent. The thermal ageing coefficient also depends on the temperature and time. Although the RCC-MRx code provides negligible thermal ageing curve and lists thermal ageing coefficients only for two aluminum alloys and one low activation steel alloy, the code suggests to account for the thermal ageing effect for other materials if the experimental data suggest so.

RCC-MRx code divides the design rules to prevent irradiation damages into two parts depending on the significance of accounting for the effect of creep. A negligible creep test, discussed in

Section 2.2.2.1, decides whether creep effect and corresponding addition analysis and rules can be neglected. Similarly, the code also provides a negligible irradiation test to determine if irradiation damages are significant. If this test is not passed, rules for significant irradiation must be applied. The code provides the negligible and maximum amount of displacement per atoms (dpa) for five austenitic steel alloys as a function of temperature. Two of the alloys have same composition but different procession conditions – one is solution annealed and the other is work hardened. Based on the values provided for all the five austenitic steel alloys, the negligible and maximum allowable dpa depend on the material compositions but not the procession conditions. Since the focus of this report is creep-fatigue damages, we only discuss rules to prevent damages under significant creep – significant irradiation conditions.

Rules for significant creep – significant irradiation provided in RCC-MRx code are only applicable for solution annealed or work-hardened austenitic stainless steel. The code also limits the applicability of these rules with two more conditions – irradiation damage must be less than the maximum allowable dpa and the temperature cannot exceed 625°C. The explanation for these two conditions, as mentioned in the code, is that the accumulation of significant irradiation and significant thermal creep was specifically studied for annealed 316 and 316L grade stainless steel in the temperature range between 450°C and 625°C. As such irradiation material properties are provided for these type of materials. There are three type of austenitic steels for which irradiation properties are provided – (a) X2CrNiMo17-12-2(N) solution annealed or simply 316L(N), (b) X2CrNiMo17-12-2, X2CrNiMo17-12-3, and X2CrNiMo18-14-3 solution annealed which are 316L, and X2CrNiMo17-12-2 with around 20% work hardening i.e. work hardened 316L.

3.3.2.1 Negligible Irradiation Test

In this test, the maximum fluence received throughout the entire life of the component is compared with the value defined for irradiation to be considered negligible, at the maximum operating temperature. If this condition is not met, the code provide another check which uses a fraction rule after breaking the total service time into intervals with approximately constant temperature and constant flux. In this check, the effect of irradiation and the additional corresponding analysis may be neglected if $\sum_i^N \left(\frac{t_i.\varphi_i}{(\Phi_{allowable})_i}\right) \leq 1$. where N is the total number of intervals the total operating period is broken into; φ_i is the irradiation flux during time duration t_i; and $(\Phi_{allowable})_i$ is the maximum allowable fluence at maximum temperature, θ reached during i interval. Although irradiation flux is mentioned here as the unit for irradiation damage, the code actually uses different units to quantify irradiation damages for different materials. For non-alloy and low alloy steels and zirconium alloys the irradiation damage is expressed as irradiation flux in fast neutrons E>1Mev per cm^2 and fast fluence can be deduced by integration over time. On the other hand, irradiation damage is expressed using the displacement per atoms (dpa) calculated by Norgett-Robinson-Torrens method for austenitic stainless steels [94].

3.3.2.2 Rules for Prevention of Type P Damages under significant creep – significant irradiation condition

As discussed in Section 2.2.2.2, Type P damages in RCC-MRx code are those that occur due to primary loads. To guard a structure against these damages under significant creep – significant irradiation condition, the rules for significant creep – negligible irradiation must be checked before

the additional irradiation related rules are applied. In this section, only the additional rules are provided.

In the case of negligible irradiation, the immediate Type P damages are prevented by limiting only the primary stress with time-independent allowable stress, S_m. When irradiation is significant, other stresses are also limited. For Level A criteria, in the case of elastic analysis:

$$\overline{P_m + Q_m} \leq S_{em}^A(\theta_m, G_{tm})$$

$$\overline{P_L + P_b + Q + F} \leq S_{et}^A(\theta, G_{tm})$$

Here, $\overline{P_m + Q_m}$ is the general membrane primary and secondary equivalent stress and $\overline{P_L + P_b + Q + F}$ is the total primary and secondary equivalent stress. The allowable stresses S_{em} and S_{et} are membrane allowable elastic stress and total allowable elastic stress, respectively, for the average temperature θ_m in thickness and for G_{tm} the average value in the thickness of G used to quantify irradiation at the given time. θ_m and G_{tm} are calculated on the length of the supporting line segment. If required, stress due to irradiation swelling must be included. Calculating stress due to irradiation swelling requires a structural analysis taking into consideration the irradiation swelling law and, if necessary, the irradiation creep law that could partially offset these stresses.

S_{em} and S_{et} are functions of irradiation G, temperature θ, Level of criteria X, and elastic-follow-up factor r.

$$S_{em}^X(G, \theta, r) = \frac{1}{k_x}\left[\frac{r}{r+1}R_m(G, \theta) + \frac{E}{100(r+1)}\left(A_{gt}(G, \theta) - \varepsilon_p(S_m^X)\right)\right]$$

$$S_{et}^X(G, \theta, r) = \frac{k_B}{k_x}\left[\frac{r}{r+1}R_m(G, \theta) + \frac{E}{100(r+1)}\left(\left(\frac{A_{gt}(G,\theta)+A_t(G,\theta)}{2}\right) - \varepsilon_p(S_m^X)\right)\right]$$

where k_x is the design margin, k_B is 1 for brittle materials and 1.5 for ductile materials. Figure 3 illustrates how S_{em} and S_{et} are determined from tensile stress strain curves. As illustrated in Figure 3 [95], the maximum point of the tensile curve (R_m, A_{gt}) is used to limit only the general membrane stress. It is to avoid locating the deformation by reduction in area that appears after this maximum and is specific to the uniform membrane load used in the test. This is very conservative because this type of stress is rarely uniform in complex structures. Traditional construction starts from this point and adds margins leading to the membrane's elastic allowable stress S_{em}. For total stress, the traditional elastic-follow-up construction starting from point (R_m, (A_{gt}+A_t)/2) and the addition of margins lead to total elastic allowable stress S_{et} .

For Level C and D criteria, same rules are applied but by replacing $S_{em}^A(\theta_m, G_{tm})$ and $S_{et}^A(\theta, G_{tm})$ by $S_{em}^C(\theta_m, G_{tm})$ and $S_{et}^C(\theta, G_{tm})$, respectively.

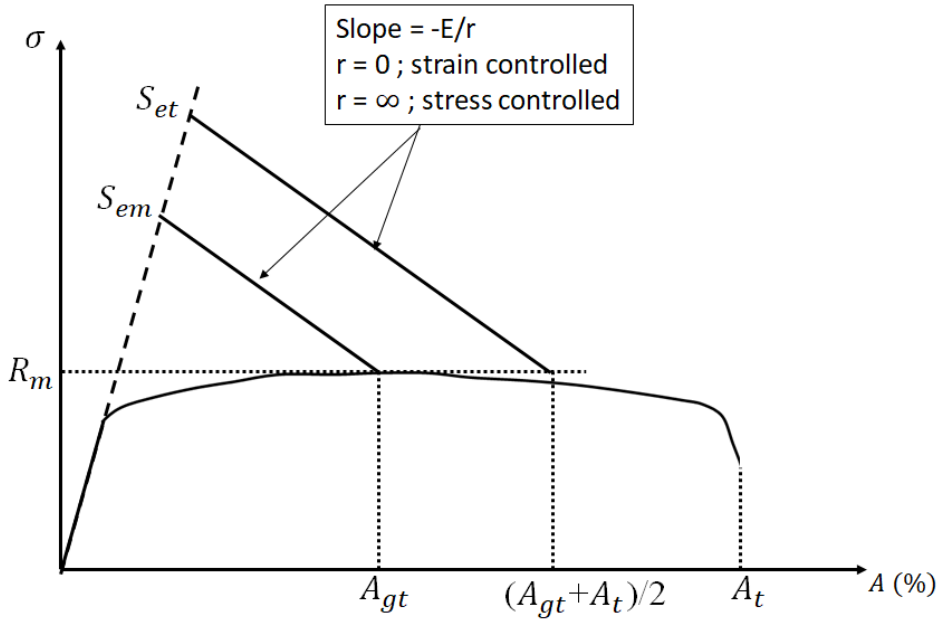

Figure 3 Illustration of determining S_{em} and S_{et}.

The significant creep – negligible irradiation rules to prevent time dependent Type P damages are applicable for significant creep – significant irradiation but with a 0.1, instead of 1.0, limit on creep and creep rupture usage fraction is 0.1 instead of 1.

The code excludes limit analysis when irradiation is significant.

3.3.2.3 Rules for Prevention of Type S Damages under significant creep – significant irradiation condition

To prevent ratcheting under significant creep – significant irradiation condition, rules for significant creep – negligible irradiation are applied. If irradiated material properties are not available, material properties without irradiation can be used justifying conservatism of the approach. Criteria, in Ductility especially, must be assessed and proven to be sufficient for the application.

Similarly, the code uses the same creep-fatigue interaction diagram to check design under significant irradiation conditions. In this case, fatigue damage is determined from design fatigue curves under irradiation condition. However, code allows the use of regular design fatigue curves if fatigue curves under irradiation is not available for the material concerned. To determine creep damage the code allows the use of minimum rupture stress, S_r without irradiation. However, the allowable envelop in the creep-fatigue interaction diagram (without irradiation) must be checked by multiplying the creep rupture usage fraction by 10.

3.3.3 ITER design criteria

The code does not provide any rule for corrosion driven damages. However, it provides a provision for corrosion and erosion which is very similar to the provision provided in RCC-MRx code. It says if the component is subject to in-service thinning resulting from surface corrosion and erosion,

the component should be protected by providing either a certain additional thickness or protective cladding. The structural analysis and design checks should treat the corrosion allowance in the most conservative manner. The analysis must check the behavior of the structure in its original condition as well as in the condition resulting from total or partial loss of the corrosion allowances. In general, the nominal thickness including corrosion allowance shall be used for checking ratcheting and fatigue damage, and the minimum thickness shall be used for checking other damages, particularly the primary membrane stress limit.

The ISDC high temperature design rules are categorized into two parts – rules to prevent M-type damage and rules to prevent C-type damage. M-type damages are those due to primary loadings – 'M' means monotonic – and C-type damages are due to cyclic loadings – 'C' means cyclic. As rules for preventing irradiation driven damages in RCC-MRx code was developed based on ISDC, some of the rules in ISDC are similar to those in RCC-MRx. At the same time, some rules in ISDC are similar to those in ASME. In general, the primary load design rules in ISDC are similar to RCC-MRx but with few changes in design margins, whereas the ratcheting rules for elastic analysis are similar to those in ASME code. Although the ISDC code considers creep-fatigue interaction as one of the factors in time-dependent fatigue damage, design rules for time-dependent fatigue are left out to be added in future.

3.3.3.1 Negligible Creep Test

For a component or a part of a component, thermal creep is negligible over the total operating period if $\sum_i^N \left(\frac{t_i}{T_i}\right) \leq 1$. Here, N is the number of intervals to which the total operating period is broken into, t_i is the duration of interval i, and T_i is the allowable time obtained from negligible creep curve corresponding to the maximum temperature during interval i. If this test is not passed high temperature rules are applied.

High Temperature Rules for Prevention of M-type Damages

These rules are basically analogous the primary load design in ASME code and rules to prevent Type S damages in RCC-MRx code. Rules in the case of elastic analysis are discussed first.

To prevent immediate plastic collapse and plastic instability, Level A criteria to be verified are:

$\overline{P_m} \leq S_m(\theta_m, G_m)$

$\overline{P_L} \leq \min [1.5\ S_m(\theta_m, G_m), S_y(\theta_m, G_m)]$; in local non overlapping areas

$\overline{P_L} \leq 1.1\ S_m(\theta_m)$; in local overlapping areas

$\overline{P_L + P_b} \leq K_{eff}(\theta_m, G_m)\ S_m(\theta_m)$

These rules are similar to those in RCC-MRx code with small changes. Note that, for comparison purposes, all the symbols in ISDC code have been changed here according to the nomenclature used in RCC-MRx code and therefore they may not match with the ISDC code but they represent the same entity.

In both the codes, the general primary membrane stress intensity, $\overline{P_m}$ is limited by allowable stress S_m, however S_m is only function of temperature, θ in RCC-MRx code whereas ISDC code treats

S_m as function of both temperature and fluence, G. S_m in ISDC code is defined as the least of the following in Table 7.

Annealed austenitic stainless steels	**Other materials**
1/3 of S_u at room temperature	1/3 of S_u at room temperature
1/3 of S_u at temperature, θ	1/3 of S_u at temperature, θ
1/3 of S_u at temperature, θ and under irradiation, G	1/3 of S_u at temperature, θ and under irradiation, G
2/3 of S_y at room temperature	2/3 of S_y at room temperature
0.9 times S_y at temperature, θ	2/3 of S_y at temperature, θ
0.9 times S_y at temperature, θ and under irradiation, G if $S_u/S_y \geq 2.0$ or, 2/3 of S_y at temperature, θ and under irradiation, G if $S_u/S_y < 2.0$	2/3 of S_y at temperature, θ and under irradiation, G if $S_u/S_y \geq 2.0$

Table 7 ISDC allowable stresses.

The reason to use temperature and irradiation dependent S_m values is that a material can harden or soften under irradiation. In case of the former S_m is controlled by the unirradiated value, while it is controlled by the irradiated value for the latter case.

Both RCC-MRx and ISDC code apply same limit on local primary membrane stress for overlapping areas. For non-overlapping areas the RCC-MRx code directly use 1.5 S_m, while ISDC code use the minimum of 1.5 S_m and the yield strength. The ISDC code multiplies K_{eff} with S_m for limiting the total primary stress. K_{eff} is effective bending shape factor which account for the increased maximum bending moment carrying capability of an elastic-plastic material with limited ductility as compared to that of an elastic-brittle material. ISDC considers this factor as a function of temperature and irradiation. The value of K_{eff} may be reduced due to the loss of ductility with irradiation. The RCC-MRx code does not use K_{eff}, instead multiplies S_m with a fixed number 1.5.

The Level A criteria to prevent cracking due to immediate plastic flow localization is

$\overline{P_m + Q_m} \leq S_{em}^A(\theta_m, G_{tm})$

and to prevent immediate local fracture due to exhaustion of ductility is

$\overline{P_L + P_b + Q + F} \leq S_{et}^A(\theta, G_{tm})$

These two rules are to account for irradiation effect and are the same as in RCC-MRx code. Definition of S_{em}^A and S_{et}^A are provided in Section 3.3.2.2.

To account for creep effect the following rules are applied for Level A criteria.

$U(\overline{P_m}) \leq 1$

$U(\overline{P_L + \Phi P_b}) \leq 1$

RCC-MRx code multiplies $\overline{P_m}$ with a factor – equal to or higher than 1 depending on the classification of membrane stresses – to determine the creep usage fraction, U due to primary membrane stress, whereas ISDC code does not consider any additional margin. Φ in the second

equation is the creep bending shape factor. In RCC-MRx code it depends only on geometry while it is also function of temperature and irradiation in ISDC code.

The ISDC code also allows the use of elasto-visco-plastic analysis. To check for different failure modes separate analyses are performed to determine the maximum loadings that can be applied to the structure without failure. Then the code applies safety margins on the loadings determined from analysis to determine design loadings. The code provides different safety margins for different type of failure mode and Level criteria as well as for different type of loadings – mechanical and thermal. Followings are the conditions to be satisfied to determine the maximum loading for different failure modes.

For time-dependent plastic collapse, the elasto-visco-plastic collapse load is the least of the loads at which the inelastic (plastic plus creep) part of the significant mean membrane (the greatest positive principal strain of the membrane strain tensor) strain should be equal to the elastic part.

The inelastic part of the significant membrane plus bending strain should be equal to the elastic part.

In case of avoiding time-dependent exhaustion of membrane ductility the condition is

$$\sum_{i=1}^{n_{blocks}} \frac{significant\ mean\ plastic\ strain\ increment}{minimum\ uniform\ elongation} + \sum_{i=1}^{n_{blocks}} \frac{significant\ mean\ creep\ strain\ increment}{minimum\ creep\ ductility}$$

and the condition to avoid local creep cracking is that the accumulated creep usage factor should be less than 1.

Note that, strain linearization on the supporting line segment is required to determine significant mean strains. The method of strain linearization is similar to that of stress linearization. In strain linearization each strain tensor is divided into three parts – mean, bending, and non-linear strain tensors. Then significant mean strain is determined by taking the greatest positive principal of strain of the mean strain tensor. The significant mean plus membrane is determined from the sum of mean and bending strain tensors while significant local strain is determined from the sum of all three strain tensors. Of course the total mechanical strain tensor is first separated into elastic and inelastic portion before strain linearization is performed on each of the elastic and inelastic strain tensors.

Rules for Level C and D criteria are the same as those for Level A criteria but with a lower safety margin.

3.3.3.2 High Temperature Rules for Prevention of C-type Damages

C-type damages in the ISDC code are ratcheting and time-dependent fatigue. The code acknowledges creep-fatigue interaction within time-dependent fatigue damage, however no rules

are yet provided to estimate fatigue life of structures when creep effects are relevant. Only rules to avoid ratcheting are provided.

For elastic analysis, the code provides four different tests – A-1 (IRB 3541.1), A-2 (IRB 3541.2), A-3 (IRB 3541.3), and B-1 (IRB 3541.4) to guard against ratcheting. Any of these test can be used. These tests are exactly the same as tests A-1 (HBB-T-1322), A-2 (HBB-T-1323), A-3 (HBB-T-1322), B-1 (HBB-T-1332), respectively, in Section III Division 5 of ASME code. Test B-1 is the most popular one. This method uses the Bree diagram to account for plasticity and the O'Donnell Porowski approach to account for creep. First, maximum primary stress intensity and maximum secondary intensity range are determined from elastic analysis under primary and secondary loading, respectively. These values are then used to determine the creep stress parameter, Z from the Bree diagram which is multiplied with yield strength at low temperature extreme of the cycle to determine the effective creep stress, σ_c. Once effective creep stress is determined for individual loading blocks, creep strain increments for each block is then determined from isochronous stress strain curve for $1.25\sigma_c$. The code limits the accumulated creep strain to 1%.

If elasto-visco-plastic analysis is used, the following two limits must be satisfied at all times.

$$\sum_{\substack{i=1 \\ blocks}}^{N} \frac{significant\ mean\ plastic\ strain\ increment}{minimum\ uniform\ elongation} + \sum_{\substack{i=1 \\ blocks}}^{N} \frac{significant\ mean\ creep\ strain\ increment}{minimum\ creep\ ductility} \leq 0.5\lambda_1$$

and

$$\sum_{\substack{i=1 \\ blocks}}^{N} \frac{significant\ local\ plastic\ strain\ increment}{\frac{minimum\ true\ strain\ at\ rupture}{triaxiality\ factor}} + \sum_{\substack{i=1 \\ blocks}}^{N} \frac{significant\ local\ creep\ strain\ increment}{\frac{minimum\ true\ strain\ at\ creep\ rupture}{triaxiality\ factor}} \leq \lambda_2$$

where λ_1 and λ_2 are safety factors which depend on level criteria.

3.3.4 R5

Environmental effects causing wall thinning (e.g. corrosion and erosion) or changes in material properties (e.g. irradiation, embrittlement, etc.) are not explicitly considered in R5. However there is an explicit interest in including the interaction between environmental effects and creep fatigue failure modes, the last sentence in R5 Volume 1 Paragraph 3 states: "The interaction of the corrosion of components and the other modes of failure considered by R5, may be a relevant consideration in future issues of R5". R5 is an assessment procedure for fitness-for-service evaluation. It requires and allows using actual, measured material properties from the actual

component in the degraded condition. Therefore, some effect of corrosion can be included by using degraded, measured properties.

3.3.5 API-579/ASME FFS-1

FFS-1 does not directly incorporate environmental effects for creep or fatigue or creep-fatigue. For component subject to creep regime, FFS-1 suggests using the component geometry determined by inspection. Furthermore the metal loss for future operations can be predicted by utilizing historic corrosion data for the component of interest (or data from a component subject to similar conditions) or by using material specific corrosion design curves. This means that if corrosion or erosion are of concern one should perform the stress analysis using the future reduced wall thickness.

3.4 Recommendations

3.4.1 Development of an engineering assessment method for creep-fatigue initiation in harsh environments

Of the design and fitness-for-service methods surveyed here only one, RCC-MRx, provides any assessment rules at all for creep-fatigue damage in concert with detrimental environmental conditions. Ultimately, fully developing an assessment methodology of this type will require system-specific experimental data, for example assessing the effect of long-term exposure to the particular plant coolant chemistry or the particular radiation dose experienced by a component. However, even provided with such a dataset there is currently no guidance on how to translate that data into acceptance criteria.

A general approach for evaluating creep-fatigue for components subject to neutron irradiation and/or corrosive coolants will need to be developed in order to assess particular designs. U.S.-based advanced reactors will likely be design to the Section III, Division 5 criteria and so the most straightforward path towards assessing environmental creep-fatigue would be to determine how to alter the design data used in these procedures to account for environmental effects while keeping the overall design method to same.

Turning then to the ASME creep-fatigue assessment procedures, environmental effects might alter the material's rupture life, its fatigue life, and/or the creep-fatigue interaction. A general method could be developed for specifying what experimental data is required to determine these modified design criteria or different combinations of radiation dose and coolant exposure. The final approach would be similar to the method adopted in RCC-MRx.

There may even be sufficient literature data to develop preliminary design data for the Class A materials accounting for irradiation damage over the range of doses expected in advanced reactors. A literature survey would need to be completed and the data collated and interpreted. One gap is likely to be creep-fatigue testing to determine the interaction diagram. Another gap will likely be long-term creep testing on irradiated material. Both could be addressed by introducing adequately conservative design factors. Again, this appears to be the RCC-MRx approach, as the factor of 10 applied to the creep damage in non-negligible radiation environments is likely a conservative approximation, rather than based on specific data.

The outcome of such a development effort could be the general assessment approach, potentially specific design factors accounting for irradiation damage, and guidance on what sort of testing would be required to establish complete design data for particular combinations of coolant exposure and radiation dose. Clearly defining an approach would give regulators and vendors a common framework from which to assess the effects of environment on creep-fatigue.

Such an assessment methodology would likely only cover relatively short-term effects because long-term testing under the expected reactor operating conditions would likely not be completed before the plant goes into service. Alternative means could be used to ensure component integrity during long-term plant operation.

3.4.2 In-situ surveillance programs for creep and creep-fatigue damage

It seems unlikely that whatever method used by vendors to justify their design against creep-fatigue in adverse environments will be directly validated by experimental data out to the plant design life. There are too many potential combinations of environmental conditions to generate a comprehensive database for all possible advanced reactor designs. Furthermore, the actual environmental conditions in an operating reactor will not be precisely known in advance and could vary during plant operations.

Accelerated testing in representative environmental conditions could be used to generate design correlations using empirical or physically-based extrapolation methods. However, an alternative means would be required to validate the extrapolation techniques for actual service conditions.

An in-situ surveillance program for creep-fatigue properties could be used to ensure the structural integrity of components accounting for the actual, in-service plant conditions. The core of a such a program would be to insert surveillance specimens at critical locations inside the reactor so that they experience the actual plant environmental conditions – temperature history, exposure to coolant, irradiation, etc.

A surveillance program for creep-fatigue (or creep) damage would also need to ensure that the monitoring specimens experience a cyclic mechanical load representative of the corresponding component. For an operating reactor the loading mechanism would likely need to be passive, not requiring any control or loading mechanisms penetrating the primary coolant boundary. Passive loading would also simplify the program of placing specimens at critical locations, as the design would not need to be complicated by providing ports for controlling the load on the specimens. One possibility for such passively loaded specimens would be a bimaterial specimen that uses differential thermal expansion to provide the mechanical load. Reference [96] provides preliminary analysis demonstrating the viability of the concept. However, more work would be required to translate the concept into a complete method for sizing specimens to replicated a set mechanical load, given some temperature history. For example, the specimens would also need to be small in order to minimize the disruption to the flow of coolant and to ease handling requirements when the specimens are removed from the reactor. The specimens would need to be designed to fail in the expected, gauge region, rather than, for example, at the bimaterial joint.

However, given the availability of suitable passive surveillance specimens, how could they be used to guard against environmental degradation and premature creep-fatigue failure? At a minimum, the methodology would require knowing the coolant temperature as a function of time at the specimen location. This information should be available as the plant temperatures are key information in the reactor control system. Volumetric heating effects, like gamma heating, might cause discrepancies between the specimen and coolant temperatures. Monitoring specimens are likely to be relatively small which should minimize these effects and help ensure the specimen stays in thermal equilibrium with the monitored coolant stream. However, if necessary, these effects could be accounted using models to correct the coolant temperature. Given only the temperature history, a model of the test specimen could be used to extract the mechanical loading on the gauge region.

The simplest model for a program only provides the opportunity to view the specimens during plant outages. The only information that could be extracted is whether the specimen gauge failed in the period between the last and current outages, gauge markings could be used to measure the residual strain accumulated in the gauge, and melt wires used to validate the temperature readings extracted from the plant control system

In this simplest model two methods could be used to monitor creep-fatigue damage in the plant components. The first would be to design the specimens as canaries for certain critical components. Critical locations would need to be identified, likely based on the design creep-fatigue assessment, possibly accounting for short-term environmental degradation using the method outlined above. Then, using whatever design criteria the vendor uses to design the component itself, the surveillance specimen would be sized so that it would be expected to fail before the corresponding critical location in the actual component. The easiest method would be if the specimen could be placed adjacent to the critical location in the operating plant. By definition then the surveillance component would experience the same environmental conditions and temperature history. The specimen could then be sized to experience *greater* mechanical loading than the actual component, so that the specimen will fail first. In essence, the surveillance specimen serves as a "canary" for the critical component location. The increased loading would need to be calibrated so that, at a minimum, the specimen would fail one full outage cycle before the component.

The basic surveillance program would consist of viewing the specimens at each outage and determining whether the gauge section has failed. If the specimen fails prematurely then there was some non-conservative assumption made in the design of the corresponding component and the plant operations would need to be altered. A more advanced program could be designed with multiple surveillance specimens for each critical location, each designed to fail at different times. For example, specimens could be designed to fail 20 years before the component, 10 years before, 5 years before, etc. The failure (or not) of these specimens could be used to provide additional prior warning on upcoming environmentally-assisted creep-fatigue failure. That is, if the 20 year specimen actually fails 21 years before the component design life that does not imply that plant operations must be immediately altered. Instead, the plant operator would have time to determine an appropriate modification strategy. On the other hand, if a 1 year specimen fails 10 years before the component design life then immediate changes to the plant would be required.

The alternative approach assumes that some out-of-reactor test could be used to ascertain the remaining life of a particular surveillance specimen. To our knowledge, no such method exists for creep-fatigue failure, but the MPC Omega method is an equivalent methodology for pure creep rupture failure [28]. Taking the Omega method as an example, specimens would be sited near critical locations in the reactor and sized to experience the *same* mechanical load. These would be removed and tested to determine the current creep rate, which in turn can be turned into a remaining life to creep rupture with the MPC Omega method. Notionally then this remaining life includes the effect of the actual environmental conditions. Conventionally, this testing is destructive (conventional rupture testing) and so in actuality multiple specimens would be required for a single critical component. Another approach might be to measure the creep rate nondestructively and then return that same specimen to the reactor, but the ability to accurately measure creep rates with microindentation or some other nondestructive method would need to be developed.

For both surveillance modes – canaries and life prediction – methods will need to be developed for configuring passive surveillance specimens to match a set of target thermomechanical loading. Specimens will need to be designed so that this loading remains stable – creep and high temperature cyclic plasticity will tend to alter the loading hysteresis over time. In general, it will be easier to achieve the bounding loadings required for a canary program, as opposed to the matching loadings required for the life prediction problem. However, even in the life prediction mode bounding loadings that produce shorter cyclic lives than the corresponding component are acceptable. When using a bounding load, the predicted lives will simply be shorter than the actual component life, which is an acceptable, conservative approximation.

Assuming the availability of advanced, wireless sensing equipment further simplifies the development of a creep-fatigue surveillance program. Some sensing capability that could determine whether the gauge of a test specimen has failed would eliminate the need to physically view the specimen during outages. This would reduce the component design issues associated with inserting creep-fatigue specimens into the plant and could reduce the required lead time in the canary approach. The ability to monitor the strain of the specimen in real time opens up many more possibilities, at the very least eliminating the need to do ex-situ testing to determine the remaining life in the Omega approach. However, the required remote sensing technology is still in the basic research stage and reactor vendors would then need to demonstrate the reliability of the sensors themselves, which might require a separate testing program. In the near-term remote sensing is likely to be used as a complement to more traditional physical property monitoring, rather than as a replacement.

Overall then, we strongly recommend starting to develop the technical basis for a creep-fatigue surveillance program now, so that reactor designers can design components that can accommodate in situ test specimens. Work is needed on developing families of passive test specimens, formulating acceptance criteria following either or both of the general approaches described in this subsection, and on developing sensing and non-destructive testing capabilities to ease the burden of physical monitoring during outages and/or ex-situ testing of irradiated samples.

3.4.3 Engineering assessment methods for high temperature cladded components

One potential strategy for managing environmental effects could be to use cladded reactor components. In this concept the base component will be fabricated from some existing, nuclear-qualified structural material. Some relatively thin clad material will be joined to this base component facing the reactor coolant. The clad material will not carry structural load, but rather is there to protect the base component from environmental damage caused by the coolant chemistry.

Clads are widely used in the petrochemical industry. However, design rules are limited and to our knowledge no rules exist for evaluating the integrity of a clad/base system under high temperature cyclic load. If the clad is a safety-critical part of the overall reactor system then regulators will need methods for evaluating the mechanical reliability of the cladded component.

The current Section III, Division 5 rules do provide some design guidance for cladded Class A components. Subpart HBB-2121(c) allows the use of non-Code qualified clad materials if the clad thickness is less than 10% of the base (Code-qualified) material thickness. The stress classification tables specify that differential thermal expansion should be classified as a peak stress. Subpart HBB-3227.8 states that designers should not count the clad in the primary load or buckling design, but mandates that they consider the clad for ratcheting and creep-fatigue loading. However, the current Code does not provide methods for evaluating creep-fatigue damage in a cladded component.

The authors and others have begun to formulate design rules for high temperature nuclear cladded components [97], however work remains to be done to formulate a complete set of design and evaluation rules. The current DOE-sponsored effort, which is not currently active, focused on design simplifications that can be made for clad materials that are either much more compliant than the base metal (e.g. pure nickel on stainless steel) or much stiffer than the base metal (e.g. tungsten on stainless steel), but reactor designers may use combinations of materials that do not fall into either of these categories. There is also the issue of interface integrity under high temperature, cyclic load. The strength of the bimaterial interface will depend on the particular manufacturing technology used in assembling the system (weld clad overlay, coextrusion, cold spray, etc.) and so developing a universal assessment method will be difficult. One option is to develop a standardized test that would ensure sufficient clad/base joint integrity at high temperatures, for cyclic load so that either the base material or the bulk of the clad material would fail before the interface. Conventional design rules could then be used to assess the structure assuming a perfect material interface. However, no such testing method currently exists.

3.4.4 A method for establishing corrosion allowances

An alternative to a detailed design assessment could be to establish adequate corrosion allowances for the relevant degradation mechanisms. This approach is commonly used for general corrosion in the petrochemical industry – section thicknesses are increased by the amount expected to be lost in-service. A similar approach could be taken for local mechanisms as well. For example, for chromium loss in molten salt systems the depth of grain boundary attack could be measured or predicted and wall thicknesses increased. For local mechanisms like this a general corrosion allowance is very conservative – the material properties are degraded but do not fall to zero – but it may be a viable strategy for some vendors.

There are two potential problems with this approach. The first is how to predict depth-of-attack for long service lives. Empirical extrapolation methods calibrated to short term tests may need to be developed. However, corrosion in some potential future reactor systems is highly dependent on the coolant chemistry and so standard crucible tests in sealed environments may not be

sufficient. Furthermore, some reactor concepts rely on controlling the coolant chemistry and so a vendor would want to account for this in their test data. An alternative approach could be to develop mechanistic corrosion models that can accurately predict corrosion rates for long service times. If a vendor relies on such a model, regulators will need some method of assessing the model for suitability and accuracy.

4 Creep cracking near welds

4.1 Mechanisms

This subsection focuses on Type IV cracking in weldments in ferritic and ferritic-martensitic steels. This mechanism has been identified as a particular concern for future high temperature reactors. The discussion below on design, fitness-for-service, and recommendations covers crack growth in high temperature reactors in general.

A major concern for low alloy ferritic steels is Type IV cracking. Type IV cracking is a long-term failure mechanism of weldments associated to the presence of a heat affected zone (HAZ). The HAZ is the region of material influenced by the heat flux and temperature gradient caused by the welding process. In HAZ the microstructure of the base metal evolves during the welding process generating a non-homogenous distribution of grain sizes and metal phases. The microstructure of HAZ becomes more complex as more weld passes are performed, which is typically required for thick components.

The HAZ of a multi-pass weld can be divided into different regions [98] that can be classified as follows while moving from the solidified weld to the unaffected base metal:

1. coarse-grain HAZ (CGHAZ)
2. fine grain HAZ (FGHAZ)
3. intercritically reheated coarse grain HAZ (ICCGHAZ)
4. subcritically reheated HAZ (SCCGHAZ)

A CGHAZ and FGHAZ are generated for each weld pass. In CGHAZ there is a rapid growth of prior austenite grains due to the high temperature, while in the FGHAZ the grain growth of prior austenite grains is slower. At each subsequent weld pass the already present CGHAZ is reheated and new microstructures are generated depending on the temperature peak [99]. Where the temperature peak is between A_{C1}, the temperature at which austenite starts to form, and A_{C3}, the temperature at which austenite transformation is completed, an ICCGHAZ forms, while further away from the fusion line, where the temperature peak is still high but below A_{C1} the formation of a SCCGHAZ is observed.

The different temperature peaks also affect the phase of the material in the HAZ. In the CGHAZ, if the cooling rate is slow pearlite and or upper bainite forms, instead if the cooling rate is high martensite and lower bainite are generated. The first two phases are undesirable because of their low toughness. The second group of phases are acceptable even though they are brittle after cooling because they have a high toughness after tempering. The FGHAZ exhibit a fine grain prior austenite grin structure. The ICCGHAZ is characterized by a mixture of ferrite and austenite precipitates along prior austenite grain boundaries. The SCCGHAZ instead, has a microstructure very similar to the base metal because the temperature peak is below the transformation phase.

Type IV cracking is creep driven failure mechanism occurring in the outer layer of the HAZ, either in ICCGHAZ or in the FGHAZ [100]. In this region the material is more susceptible to creep damage because of the fine grain structure. Defect pile up at grain boundaries causes void

generation or particle decohesion, weakening the material. When a crack initiates then its propagation rate is high because of the weakened material.

There have been a few studies investigating the behavior of Type IV cracks. An example is the study by Shibli and Hamata [101] that reported results from the European SOTA and HIDA programs. For the SOTA program, machine welded CT specimens have been used and the crack tip was purposely placed in the CGHAZ and FGHAZ. The test temperature was $600\ °C$. Results of the SOTA program were compared against base metal creep-fatigue scatter band curves. Both kind of analyzed cracks showed a higher crack growth rate and scatter compared to the base metal. The higher scatter was observed for low C^* values where microstructural features dominates the propagation rate. For higher C^* values the scatter reduces to a similar range than the one observed in the base metal. The growth rate in HAZ was observed for all ranges of C^* and can be conservatively estimated using a factor of about 10 on the upper scatter band of the base material. Results of FGHAZ showed a larger scatter than the one obtained for the CGHAZ but always on the conservative side (e.g. lower crack growth rate for the same C^* value). It was also observed that cracks initiated in the CGHAZ would end up propagating in FGHAZ. In the HIDA program the temperature was higher, $625°C$, and specimens with different geometry were used. Crack growth rate in the HAZ were about factor of 10 higher than in the base metal. Note that welds were all heat-threated at $760°C$ for 2 hours. Results of both testing programs agree and show that creep-crack growth rate can be predicted using base metal material properties and a scale factor, at least for ferritic steels.

The crack incubation time is the other factor that must be considered. Due to the inherent microstructure variability the scattering of HAZ the crack incubation time might be very large. To diminish the scatter and improve the crack incubation time all the steps of the welding process must be accurately controlled. The first variable in the welding process is the chemistry of the filler material. For steels such as T91, P91 and P92, it is generally recommended to use a filler material of matching composition and use a submerged arc welding process to avoid diffusion of unwanted species in the weld.

The critical properties of a weld for high temperature applications are the fracture toughness and the creep resistance. These properties can be altered by changing the chemistry of the filler. However, increase in fatigue performance generally degrades creep performance and vice versa. Therefore, the optimal filler composition depends on the application. In a recent study [102], the effect of different species on fracture toughness and creep rupture showed that the fracture toughness decreases proportionally with the boron and oxygen content and that an optimum content of nitrogen exists (440 ppm). However, boron helps improving creep rupture. Therefore, the composition of the filler material should be optimized to achieve, if possible, the desired material properties.

Another critical aspect of the welding process is welding thermal cycle. It is widely accepted that preheating of the base metal is fundamental step to obtain the appropriate cooling rate after welding. For performing a SAW on a ferritic steel such as P91, P92 and T91, a preheat temperature between $\approx 200 - 250°C$ is usually adopted. After the welding process is complete, a 2-3 hours post-weld soaking should be allowed to prevent hydrogen induced cold cracking [103] followed

by a slow cooling up to $80°C$ for thick walled component. This temperature should be held for some time before performing tempering.

Tempering should be performed below the A_{C1} temperature to prevent the formation of martensite thus resulting in untempered material. Care should be taken when selecting the tempering temperature because the A_{C1} of the weld metal is likely to be lower than that of the base material and varies with the Ni+Mo wt% content [104] ($820 - 750°C$ for P91 and P92 like materials). Furthermore, the minimum allowed tempering temperature according to ASME is $735°C$. Therefore, the temperature window for performing tempering on thick component in a reasonable time might be very small. The suggested tempering time is usually between 2 to 4 hours [103].

4.2 Survey of current design practices: preventing cracking

4.2.1 ASME

The goal of the Section III, Division 5 design rules is to prevent the initiation of a creep or creep-fatigue crack. The Code does this through the primary load creep rupture and secondary creep-fatigue design procedures described above in concert with the construction practices specified in Division 5 and the in-service inspection criteria detailed in Section XI. Fundamentally then, this is a defense-in-depth approach: the design rules limit the stresses imposed on weldments, aiming to prevent the initiation of a crack, the construction rules mandate high-quality, well-inspected welds post-processed with appropriate heat treatments, and the Section XI inspection rules ensure that if a crack or defect does nucleate during service it will be located in time to take preventative action.

Focusing on the HBB design rules, the Code makes special modifications to the general base metal design rules to account for the metallurgical discontinuity caused by the weld. The Code limits designers to a small number of combinations of weld process and weld material that have good demonstrated high temperature performance (HBB-I-14.1(b)). For creep strength, both in primary load design and in creep-fatigue evaluation, the Code accounts for the reduced creep strength of some of these allowable weld combinations using a temperature- and time-dependent stress rupture factor R (HBB-I-14.10). These factors are determined experimentally using cross-weldment rupture tests. The rupture factor is the ratio of the rupture strength of a weldment to the rupture strength of base metal at the indicated combination of temperature and rupture life. This factor is applied to the base metal rupture stress used in the creep-damage calculation for creep-fatigue evaluation and the reduced rupture stress supplements the allowable stress S_t for primary load design. For the fatigue damage calculation, a weldment is only allowed half of the design cycles to failure as for the equivalent base material. The creep-fatigue diagram remains the same as the base material.

The general approach for creep-fatigue design of weldments then follows the base material approach of applying factors to the creep and fatigue damage and then using a creep-fatigue interaction diagram representing nominal material properties. The weld factor for creep rupture is determined experimentally using cross-weld rupture tests. The allowable number of fatigue cycles for welds specified in the code is almost certainly conservative, given the large factors already applied to base material experimental data to make the design fatigue curves and the further, additional reduction for weldments.

The Section III, Division 5 design criteria do not provide a procedure for evaluating fracture under high residual stresses, either for base or weld material. The rational is that high temperature cyclic service will rapidly reduce any initial residual stresses caused by manufacturing processes, the Code requires post-weld heat treatments to reduce residual stress and increase weld ductility, where appropriate, the Code limits the allowable weld processes and materials to those with adequate high temperature ductility, and that brittle material failure is unlikely at high temperatures where the Class A materials all have substantial ductility.

However, HBB-3241 does note that residual-stress induced cracking is a possibility during shutdown conditions after some period of high temperature service. The very creep deformation that the Code relies on to eliminate residual stresses during high temperature operation will cause residual stresses when the component temperature drops below the creep range. The Code Design procedures will provide an estimate of the residual stress distribution during these periods of operation and Section III procedures for preventing nonductile crack growth could be applied given this information.

This leaves the possibility of non-ductile failure near welds during the initial plant startup or during the first few operating cycles, before creep and cyclic plasticity eliminate any initial weld residual stress fields. The Code currently does not provide design rules guarding against this possibility.

The Code does not contain guidance on the interaction of corrosive environments or irradiation damage on the performance of welds.

4.2.2 RCC-MRx

The RCC-MRx general design rules for welds are covered in RB 3290. These design rules are basically the base metal rules with modification made to account for the metallurgical discontinuities in welds. These design rules are applied only after satisfying all the rules regarding welding operations and their implementation. These rules are provided in Tome 4 and include checking the suitability of materials for welding, acceptance testing of filler materials, welding procedures, examination of welds, etc. These rules are provided to make sure a high quality weld is produced.

The general design rules for weld are discussed here in reference to the base metal rules discussed in above. The code allows performing elastic analysis with base material properties, but then limits the structural response with allowable stresses specific to the weld. These allowable stresses are

deduced from base metal allowable stresses by multiplying with a weld joint coefficient, n and another coefficient to add extra margin on the design which is depending on the allowables:

$S_{m,weld} = n\, J_m S_{m,base\ metal}$

$S_{t,weld} = n\, J_t S_{t,base\ metal}$

$S_{r,weld} = n\, J_r S_{r,base\ metal}$

where J_m is the weld properties coefficient, J_t is the coefficient of weld creep properties, and J_r is the coefficient of weld rupture properties. These coefficients are temperature dependent and always less than or equal to 1. J_m values are determined by dividing the mean tensile strength measured on the welded joint by the base metal mean experimental tensile strength. J_t and J_r are determined by performing time- and temperature-dependent rupture tests of the welded joint and then taking the ratio between respective strength of the welded joint to that of base metal. The weld joint coefficient, n depends on the type of joint and the extend of examinations made on the weld.

For ratcheting calculation, the code uses the base metal approach but using the allowable stress of the weld and reducing the limits on the ratcheting strain by a factor of 2. For creep-fatigue damage calculation, the code uses the base metal creep-fatigue interaction diagram. However, the creep damage is calculated by replacing the base metal S_r by weld S_r. The fatigue damage is calculated using the design fatigue curves provided for the weld and for a strain range that is determined by stress range found from elastic analysis divided by a fatigue strength reduction factor, f. This factor depends on the type of joint and the extend of checks made on the weld. It is intended to take account of local strain concentrations in the welded joint or at its surface. The weld design fatigue curves are determined by applying a factor of 2 on the strain range and 20 on the number of cycles.

Limit analysis for primary load design under significant creep condition is carried out with a creep usage fraction calculated by using S_r for weld, if an elastoplastic analysis is used.

The code does not allow inelastic analysis for creep-fatigue design unless the fatigue strength reduction factor, *f* and joint efficiency, *n* are equal to 1. If they are equal to 1, inelastic analysis can be used without considering the weld.

The RCC-MRx code does not provide any rules to address the effect of irradiation on the performance of weld.

The provision, mentioned above, to account for in-service thinning of the base metal due to corrosion, erosion, and wear is also applicable for weld.

4.2.3 ITER design criteria

The ISDC code provides design rules for irradiation damage only when creep is negligible. It does not contain high temperature design rules while considering the effect of irradiation on welds.

4.2.4 R5

The base metal procedure can be used for assessing weldments. The only modification required is to penalize the equivalent strain rage $\Delta\bar{\varepsilon}_t$ by using the fatigue strength reduction factor (FSFR). For dressed weldments the $\Delta\bar{\varepsilon}_{t,weld} = \Delta\bar{\varepsilon}_t FSFR$. For undressed weldments an even more

conservative approach is used by also adding the equivalent creep strain range $\Delta\bar{\varepsilon}_{t,weld} = \Delta\bar{\varepsilon}_t FSFR + \Delta\bar{\varepsilon}_c$. Typical values of $FSFR$ ranges from 1.5 to 4.0 depending on the weld and load type.

4.2.5 API-579/ASME FFS-1

4.2.5.1 Creep damage

For a Level 1 or Level 2 assessment if the component of interest contains a weld then $14°C$ $(25°F)$ should be added to the maximum operating temperature.

For a Level 3 assessment the procedures for computing creep-rupture can be used with the following modifications:

- Procedure 1 accounts for welds by setting the value of the creep adjustment factor used in the omega model $\Delta_{\Omega}^{\mathrm{sr}} = -0.5$.
- Procedure 2 accounts for welds by reducing the allowable accumulated inelastic strain by a factor of 2:
    - 2.5% anywhere in the structure
    - 1.25% when considering only primary bending and membrane stress
    - 0.5% when considering only primary membrane stress

  Furthermore, special consideration is given near welds for materials exhibiting a minimum yield strength greater or equal to 345 MPa (50 ksi). In this case the allowable creep damage D_c must be smaller than 0.5 for any location within 25mm form the weld's bevel.

  This supplemental check for weldments and adjacent base material is recommended for high strength materials because compliance with the total accumulated strain criterion is not sufficient to preclude failure from creep damage.

4.2.5.2 Fatigue damage

API-579/FFS-1 provides fatigue curves specifically for various types of weldments.

4.2.5.3 Creep-fatigue interaction

The modifications described above to the creep damage and fatigue damage provisions apply when computing creep-fatigue interaction in a weld.

4.2.5.4 Creep-fatigue in dissimilar metal welds

FFS-1 provides a special method for evaluating creep-fatigue in dissimilar metal welds.

Laboratory experiments and on-the-field measurements show that creep rupture is the dominant failure mode in dissimilar metal welds (DMW). Such data also shows that fatigue loading enhances creep damage even for low stresses. Therefore, creep-fatigue interaction must be properly accounted for in DMW procedure. The procedure outlined below address creep-fatigue interaction

by including an appropriate model accounting for thermal mismatch, sustained primary stresses, and cyclic secondary loads

Creep damage localizes in the heat affected zone on the ferritic side of the weldment. Failure can occur by one of two modes:

I. Inter-granular cracking: it is usually observed at prior austenite grain boundaries in region confined between one or two grains from the weld's interface. This failure mode is commonly observed in DMWs with nickel or steel-based filler metal. Inter-granular cracking generally initiate at surface. Failure occurs because of crack bridging.
II. Interfacial voiding: it usually occurs at the interface between parent and welded metal due to the presence of multitude of carbides from which decohesion starts. Failure occurs due to crack bridging. This failure mode is only observed in DMW in which a nickel filler material has been used.

For failure Mode I the assessment procedure considers the total creep damage to be the sum of three different contributing mechanisms: the damage due to the differential thermal expansion between the weld and the parent material, the damage generated by the presence of primary loads and the damage associated to secondary load. The above three creep-fatigue damage contributions summed together are the total creep-fatigue damage that as usual is given in term of life fraction (e.g. the creep-fatigue damage limit is 1). The procedure steps are outlined below:

- Divide the load histogram into steady into the M different types of loading and define N as the total number of observed dwell.
- Compute the intrinsic creep damage as function of the difference in thermal expansion coefficients between the base and the filler material:

$$D_{Ic}^{I} = \sum_{j=1}^{M} k_1 n_j \left(\varepsilon_j^T\right)^{\gamma} + \sum_{i=1}^{N} k_2 t_i (\sigma_i^T)^{\beta} \; 10^{f(T_i)}$$

  where $\varepsilon_j^T = \Delta\alpha_j \Delta T_j$, $\sigma_i^T = \frac{E_i \Delta\alpha_i (T_i - 70)}{2}$, $k_1, k_2, \gamma\, \beta$ and $f(T_i)$ are constants defined in FFS-1 Table 10.4 (which is not reported in this document) and E_i is mean value of Young's modulus for the i^{th} dwell.
- Determine the creep fatigue damage caused by primary and secondary loads, D_{Pc}^{I} and D_{Sc}^{I}, respectively:

$$D_{Pc}^{I} = \sum_{i=1}^{N} k_3 n_j (\sigma_i^P)^{\gamma}$$

$$D_{Sc}^{I} = \sum_{j=1}^{M} k_4 n_j \left(\varepsilon_j^S\right)^{\gamma} + \sum_{i=1}^{N} k_5 t_i \left(\sigma_i^S\right)^{\beta} \; 10^{f(T_i)}$$

  where k_4, k_5 are constants defined in FFS-1 Table 10.4, $\varepsilon_j^S = \frac{\sigma_i^S}{E_i}$ and represents the strain due to secondary loads and σ_i^S is the secondary stress.
- Determine the total creep damage for Mode I as the sum of all the compute contribution

$$D_c^I = D_{Ic}^I + D_{Pc}^I + D_{Sc}^I$$

- If the creep total creep damage for Mode I $D_c^I \leq 1$ then the component is suitable for continued operations

For failure Mode II the assessment procedure considers the total creep damage to be the sum of two different contributing mechanisms: the creep-fatigue damage created by primary loads and the creep-fatigue damage created by secondary load. The above two creep-fatigue damage contributions summed together are the total creep-fatigue damage that as usual is given in term of life fraction (e.g. the creep-fatigue damage limit is 1). The procedure is the following:

- Divide the load histogram into steady into the M different types of loading and define N as the total number of observed dwell.
- Compute the creep damage caused by primary load as a function of all dwell and half cycles:

$$D_{Pc}^{II} = \sum_{i=1}^{N} k_3 t_i \left(\frac{\sigma_i^P}{1 - k_6 10^{g(T_i)} (TW_i + 0.5t_i)^{\frac{1}{3}}} \right)^{\beta} 10^{f(T_i)}$$

  where k_3, k_6 and constants in Table 10.5 (not reported here for brevity) and

$$TW_i = \begin{cases} \bar{t}_i & for\ t_i \le MT_i \\ 2MT_i - \bar{t}_i & for\ MT_i < t_i \le 2MT_i \\ 0 & for\ t_i > 2MT_i \end{cases}$$

  where $\bar{t}_i = \sum_{k=1}^{i-1} t_k 10^b$, $MT_i = 10^c$, $b = 25665 \left[\frac{1}{(T_i+460)} - \frac{1}{(T_k+460)} \right]$ and $c = \left[\frac{38500}{(T_i+460)} - 20 \right]$.
- Compute the damage caused by secondary loads as:

$$D_{Sc}^{II} = \sum_{j=1}^{M} k_4 n_j \left(\varepsilon_j^S \right)^{\gamma} + \sum_{i=1}^{N} k_5 t_i \left(\frac{\sigma_i^P}{1 - k_6 10^{g(T_i)} (TW_i + 0.5t_i)^{\frac{1}{3}}} \right)^{\beta} 10^{f(T_i)}$$

  where k_4, k_5, k_6 are constants defined in FFS-1 Table 10.5 and $\varepsilon_j^S = \frac{\sigma_i^S}{E_i}$ is strain caused by secondary stresses.
- Determine the total creep damage for Mode I as the sum of all the compute contribution

$$D_c^{II} = D_{Pc}^{I} + D_{Sc}^{I}$$

- If the creep total creep damage for Mode I $D_c^{II} \le 1$ then the component is suitable for continued operations

4.3 Survey of fitness-for service practices and damage tolerant design

4.3.1 ASME Boiler and Pressure Vessel Code, Section XI

Section XI of the ASME Code provides in-service inspection criteria suitable for high temperature reactors. However, if a flaw is discovered Section XI currently does not provide fitness-for-service criteria suitable for flaw growth at high temperatures. This is a known gap in the ASME Code and is currently being addressed by a joint Section III/Section XI Working Group on High Temperature Flaw Evaluation. The working group will begin with flaw evaluation procedures for base materials. Its current work does not address weldments nor does it address environmental effects.

4.3.2 RCC-MRx

4.3.2.1 Preventing fast fracture

The RCC-MRx code provides rules to prevent fracture that initiates from any existing defect but not preceded by an appreciable plastic deformation of the material. Fast fracture is generally caused by unstable propagation of a crack. Two types of fast fracture are considered – ductile tearing which occurs when a small volume of highly stressed material at the tip of the defect fractures through plastic instability while bulk of the structure behaves elastically and brittle tearing which is the result of material cracking without detectable local plastic deformation.

Rules to prevent fast fracture in RCC-MRx code are provided in Appendix A16. The code provides a conventional analysis method as well as a detailed analysis method. The conventional analysis method checks the design against postulated defects without direct connection to possible manufacturing defects or in service deterioration. On the other hand, detailed analysis method consists of determining the size of a critical defect that just barely meets the recommended safety factors. The structure is then declared safe against fast fracture by demonstrating that any defect larger than the critical defect is not possible considering the manufacturing process used and the inspection during fabrication and operation.

In conventional analysis method, the value of J-integral must meet the following criteria:

$J(\lambda M + T, a_{ref}) \leq J_{intiation}$; for preventing tear initiation

$J(\lambda M + T, a_{ref} + \Delta a) \leq \frac{J_R(a_{ref}+\Delta a)}{\delta}$; for preventing defect instability

where J-integral is calculated considering the mechanical, M and thermal load, T specified by C and the depth, a_{ref} of a postulated reference crack. The depth a_{ref} is to be considered equals ¼ of the thickness of the part but not exceeding 20mm. Acceptable calculation methods for J are provided in Appendix A16 Section A16.7000 of the code. $J_{intiation}$ is the fracture toughness at initiation and is determined as per standard ISO 12135 or ASTM E1820. J_R is determined from tear resistance curve based on standard ISO 12135 or ASTM E1820. δ is a factor on J_R curve and varies depending on the Level criteria. δ is defined in the Equipment Specifications and justified by statistical load dispersion on the tear resistance curve. An additional factor, λ on mechanical load is applied whose value depends on the type of check and the Level criteria.

4.3.2.2 Defect and leak before break assessment

In Appendix A16, the RCC-MRx code provides methods to perform defect assessment as well as methods for leak before break analysis.

In order to perform a defect assessment, the effective length and height of the crack has to be determined. The code provides instructions with figures to characterize and determine the respective effective dimensions of different type of cracks. Once the geometry of the crack is determined, the defect assessment is a two-step analysis method. The first step is the calculation

of the defect evolution, while the second step is the verification that the presence of the defect will not induce any risk of rupture and instability during the rest of the service life.

If the component experiences significant creep deformation, the first step is to check for creep-fatigue initiation. In this step, the total usage fraction for initiation, A and total usage fraction for rupture, W are determined for the number of cycles prior to initiation. Strain range and stress relaxation profile from elastic analysis are used to determine the usages fractions. The usage fractions are then checked with the creep-fatigue interaction diagram. If the (A, W) point falls within the creep-fatigue envelop, only fast fracture and plastic instability are checked in the second step. Otherwise, an additional creep-fatigue propagation analysis is required to perform for the rest of the service life.

In creep-fatigue propagation analysis, the geometry of the defect at the end of service life is checked given its current geometry. The rate of fatigue and creep propagation are determined first and then add together to determine the final size of the defect.

The leak-before-break analysis determines whether it is possible to detect, under in-service conditions, a leak of a fluid containing structure before the defect, the origin of the leak, induces rupture of the structure. For this analysis, the code provides simplified methods based on fracture mechanics concept.

4.3.3 ITER design criteria

Likely due to the high radiation doses structural components will experience in ITER, the ITER design criteria focus on fast fracture in embrittled material.

Since irradiation can reduce the fracture toughness of most materials, the ISDC code provide rules for preventing fast fracture originating from postulated flaws. The depth of the postulated crack, a_o is considered as the maximum of 4 times the largest undetectable crack length by NDE and ¼ of the wall thickness. Rules are provided for both elastic and elastic-plastic analyses.

In elastic analysis, mode I stress intensity factor , K_I has to be calculated for a postulated surface crack with depth, a_o and minimum length $10a_o$ subjected to the prescribed loading. The elastic analysis rules are

$K_I \leq \gamma_1 K_C(\theta, G_{tm})$; for preventing global fast fracture due to primary plus secondary membrane loadings

and

$K_I \leq \gamma_2 K_C(\theta, G_{tm})$; for preventing local fast fracture due to all primary and secondary loadings, including peak. Here γ_1 and γ_2 are the safety factors.

If the postulated crack for the global and local fast fracture analysis is embedded in a yielded region, elastic-plastic fracture mechanics methodology should be used. The acceptance criterion is based on J-integral determined for all the loadings.

$J_I \leq \gamma_3 J_C(\theta, G_{tm})$

Note that, both the minimum fracture toughness, K_C and minimum critical J-integral are function of temperature, θ and thickness averaged fluence, G_{tm} to account for the effect of irradiation.

4.3.4 R5

4.3.4.1 General procedure

This procedure is described in R5 Volume 4/5 and is used for assessing the suitability of a structure containing defect operating at high temperature and subject to creep-fatigue loading conditions. This procedure can be used for different purposes: to find the loads so that a certain service life is achieved; and to identify the initial defect size which will grow to the maximum acceptable size given the operating conditions and the combination of loadings geometry, and material properties for which the crack tip behavior has a negligible effects on total service life.

The core of this procedure is the creep-crack growth evaluation for which R5 provides two different methods. For Method I cyclic and creep crack growth rates are computed separately and then summed together to obtain the total crack growth rate. For cases in which plasticity is negligible the fatigue assessment is based on the elastically calculated ΔK, otherwise ΔK is modified to account for plasticity using ΔJ. Creep crack growth during dwell is computed via the C^* parameter.

Method II is simpler than Method I and assumes that creep influences the cyclic contribution to crack growth and therefore no explicit calculations of creep crack growth are required. For this purpose, a high-strain creep model is used to account for the effects of creep damage occurring during dwell and cyclic loading. The underlying assumption is the defect is small enough to be embedded inside the cyclic plastic zone.

The procedure outlined below is applicable only to austenitic and ferritic steels, and does not consider leak-before-break for pressurized components. Defects are assumed to be embedded in a homogeneous material (either be parent or weld metal), or in non-homogeneous weldments. Both displacement controlled and stress controlled crack behavior is considered.

The procedure is outlined below:

- Establish the cause of cracking. This step is critical as it ensures that the procedure is applicable. Caution should be used if the defect is formed during service due to creep because if significant creep damage is found away from a crack tip this might indicate over-heating and or over-stressing. Caution should also be used if cracks are found in a material having sustained extensive creep damage. When this is found to be the case all crack growth calculations should use material properties fully representative of the present material damage state. If there is evidence of environmental assisted cracking, this procedure should not be used.
- Characterize the defect. The geometry and location of a defect are required for using this procedure. Once the actual geometry of the defect is known it must be simplified before the procedure can be applied: through wall cracks are idealized by their circumscribing rectangle and embedded surface crack are characterized by a semi-ellipse whose axes are derived from a rectangle circumscribing the actual defect. Calculations for elliptical defects

must be performed twice, one for each ellipse axis. The procedure below only applies to Mode I loading.

- Define past and planned future loading conditions and resolve them into loading cycles. Specification of the service conditions must include load, temperature and to-date and planned service life. Furthermore, the load history must include time dependent, time independent and fault loadings.
- Identify the material parameters. Time dependent, time independent and cyclic material properties are required for the evaluation. Furthermore, one might also want to consider the effect of thermal ageing on material properties. The required material date are:
    - Elastic and physical constants, such as elastic modulus E, Poisson's ratio ν, coefficient of thermal expansion α, etc.
    - Monotonic tensile data such as the 0.2% proof stress
    - Creep rupture data
    - Creep deformation data
    - Creep ductility data
    - Fracture toughness
    - The shakedown factor, K_s
    - Cyclic stress-strain data
    - Creep crack incubation data. For situation where fatigue is insignificant it might be possible to discount the incubation period. The incubation period might be computed as a function of a critical crack tip opening displacement δ_i or using the C^* parameter in the following relationship $t_i(C^*)^\beta = \gamma$, where β and γ are material properties.
    - Creep crack growth data. This kind of data are expressed in terms $\dot{a} = A(C^*)^q$ where A and q are material parameter. Further, when using C^* to compute the crack growth rate, there is a limit on the dimensionless crack velocity: $\lambda = \dot{a}\sigma_{ref}^2/EC^* \leq 0.5$.
    - Cyclic crack growth data. The type of cyclic crack growth data utilized for this analysis dependents on the method.
        - For Method I the relationship used to compute the cyclic component of the of the creep fatigue crack growth is $\left(\frac{da}{dN}\right)_f = C\Delta K_{eff}^l$ where C and l are material and temperature dependent parameters.
        - For Method II the relationship used to compute the cyclic component of the of the creep fatigue crack growth is $\left(\frac{da}{dN}\right)_f = B'a^Q$ where B' and Q depend on material, temperature, environment and strain range. This method can only be applied if the crack is embedded in the cyclic plastic zone at the surface ($a_{min} \leq a \leq r_p$ where a is the crack size $a_{min} = 0.2\ mm$ and r_p is the plastic zone size on the surface.)

    The main source of data for this procedure is R66.

- Perform an elastic stress analysis of the defect-free body at the extremes of the service cycles identified before. A ratcheting analysis of the uncracked component/structure should also be performed. The procedures used to assess shakedown are the same ones used in Volume 2/3. If shakedown is demonstrated, then one must check that the crack has negligible effect on the elastic compliance of the structure/component. For the crack propagation analysis, the elastic follow up factor resulting from the shakedown analysis of the uncracked body is increased by unity and the modified elastic follow up factor is used in the crack propagation analysis. The size of the surface plastic zone must also be identified as this might influence the method selected for calculating the crack growth rate. The procedure to compute the cyclic plastic zone size is the same as that in Volume 2/3. The stress intensity factor ratio $R = K_{min}/K_{max}$ must also be computed by using the result of the shakedown analysis. This is because due to creep the shakedown analysis will provide a lower value of R. For the creep crack growth analysis, one also needs the reference stress at the beginning of dwell:

$$\sigma_{ref}^{p} = \frac{P\sigma_y}{P_L(\sigma_y, a)}$$

  where P is the primary stress resulting from the shakedown analysis at dwell, P_L is the plastic collapse load assuming a yield stress σ_y and a crack size a.
- Check the stability of the structure under time independent loading utilizing the procedure described in R6. This procedure requires the use of the initial residual stresses present in the component.
- Check the significance of creep damage, fatigue damage and creep-fatigue damage interaction.
  - The effect of creep can be neglected if the ratio of hold time t over the maximum hold time t_m at the reference temperature T_{ref} for the whole loading history is smaller than unity (e.g. $\sum_{j=1}^{J} n_j \left[\frac{t}{t_m(T_{ref})}\right]_j \leq 1$) where t_m should be determined using Figures A6.6 and A6.7 in R5 Volume 4/5.
  - Cyclic loading can be neglected if: i) the creep behavior is not perturbed by cyclic loading both locally and globally, and ii) the creep crack growth rate due to cyclic loading is smaller than $1/10^{th}$ of the estimated creep crack growth rate. To determine if the creep behavior is perturbed by cyclic loading from the global structural response, the same test for checking the significance of cyclic loading for the uncracked structure is used (see Volume 2/3 Section 6.2.2 for more details.) To determine the local effect of cyclic loading on the creep behavior one needs to show that for the most severe cycles the size of the cyclic plastic zone r_p^{crack} is much smaller than the crack or any sectional characteristic dimension of the structure (e.g. remaining ligament size.) For cyclic loading the allowable elastic stress is two times the yield stress (e.g. $2\sigma_y$), therefore one can compute $r_p^{crack} = \beta\left(\frac{\Delta K}{2\sigma_y}\right)^2$ where β can be is $1/2\pi$ and $1/6\pi$ for plane stress and plain strain condition, respectively.

If all requirements are satisfied then the effect of cyclic loading on creep crack growth can be neglected.

- Check for the significance of creep fatigue interaction. Even if both creep and fatigue are shown to be significant the latter has little effect on the total crack growth rate if the creep-crack growth is accounted for explicitly. i) If creep behavior is perturbed by cyclic loading but the creep crack growth rate due to cyclic loading is still smaller than 1/10th of the estimated creep crack growth rate. ii) When a crack propagates through a material exhibiting high creep damages (e.g. $D_c \geq 0.8$).

  For case i) the coefficients C and l of $\left(\frac{da}{dN}\right)_f = C\Delta K_{eff}^{l}$ should be determined experimentally for relevant conditions. For case ii) R5 suggests following the guidelines provided in BS 7910 [105] which recommends evaluating the penalty factor experimentally for creep damage $D_c \geq 0.8$. Other sources [106] recommend enhancing the creep damage by a factor $\frac{1}{(1-D_c)}$ for any value of D_c.

- Calculate the rupture life t_{CD} based on defect size. The rupture life t_{CD} can be estimated as: $t_{CD} = t_r\left[\sigma_{ref}^{P}(a)\right]$ where t_r is the rupture time at the stress level σ_{ref}^{P} where σ_{ref}^{P} is the stress level considering primary stress loads for a crack of size a. If the computed rupture life is less than the required service life then one does not need to perform crack growth calculations. Otherwise, one needs to calculate the crack growth.
- Calculate the three different characteristic times due to the different crack propagation stages.
  - Calculate the crack incubation time t_i (optional). The incubation time is defined as the time from the beginning of the assessed period of high temperature operation for which the crack growth rate is insignificant. If this step is neglected, the incubation time is assumed to be zero. The incubation time can be estimated as

$$\varepsilon_c\left[\sigma_{ref}^{p}(a_0), t_i\right] = \left[\frac{\delta_i}{R'(a_0)}\right]^{\frac{n}{n+1}} - \frac{\sigma_{ref}^{p}(a_0)}{E}$$

    See appendix A2 in R5 Volume 4/5 for more details.

  - Calculate the redistribution time t_{red}. The redistribution time t_{red} is the time required for stresses to redistribute due to creep since the beginning of dwell up to widespread creep conditions. The redistribution time t_{red} can be expressed as

$$\varepsilon_c\left[\sigma_{ref}^{p}(a), t_{red}\right] = \frac{\sigma_{ref}^{p}(a)}{E}$$

  - Calculate the time to achieve steady cyclic state t_{cyc}. This is required to account for the effect of the early cycles. When the damage due to cyclic loading is significant one must estimate the t_{cyc}. For the case where only primary loads are present the equation below can be used:

$$\varepsilon_c\left[\frac{\sigma_{ref}^{cyc=1} + \sigma_{ref}}{2}, t_{cyc}\right] = Z\frac{\sigma_{ref}^{cyc=1} - \sigma_{ref}}{E}$$

where Z is the elastic follow up factor computed accordingly to Appendix 3 of Volume 4/5, and $\sigma_{ref}^{cyc=1}$ is the reference stress for the first cycle and σ_{ref} is reference stress for steady cyclic conditions. $\sigma_{ref}^{cyc=1}$ can be estimated using the Neuber rule.

- Calculate crack tip parameters. There are a variety of crack tip parameters that need to be computed before assessing the actual crack growth rate.
  - Calculations of ΔK_{eff}: if cyclic plasticity is not observed for the uncracked structure then $\Delta K_{eff} = q_0 \Delta K$, where q_o is the time fraction the crack is considered to be open and is related to the value of R. If $R \geq 0$ then $q_0 = 1$, if $R < 0$ then $q_0 = \frac{1-0.5R}{1-R}$. If cyclic plasticity is present than one should use ΔJ instead of ΔK (more detail in Volume 4/5 Appendix A3) to determine R.
  - Calculate the value of the characteristic length R' as $R' = \left(\frac{K_p}{\sigma_{ref}^p}\right)^2$. Note that the value of R' is different while moving along an elliptic crack rim. Therefore, it should be evaluated separately for the deepest point on the crack rim and at the surface.
  - Estimate the value of C^* as $C^* = \sigma_{ref}^p \dot{\varepsilon}_c \left[\sigma_{ref}^p(a), \varepsilon_c\right] R'$. Here ε_c is the accumulated creep strain and $\dot{\varepsilon}_c$ is the creep strain rate associated with the reference stress level σ_{ref}^p. A strain hardening rule must be used.
- Calculate the increment in crack size due to creep crack growth rate $\left(\frac{da}{dN}\right)_C$. Three regimes may be considered: i) steady-state creep crack growth (e.g. $t > t_{red}$), ii) non-steady state creep crack growth (e.g. $t < t_{red}$), and iii) early cyclic creep crack growth (e.g. $t < t_{cyc}$). Note that in order to use the following one needs to demonstrate that the non-dimensional crack velocity satisfies the condition: $\lambda = \dot{a}\sigma_{ref}^2 / EC^* \leq 0.5$.
  i. For steady state creep, the crack growth per cycle due to the dwell time t_h can be compute as:

$$\left(\frac{da}{dN}\right)_C = \int_0^{t_h} A(C^*)^q dt$$

  ii. For non-steady state creep, there are two cases: a) the case for which the total time for the assessment t is greater than t_{red}, and b) the case for t smaller than t_{red}.
    a. For the first scenario a simplified approach can be utilized assuming that between incubation and redistribution time the crack will grow twice as fast as after redistribution:

$$\begin{cases} \dot{a} = 2A(C^*)^q & t_i \leq t < t \\ \dot{a} = A(C^*)^q & t > t_{red} \end{cases}$$

    b. In this case a more rigorous treatment is required. This involves the use of the $C(t)$ parameter rather than the C^* parameter. R5 provides an interpolation rule to obtain $C(t)$ from C^*:

$$\frac{C(t)}{C^*} = \frac{\left(1+\frac{\varepsilon_c}{\varepsilon_e}\right)^{\frac{1}{1-q}}}{\left(1+\frac{\varepsilon_c}{\varepsilon_e}\right)^{\frac{1}{1-q}} - 1}$$

where q is the exponent of the creep crack growth rate equation, $\varepsilon_c$is the accumulated creep strain at time t and ε_e is the elastic strain.
The creep crack growth per cycle can then be computed as

$$\left(\frac{da}{dN}\right)_C = \int_0^{t_h} A\big(C(t)\big)^q dt$$

iii. Early creep crack growth estimate is required for times for which shakedown has not been achieved yet. In this case the parameter C^* is replaced with

$$\bar{C}^* = \frac{\sigma_{ref}^{cyc=1} + \sigma_{ref}}{2}\dot{\varepsilon}R'$$

where $\dot{\varepsilon}$ is evaluated as $\varepsilon_c = Z\frac{\sigma_{ref}^{cyc=1}-\sigma_{ref}}{E}$. It should be noted that the above equation is insensitive to the time to shakedown t_{cyc} but is proportional to the accumulated creep strain ε_c. The creep crack growth per cycles before structural shakedown can then be computed as

$$\left(\frac{da}{dN}\right)_C = \int_0^{t_h} A(\bar{C}^*)^q dt$$

- Combining cyclic crack growth due to creep and cyclic loading. The way creep and cyclic crack growths are combined depends on the crack and plastic zone size. As mentioned before if the characteristic crack length is greater than the cyclic plastic zone then one should use Method I. If the crack is growing inside the cyclic plastic zone then one should use Method II.
  - Method I: In this case the total cyclic crack growth is defined as the sum of creep and fatigue cyclic crack growths:

    $$\frac{da}{dN} = \left(\frac{da}{dN}\right)_f + \left(\frac{da}{dN}\right)_C$$

    where $\left(\frac{da}{dN}\right)_f = C\Delta K_{eff}^l$.
  - Method II: In this case the total cyclic crack growth is modified by a fatigue damage enhancement factor dependent on the creep surface damage D_c^{surf}:

    $$\frac{da}{dN} = \left(\frac{da}{dN}\right)_f \frac{1}{\left(1-D_c^{surf}\right)^2}$$

    where $\left(\frac{da}{dN}\right)_f = B'a^Q$ and D_c^{surf} is the sum of the creep damage fraction $\left(d_c^{surf}\right)_j$ accumulated for each cycle j, and $\left(d_c^{surf}\right)_j = \int_0^{t_{h,j}} \frac{\dot{\bar{\varepsilon}}_c}{\bar{\varepsilon}_f(\dot{\bar{\varepsilon}}_c)} dt$.

    It should be noted that when $D_c^{surf} = 1$ then $\frac{da}{dN} = \infty$. This should be interpreted as the exhaustion of creep ductility inside the cyclic plastic zone and that the crack

will propagate up to the edge of the plastic zone very quickly. In this case one should revert to using Method I.

- Update the crack size at the end of the assessed period. This step simply involves computing the total crack growth increment due to all the cycles: $\Delta a_g = \sum_{j=1}^{N} \left(\frac{da}{dN}\right)_j$
- Recalculate the rupture life with the updated crack geometry.
- Recheck the structural stability under time independent load with the updated crack geometry.
- Perform a sensitivity analysis of the inputs.

The procedure outlined in the previous section also applies to welds and exhaustive explanations are given in R5 Volume 4/5 Appendix 4. For a similar metal weld joint one should use the procedure described in Volume 7 that has been summarized in this report. For dissimilar metal weldments the biggest change to the procedure outlined above is to use different material data. The defect is assumed to be embedded in the heat affected zone. Material properties should then be select appropriately, following the guidance of Volume 4/5 Section A4.4.2.

4.3.4.2 Volume 6: Assessment procedures for dissimilar metal welds

Volume 6 of R5 provides a simplified assessment procedure for dissimilar metal weldments (DMW) based on experimental results and experience. The procedure applies to butt welded pipe and tube geometries operating in the creep regimes. The procedure is supposed to be general enough to account for a variety of material and weld geometries. However, it assumes the availability of experimental data for the assessed geometry and material combinations. This procedure is therefore limited to a small number of material combinations and weld design because of the lack of data.

As a first step one is required to collect the following data for the loadings: pressure, system self-weight, differences in coefficients of thermal expansion across the weld, through wall temperature gradients and other system loading (e.g. cold pull, thermal expansion, temperature variation of the whole pipe network, etc.). The structure's self-weight and the pressure contributes to primary stresses. Ideally other loads relax with time and can be considered as secondary. However, because of possible high value of the elastic follow up factor they will be considered primary.

This procedure as built upon the following assumptions:

- Metallurgical features of the weld are reproducible
- Material properties across the weld are known at every location with reasonable accuracy (if not, experiments are required to apply the procedure)
- Failure is a combination of creep and cyclic loading
- A rupture stress can be identified for the weld region of interest
- The leading failure mechanism is creep due to primary loading
- The stresses at the mean diameter of the structure calculated via elastic analysis are reasonable

The procedure includes three types of damage accumulation mechanisms: i) creep due to primary stress, ii) cyclic loading, and iii) creep damage due to relaxation. For each of the above mechanisms, a damage fraction is computed, and when their sum is equal or exceeds unity, weld

failure is assumed. If A, B and C are the damage fractions associated with the above mechanisms, the assessment passes if $A + B + C < 1$.

The first step in the procedure is to assess the loading history and resolve it into cycles. Actual geometries resulting from inspection and actual service loading should be used. Using design geometry and load may result in overestimating the weldment life.

A pessimistic assessment may be achieved by using the minimum recorded wall thickness of the DMW at the ferritic interface and assuming it for the entire wall. The hoops stress used for the assessment calculation should always be the one resulting from the minimum wall thickness.

The creep life fraction under steady condition, A, is determined as

$$A = \sum_{i=1}^{I} \frac{t_i}{t_f\left(\sigma_{rup}^{i}, T_i\right)}$$

where t_i is the time under loading condition i, t_f is the time to rupture for a given rupture stress σ_{rup}^{i} (defined as $\sigma_{rup}^{i} = \left(\frac{\sigma_a^2 \bar{\sigma}^2}{MF}\right)^{0.25}$) at the median section temperature T_i. The rupture time t_f is computed using the logarithmic relationship given in Appendix 1 of volume 4.5. Moreover, MF is the multiaxial correction factor defined as $MF = \frac{\bar{\sigma}}{\sigma_h} + \sigma_a + \sigma_r$ and $\bar{\sigma}$, σ_h, σ_r and σ_a are the von Mises equivalent, hoop, radial and axial stress, respectively.

The used fraction B for time independent fatigue life is computed via Miner's rule:

$$B = \sum_{j=1}^{J} \frac{N_j}{N_f\left(\Delta\bar{\varepsilon}_j\right)}$$

where N_j is the number of applied cycles with an equivalent strain range $\Delta\bar{\varepsilon}_j$ and N_f is the number of allowable cycles before failure happens given $\Delta\bar{\varepsilon}_j$. The equivalent strain range $\Delta\bar{\varepsilon}_j$ can be determined either by applying a fatigue reduction strength factor (FSFR) to the parent metal or by computing it as the separate contribution of different strain ranges:

$$\Delta\bar{\varepsilon}_j = \Delta\bar{\varepsilon}_{el} + \Delta\bar{\varepsilon}_{pl} + \Delta\bar{\varepsilon}_{vol} + \Delta\bar{\varepsilon}_T$$

where $\Delta\bar{\varepsilon}_{el}$, $\Delta\bar{\varepsilon}_{pl}$, $\Delta\bar{\varepsilon}_{vol}$ are the elastic, plastic, volumetric strain ranges as per Volume 2/3 (see relevant section) and $\Delta\bar{\varepsilon}_T$ is thermal strain range. The term $\Delta\bar{\varepsilon}_T$ is a function of the mismatch in the coefficients of thermal expansion between the parent and the weld material and the temperature range:

$$\Delta\bar{\varepsilon}_T = 1.5\Delta\alpha\Delta T$$

The number of cycles to failure N_f is obtained by using the appropriate curves (parent material if FSFR or cross weld specimen if using the computed $\Delta\bar{\varepsilon}_j$).

The used creep life fraction under transient condition C is evaluated as:

$$C = \sum_{k=1}^{K} N_k \frac{\alpha \Delta T_k}{\varepsilon_{fk}}$$

where α is coefficient of thermal expansion for the local material inside the weld, ΔT_k is the temperature jump between two different operating condition, which are temperature variation between the beginning of a cycle and start of dwell or the end of cycle and the beginning of a new one (see Figure A5.1 in Volume 6). If no data are available $\varepsilon_{fk}$is set to be 5%.

4.3.4.3 Volume 7: Behavior of similar weldments: Guidance for steady creep loading of ferritic pipework components

The aim of this procedure is to assess the life of a welded ferritic pipeline subject to steady creep loading conditions. This procedure is referenced several times in R5 Volume 4/5 and is fully compatible with it. This procedure has been developed for welds with parent and welded material 0.5CrMoV and 2CrMoV, respectively. However, it can be used for all instances in which the parent and welded material have similar composition, creep crack growth is driven by C^* or $C(t)$ and appropriate material data regarding the welded zone are available.

In this procedure a weld is considered to be composed of different microstructures while moving across the weld. For each microstructure relevant material properties need to be available.

This procedure is applicable when loads and temperatures vary slowly in time. In general, it is assumed that creep rather than fatigue is the major contributor to failure. Variation in stress and temperature are accounted for by integrating continuum creep and fatigue crack growth rates. Furthermore, the procedure accounts for both primary and secondary loads. This procedure only applies to Mode I crack growth.

Creep crack growth and damage are computed as functions of the operating time t. The crack size at the beginning of the assessment is denoted as a_0. Incubation may be included in the evaluation if necessary. It is conservative to assume a zero incubation time.

Several weldment material properties at different location across the weld are required to perform this assessment. Required material properties for each area can be summarize as follows:

- Creep rupture
- Creep deformation
- Creep rupture ductility
- Creep crack growth rate
- Fracture toughness
- Yield and ultimate tensile stress
- Elastic constants (Young's modulus and Poisson's ratio)
- Incubation time as function of the critical crack opening displacement δ_i or C^*.

In general, use of lower bound material properties would lead to an overly conservative life estimate. Experience suggests that the use of average material properties is acceptable and it would still produce conservative results. Safety factors are not used in the assessment. Instead, an enhanced service life $t_2 = 1.25t_1$ is assume, where t_1 is the future planned service operation time. This is justified in R5 as a prevention against abrupt failure due to sudden changes in material properties. This approach is deemed to provide a qualitative margin against cliff effects.

The procedure itself requires the following steps, some of which can be bypassed depending on the conditions:

- Obtain data regarding the pipe system, the component and the investigated welded section
- Define the operating time to date as t_0 and the planned future service life as t_s. The assessment is performed on the time range between $t = 0$ and t_1, where $t_1 = t_0 + t_s$.
- Determine the loads and temperature variations for all times t such that $0 \leq t \leq t_1$. Again, loads and temperatures should not be inferred from design data but should be taken from operating conditions.
- Compute the elastic stress for the uncracked feature (e.g. stress classification line in a component) assuming homogenous parent material properties. The resulting stress field shall be linearized and categorized.
- If any feature contains a defect, it should be identified and sized. The value a_0 is the size of a defect at time t_0. Here, incubation time can be used to determine when, in time, the defect reaches the initial size. Again, if the time at which the crack is started is unknown it is safe to assume the incubation time $t_i = 0$.
- Compute the reference stress σ_{ref}, and if a crack is present, compute the primary and secondary stress intensity factor K_p and K_s, respectively. The reference stress is determined from the elastic solution for the uncracked body as $\sigma_{ref} = \left(\frac{P}{P_L}\right)\sigma_y$, where P is the primary stress, P_L is the collapse load determined according to R6, and σ_y is the yield proof stress of the material. For instances in which a defect is present the reference stress must be multiplied by a factor k (e.g. $\sigma_{ref} = k\sigma_{ref,0}$) ranging from 0.7 to 1.4, depending on the situation. The stress intensity factor K_p and K_s are determined separately from the elastic solution of the uncracked body using handbook solutions, and summed together to obtain the total stress intensity factor $K = K_P(a) + K_s(s)$. See R5 Volume 7 Appendix 3 for more details.
- Compute the initial rupture life t_{CD_0} and the continuum damage D_{C_0} for the time t_0 using the crack size a_0. The rupture life t_{CD_0} is computed using appropriate rupture life curves $t_r(\sigma_{ref}, T_{ref})$ for the given conditions. The continuum damage is a life fraction and is computed by integrating $\dot{d_C} = \frac{dt}{t_r(\sigma_{ref}, T_{ref})}$ between two times intervals. This must be done for each type of microstructure in the feature. Then for conservatism the shortest rupture life and its associate continuum damage should be selected. Check if t_{CD_0} is greater than planned service life t_1. If this is not the case the analysis should be refined or remedial action taken.

- Check time independent collapse using the procedure outlined in R6 using the crack size a_0, lower bound fracture toughness and tensile material properties. If a crack is not present this assessment reduces to comparing the reference stress with the flow stress. The flow stress is defined as the average between the yielding and rupture stress.

If the analyzed feature is uncracked, one skips the following steps and proceed to perform a sensitivity analysis of the input, otherwise the following additional steps are required.

- Assess the incubation time t_i (optional). It is conservative to assume $t_i = 0$.
- Calculate the creep crack growth rate and crack sizes up to a time $t_2 \geq t_0 + 1.25t_1$. Creep crack growth is estimated as in Volume 4/5 but using the enhanced reference stress mentioned above and its associated strain fields. This step involves computing the crack growth rate $\dot{a}$ as a function of C^* or $C(t)$ and making sure that the non-dimensional crack velocity satisfies the condition $\lambda \leq 0.5$. If the feature fails before time t_2 then the analysis should be refined or service life t_1 should be reduced.
- Calculate the continuum damage D_{C_2} up to time t_2. If $D_{C_1} > 1$ or $D_{C_2} > 1$ then the assessment fails. One can reduce the planned service life or refine the analysis. If $D_{C_2} \leq 1$ then one can proceed to the last step of the assessment.
- Recompute time independent collapse using the procedure outlined in R6 using the crack size a_1, lower bound fracture toughness and tensile material properties. Also using R6 establish the limiting crack size a_L at time t_1. Check that the limiting crack size a_L is greater than the crack size a_2. If this is the case then the feature is suitable for continued service up to time t_1. Again, a sensitivity analysis should be performed to gain confidence in the assessment.

4.3.5 API-579/FFS-1

FFS-1 provides a procedure to evaluate a component operating in the creep range with a crack-like flaw using the results from a stress analysis.

This assessment utilizes stresses, strains, operating time and temperatures at each point across the wall thickness. When an inelastic analysis is performed, it shall include a material model accounting for creep. The creep material model should be sensitive to stress, temperature and time. If at a location stress state beyond yield is computed, the material model must also include plasticity. For this analysis the mean material fracture toughness and the minimum yield and tensile strengths shall be used.

With material data and histogram identified, the following steps need to be performed:

- Determine the damage ahead of the crack tip before the crack is nucleated D_{bc}. There are two options depending if the structure is subject to steady or cyclic operations:
    - Steady operations: Procedure 1 describes creep-rupture life section to compute the creep damage as

$$D_{bc} = \sum_{m=1}^{M_{bc}} {}^{m}D_c$$

    - Cyclic operations: the fatigue damage before cracking need to be added to the creep damage:

$$D_{bc} = \sum_{m=1}^{M_{bc}} {}^{m}D_c + \sum_{m=1}^{M_{bc}} \frac{{}^{m}n}{{}^{m}N}$$

where M_{bc} is total number of cycle before the onset of cracking, n is number of applied cycles, N is number of allowable cycles for the given conditions and m is the cycle type.

- Compute the damage ahead of the crack tip for the period of time it was verified that the crack was not present ${}^{0}D_{ac}$: this involves characterizing the crack dimensions from inspection and categorizing it according to Annex 9C (Annex 9C is handbook for reference stress distribution given a crack and a component geometry.) Determine the crack characteristic dimensions a_0 and c_0. The crack damage ${}^{0}D_{ac}$ is still computed using Procedure 1 but with a modified reference stress from Annex 9C. This reference stress accounts for stress concentration due to the crack. The damage is computed as

$$ {}^{0}D_{ac} = \sum_{m=1}^{M_{bc}} {}^{m}D_c $$

- Initialize the crack size and time such that ${}^{i=1}a = a_0$, ${}^{i=1}c = c_0$, ${}^{i=1}t = 0$, where i is an index to keep track of the crack size through time.
- Starting from cycle $m = M_{bc}$ identify the cycle time ${}^{m}t$ and divide the cycle into a number of periods I. Assign at ${}^{i}t$ the time corresponding to the end of each period. Note that the higher the number of periods, the better is the accuracy of the solution. Also determine the temperature ${}^{i}T$ for each period selected from the histogram. A sensitivity analysis is recommended. For each period i:
    - Compute the stresses ${}^{i}\sigma_{ij}$ through the wall thickness and recomputed the reference stress ${}^{i}\sigma_{ref}$ according to Annex 9C.
    - Check the margin against plastic collapse of the component and that for the identified crack geometry and operating conditions for the point lies in safe zone of the failure assessment diagram (FAD). If any of the above criteria is not satisfied then the life of the component is limited by them and the procedure stops. If both criteria are satisfied then one moves to the next step.
    - Compute the damage ahead of the crack as
    - $${}^{i}D_{ac} = {}^{i-1}D_{ac} + \frac{\left({}^{i}t - {}^{i-1}t\right)}{{}^{i}L_{ac}}$$

      where ${}^{i}L_{ac}$ is the rupture time for the given loading history after crack initiation. Compute the value as:

      ${}^{i}L_{ac} = \frac{1}{\dot{\varepsilon}_{co}\Omega_m}$ if one uses the Omega Project Data at the reference stress $S_l = \log_{10}\left({}^{i}\sigma_{ref}\right)$, or

      ${}^{i}L_{ac} = \log_{10}[{}^{n}L] = \frac{1000\,LMP({}^{n}S_{eff})}{T_{refa} + {}^{n}T} - C_{LMP}$ if one uses the Larson-Miller parameter.
    - Check that the creep damage ahead of the crack is acceptable: This means simply checking that $D_{bc} + {}^{i}D_{ac} \leq D_c^{allow}$.

- Compute the new reference strain rate ${}^{i}\dot{\varepsilon}_c$ using the Omega Project model (Eq. 10.14 in FFS-1) for the reference stress $S_l = \log_{10}\left({}^{i}\sigma_{ref}\right)$.
- Compute the Mode I stress intensity factor for both the characteristic crack lengths, $K_I^{90}\left({}^{i}a,\ {}^{i}c\right)$ and $K_I^{0}\left({}^{i}a,\ {}^{i}c\right)$ using Annex 9B (FFS1 Annex 9B is a handbook of stress intensity factor given a crack and a component geometry).
- Compute the crack driving forces $C_t^{90}\left({}^{i}a,\ {}^{i}c\right)$ and $C_t^{0}\left({}^{i}a,\ {}^{i}c\right)$. The evaluation of $C_t^{90}\left({}^{i}a,\ {}^{i}c\right)$ and $C_t^{0}\left({}^{i}a,\ {}^{i}c\right)$ involves computing a relaxation time t_{relax} and a C^* value for both characteristic crack lengths. Beside all the equations, the relaxation time uses a factor of 0.91.
- Compute the crack growth rate for the time period ${}^{i}t$ as:

$$\frac{{}^{i}da}{dt} = H_C\left(C_t^{90}\left({}^{i}a,\ {}^{i}c\right)\right)^{\mu} \quad \frac{{}^{i}dc}{dt} = H_C\left(C_t^{0}\left({}^{i}a,\ {}^{i}c\right)\right)^{\mu}$$

  where H_C and μ are the coefficient and the exponent for the creep crack growth model. The value of H_C and μ depends on whether the MPC Omega Project or Larson-Miller's parameter formulation is used.
- Determine the integration time step Δt as a function of the maximum crack growth rate:

$$\Delta t = \frac{C_{intg}\, t_c}{\max\left[\frac{{}^{i}da}{dt}, \frac{{}^{i}dc}{dt}\right]}$$

  where $C_{intg} = 0.005$ for explicit time integration and t_c is the component thickness adjusted for metal loss and future corrosion allowance.
- Update the crack dimensions and time as:

$${}^{i}a = {}^{i}a + \frac{{}^{i}da}{dt}dt \quad {}^{i}c = {}^{i}c + \frac{{}^{i}dc}{dt}dt \quad {}^{i}t = {}^{i}t + \Delta t$$

- If the current time ${}^{i}t < {}^{m}t$ then one repeats all the calculations for the next time i. Otherwise, proceed to the next step

- If cyclic loading is present the crack size must be updated:

$${}^{i}a = {}^{i}a + \frac{{}^{m}da}{dN} \quad {}^{i}c = {}^{i}c + \frac{{}^{m}dc}{dN}$$

  where
  $\frac{{}^{m}da}{dN} = H_f\left({}^{m}\Delta \mathrm{K}_{\mathrm{eff}}^{90}\frac{E_{amb}}{E_r}\right)$,
  $\frac{{}^{m}dc}{dN} = H_f\left({}^{m}\Delta \mathrm{K}_{\mathrm{eff}}^{0}\frac{E_{amb}}{E_r}\right)$,
  ${}^{m}\Delta \mathrm{K}_{\mathrm{eff}}^{90} = q_0\left({}^{m}\mathrm{K}_{\mathrm{I,max}}^{90} - {}^{m}\mathrm{K}_{\mathrm{I,min}}^{90}\right)$
  ${}^{m}\Delta \mathrm{K}_{\mathrm{eff}}^{0} = q_0\left({}^{m}\mathrm{K}_{\mathrm{I,max}}^{0} - {}^{m}\mathrm{K}_{\mathrm{I,min}}^{0}\right)$.

  The parameter q_0 is a function of the stress intensity factor ratio R=$\frac{{}^{m}\mathrm{K}_{\mathrm{I,min}}}{{}^{m}\mathrm{K}_{\mathrm{I,max}}}$:

  - For $R \geq 0$ then $q_0 = 1$
  - For $R < 0$ then $q_0 = \frac{1-0.5R}{1-R}$

- If cycle m is the last cycle in the histogram the procedure continues to the next step; otherwise, one needs to analyze the next cycle beginning again by dividing the cycle in I substeps.
- If for all the analyzed locations and sub steps i the results lay within the safe region of the failure assessment diagram then guarding against plastic collapse is guaranteed and the damage in front of the crack tip is acceptable. Therefore, the component is suitable for continued operations. The component remaining life can be assessed by including additional operating cycles.

In this procedure the presence of a weld is considered by reducing the allowable accumulated inelastic strain (see Table 6) or by setting a lower bound for the strain range adjustment factor $\Delta_{\Omega}^{\mathrm{sr}}$. Furthermore, the presence of a weld is also accounted for by utilizing specific handbook solutions for the reference stress ${}^{i}\sigma_{ref}$ (Annex 9B) and for the stress intensity factors K_I^{90} and K_I^{0} (Annex 9C.)

4.4 Recommendations

4.4.1 Developing a high temperature flaw assessment method

Currently, there is no widely accepted and understood methodology for assessing flaw growth for high temperature cyclic load. ASME Section XI does not include high temperature flaw evaluation criteria, though work is in progress through the Working Group on High Temperature Flaw Evaluation, where the R5 approach is being adopted. This means that if a flaw is discovered in an operating high temperature plant, at a weld or otherwise, there is no accepted methodology for determining how plant operations must be altered to ensure a safe amount of flaw growth. Such a flaw assessment method will likely be required before plants can be licensed.

The methodology presented in API 579/ASME FFS-1 could be adopted for use in Section XI and/or used by regulators. This method is essentially the method developed for R5. The challenge here would be obtaining the required crack growth data and ensuring the data meets nuclear quality assurance requirements. Creep-crack growth data on any material is not commonly available from the open literature and so a test program may be required. Developing a consensus evaluation method that can be adopted by regulators, including minimum data requirements, may help reactor vendors understand and plan for the required testing.

4.4.2 Awaiting a consensus on Type IV cracking and austenitic reheat cracking

Currently, there does not seem to be a consensus on if Type IV cracking in ferritic-martensitic steels is a problem with current post-weld heat treatment procedures, a problem that requires design modifications (likely, in the ASME context to the stress rupture factors), or a fabrication problem caused by improper post weld heat treatment. A similar situation exists for stress relaxation cracking in austenitic alloys. A determination on if changes to design codes and construction practices is required will need to wait for additional experimental data and high temperature field experience with these materials. This consensus on ferritic-martensitic steels will likely need to emerge from the fossil energy or petrochemical industries or their representative trade associations as the U.S. currently has no operating high temperature nuclear plants. Transferring information from the non-nuclear to the nuclear industry could be done through the ASME, but will be complicated by the different design rules used by the two groups.

Similarly, information on reheat/stress relaxation cracking in austenitic steels could be gathered from non-nuclear industries in the U.S. or from foreign high temperature reactor programs. The UK Advanced Gas Reactor fleet is a promising source of information on 316H stainless steel, as those reactors have extensive operating experience with that material in the creep regime. However, at the time of this report there does not seem to be a publicly available summary of the AGR experience with 316H. Developing a mechanism for information sharing with the UK (and other foreign reactor programs) is a critical future issue to be resolved.

4.4.3 Assessing assumed flaw design at high temperatures

Lightwater reactor designers conventionally evaluate their designs against some library of assumed flaws. That is, they are required to assume the existence of a flaw with some set geometry (or a library of such flaws) and demonstrate that if such a flaw exists it will not grow unstably under the component operating conditions. This check ensures that a flaw will be detected before it could lead to rapid failure of the component.

The RCC-MRx code applies this concept to high temperatures by requiring the designer to evaluate an assumed flaw. The other high temperature codes do not adopt this approach. The common justification is that at high temperatures it is extremely unlikely that a flaw would grow unstably and so regular plant inspection would identify flaws before they could cause rapid failure of the component. Therefore, a properly integrated design and in-service inspection method mitigates the risk associated with such flaws. Accepting this approach, flaw evaluation is an aspect of fitness-for-service approaches, rather than a safety-critical high temperature design issue as regular inspection should identify any cracks in operating high temperature plants before they can rapidly grow to fail a component.

However, there is the possibility that a flaw could grow stably but relatively quickly to the critical size in between plant inspection periods. This is only likely in components that are highly stressed or see a large number of operating cycles in a short period of time.

An evaluation of prototypical components for various reactor systems could be made to assess the possibility of such rapid, but stable, crack growth under creep-fatigue loading. It seems unlikely

that rapid crack growth configurations will be found in cases not considering environmental effects. However, such a study would need to wait for the establishment of a flaw assessment procedure (4.4.1).

An exception to this assessment are situations where the environment affects material ductility or if environmentally-assisted crack growth mechanisms are present. A prime example would be irradiation embrittlement, which can lower the ductility of the material to the point where rapid cracking becomes possible even at high temperatures. Likely it is this concern that prompts RCC-MRx and (especially) the ISDC to include flaw-tolerant design approaches based on assumed flaws.

Flaw tolerant design methods will require fracture toughness data on embrittled material, but with the availability such data the implementation will be fundamentally similar to the techniques used in light water reactors. A monitoring program could be adopted, if necessary, to measure the toughness of material exposed to the reactor operating conditions.

This report did not cover environmentally-assisted cracking in detail, in part because there is little available data on potential cracking mechanisms for potential advanced reactor coolants. Inspection, surveillance, and, in the last resort, adequate fitness-for-service procedures can mitigate concerns with environmentally-assisted cracking in future reactors.

5 Conclusions

This report surveyed existing methods of creep-fatigue design and fitness-for-service assessment to identify gaps that could prevent the regulator from assessing future high temperature nuclear plant designs. Specific recommendations are addressed at the end of each of the prior sections.

Overall, the area of most concern is the interaction of creep-fatigue damage mechanisms with corrosive coolants and irradiation damage. The RCC-MRx code developed criteria for accounting for irradiation damage in the design of high temperature nuclear components, but it is unclear if the required data exists for the alloys expected for use in future U.S. plants. None of the current design or fitness-for-service methods provide rules accounting for the interaction of corrosion mechanisms with creep-fatigue damage. Environmentally-assisted cracking could be a concern for some plant concepts. In the near term, reactor designers are likely to either conservatively bound such effects, possibly by providing a corrosion allowance, or attempt to minimize corrosion in the coolant systems through the use of coolant chemistry control.

A suitable in-situ surveillance program could mitigate concerns associated with environmentally-assisted degradation methods and could even be applied to weldments through the use of welded monitoring specimens. One concept, discussed above, would use passively loaded specimens to impose creep-fatigue loading on a small test section of material. Specimen design, acceptance criteria, and monitoring strategies will all need to be developed to create a monitoring program suitable for high temperature reactors.

Such a surveillance program would be carried out in tandem with a structural monitoring and inspection program. Inspection rules for high temperature reactors exist in the current Section XI of the ASME Code. The combination of a detailed inspection program in concert with in-situ monitoring of material properties and, potentially, canary surveillance specimens, can mitigate concerns with environmentally-assisted creep-fatigue flaw initiation and growth. In the last resort, adequate high temperature fitness-for-service must be developed to assess the severity of flaws that are discovered during routine monitoring. The development of in-service monitoring programs of this type are a viable near-term solution to addressing environmental effects in future high temperature reactors.

ACKNOWLEDGEMENTS

This report was sponsored by the U.S. Nuclear Regulatory Commission (NRC), Office of Nuclear Regulatory Research (RES) under agreement NRC-HQ-25-14-D-0003. The authors would like to thank Dr. Sara Lyons for her guidance and several other NRC staff members for their helpful feedback.

REFERENCES

[1] A. Pineau, D. L. McDowell, E. P. Busso, and S. D. Antolovich, "Failure of metals II: Fatigue," *Acta Mater.*, vol. 107, pp. 484–507, 2016.

[2] M. Kamal and M. M. Rahman, "Advances in fatigue life modeling: A review," *Renew. Sustain. Energy Rev.*, vol. 82, no. October 2017, pp. 940–949, 2018.

[3] R. K. Penny and D. L. Marriott, *Design for Creep*, 2nd ed. Chapman & Hall, 1995.

[4] M. E. Kassner and T. A. Hayes, "Creep cavitation in metals," *Int. J. Plast.*, vol. 19, no. 10, pp. 1715–1748, 2003.

[5] N. J. Hoff, Ed., *High Temperature Effects in Aircraft Structures*. Pergamon Press, 1958.

[6] J. Shingledecker *et al.*, "U.S. Program on Materials Technology for Ultra-Supercritical Coal Power Plants," *J. Mater. Eng. Perform.*, vol. 14, no. 3, pp. 281–292, 2005.

[7] R. Viswanathan and J. Stringer, "Failure Mechanisms in High Temperature Components in Power Plants," *J. Eng. Mater. Technol.*, vol. 122, no. 3, pp. 246–255, 2000.

[8] R. S. Koripelli, "Load Cycling and Boiler Metals: How to Save Your Power Plant," *Power*, 2015.

[9] EPRI, "Damage to Power Plants Due to Cycling," 2001.

[10] M. Pearson and R. W. Anderson, "Reliability and durability from large heat recovery steam generators," *Proc. Inst. Mech. Eng. Part A J. Power Energy*, vol. 213, no. 3, 1999.

[11] V. Rogers, "Heat Recovery Steam Generators: Vulnerable to Failure," *Engineering360*, 2016.

[12] J. Tong, S. Dalby, J. Byrne, M. B. Henderson, and M. C. Hardy, "Creep, fatigue and oxidation in crack growth in advanced nickel base superalloys," *Int. J. Fatigue*, vol. 23, pp. 897–902, 2001.

[13] S. L. Mannan and M. Valsan, "High-temperature low cycle fatigue, creep-fatigue and thermomechanical fatigue of steels and their welds," *Int. J. Mech. Sci.*, vol. 48, no. 2, pp. 160–175, 2006.

[14] M. R. Winstone, K. M. Nikbin, and G. A. Webster, "Modes of failure under creep/fatigue loading of a nickel-based superalloy," *J. Mater. Sci.*, vol. 20, no. 7, pp. 2471–2476, 1985.

[15] L. J. Chen, G. Yao, J. F. Tian, Z. G. Wang, and H. Y. Zhao, "Fatigue and creep-fatigue behavior of a nickel-base superalloy at 850°C," *Int. J. Fatigue*, vol. 20, no. 7, pp. 543–548, 1998.

[16] J. K. Wright, L. J. Carroll, J. A. Simpson, and R. N. Wright, "Low Cycle Fatigue of Alloy 617 at 850C and 950C," *J. Eng. Mater. Technol.*, vol. 135, no. 3, p. 031005, 2013.

[17] S. Baik and R. Raj, "Mechanisms of Creep-Fatigue Interaction," *Metall. Mater. Trans. A*, vol. 13A, pp. 1215–1221, 1982.

[18] S.-L. Mannan, F.-Z. Xuan, X.-C. Zhang, Y.-C. Lin, S.-T. Tu, and X.-L. Yan, "Review of creep–fatigue endurance and life prediction of 316 stainless steels," *Int. J. Press. Vessel. Pip.*, vol. 126–127, pp. 17–28, 2014.

[19] S. W. Nam, S. C. Lee, and J. M. Lee, "The effect of creep cavitation on the fatigue life under creep-fatigue interaction," *Nucl. Eng. Des.*, vol. 153, no. 2–3, pp. 213–221, 1995.

[20] J. Wareing, "Creep-fatigue interaction in austenitic stainless steels," *Metall. Trans. A*, vol. 8, no. 5, pp. 711–721, 1977.

[21] B. Fournier *et al.*, "Lifetime prediction of 9-12%Cr martensitic steels subjected to creep-fatigue at high temperature," *Int. J. Fatigue*, vol. 32, no. 6, pp. 971–978, 2010.

[22] P. Rodriguez and K. Bhanu Sankara Rao, "Nucleation and growth of cracks and cavities under creep-fatigue interaction," *Prog. Mater. Sci.*, vol. 37, no. 5, pp. 403–480, 1993.

[23] M. Sauzay, M. Mottot, L. Allais, M. Noblecourt, I. Monnet, and J. Périnet, "Creep-fatigue behaviour of an AISI stainless steel at 550°C," *Nucl. Eng. Des.*, vol. 232, no. 3, pp. 219–236, 2004.

[24] R. V. Miner, J. Gayda, and R. D. Maier, "Fatigue and creep-fatigue deformation of several nickel-base superalloys at 650 °c," *Metall. Trans. A*, vol. 13A, pp. 1755–1765, 1982.

[25] S. Zhang and Y. Takahashi, "Evaluation of high temperature strength of a Ni-base alloy

740H for advanced ultra-supercritical power plant," in *Proceedings from the Seventh International Conference on Advances in Materials Technology for Fossil Power Plants*, 2013, pp. 242–253.
[26] R. M. Goldhoff, "Uniaxial Creep-Rupture Behavior of Low-Alloy Steel Under Variable Loading Conditions," *J. Basic Eng.*, vol. 87, no. 2, pp. 374–378, 1965.
[27] S. Y. Zamrik and D. C. Davis, "A Ductility Exhaustion Approach for Axial Fatigue—Creep Damage Assessment Using Type 316 Stainless Steel," *J. Press. Vessel Technol.*, vol. 113, no. 2, pp. 180–186, 1991.
[28] M. Prager, "Development of the MPC Omega Method for Life Assessment in the Creep Range," *J. Press. Vessel Technol.*, vol. 117, no. 2, pp. 95–103, 1995.
[29] L. M. Kachanov, "On the creep fracture time," *Izv Akad, Nauk USSR Otd Tech*, vol. 8, pp. 23–31, 1958.
[30] Y. N. Rabotnov, *Creep Problems in Structural Members*. Amsterdam: North-Holland, 1969.
[31] F. A. Leckie and D. R. Hayhurst, "Creep rupture of structures," *Proc. R. Soc. A Math. Phys. Eng. Sci.*, vol. 340, pp. 323–347, 1974.
[32] A. Dasgupta, "Failure Mechanism Models For Cyclic Fatigue," *IEEE Trans. Reliab.*, vol. 42, no. 4, pp. 548–555, 1993.
[33] S. S. Manson, G. R. Halford, and M. H. Hirschberg, "Creep-fatigue analysis by strain-range partitioning," in *Proceedings of the First National Pressure Vessel and Piping Conference*, 1971.
[34] L. F. Coffin, "The concept of frequency separation in life prediction for time," in *Proceedings of the ASME-MPC Symposium on Creep/Fatigue Interaction*, 1976.
[35] J. L. Chaboche, "Anisotropic creep damage in the framework of continuum damage mechanics," *Nucl. Eng. Des.*, vol. 79, no. 3, pp. 309–319, 1984.
[36] J. L. Chaboche, "A review of some plasticity and viscoplasticity constitutive theories," *Int. J. Plast.*, vol. 24, no. 10, pp. 1642–1693, Oct. 2008.
[37] J. L. Chaboche, "Continuous damage mechanics - A tool to describe phenomena before crack initiation," *Nucl. Eng. Des.*, vol. 64, no. 2, pp. 233–247, 1981.
[38] W. J. Ostergren, "Correlation of hold time effects in elevated temperature low cycle fatigue using a frequency modified damage function," in *Proceedings of the ASME-MPC Symposium on Creep/Fatigue Interaction*, 1976.
[39] A. Saxena, "Creep and creep–fatigue crack growth," *Int. J. Fract.*, vol. 191, no. 1–2, pp. 31–51, 2015.
[40] American Society of Mechanical Engineers, "Section III, Division 5," in *ASME Boiler and Pressure Vessel Code*, 2017.
[41] Personal Communication with R. I. Jetter, "Personal Communication with R. I. Jetter." .
[42] A. K. Dhalla and G. L. Jones, "ASME code classification of pipe stresses. A simplified elastic procedure," *Int. J. Press. Vessel. Pip.*, vol. 26, no. 2, pp. 145–166, 1986.
[43] M. H. Jawad and R. I. Jetter, *Design and Analysis of ASME Boiler and Pressure Vessel Components in the Creep Range*. ASME Press, 2009.
[44] R. L. Huddleston, "An Improved Multiaxial Creep-Rupture Strength Criterion," *J. Press. Vessel Technol.*, vol. 107, no. November, pp. 421–429, 1985.
[45] International Atomic Energy Agency, *Regulatory Practices and Safety Standards for Nuclear Power*. International Atomic Energy Agency, 1988.
[46] French Society for Design and Construction Rules for Nuclear Island Components, *RCC-MRx: Design and Construction Rules for Mechanical Components of PWR Nuclear Installations: High Temperature, Research, and Fusion Reactors*. AFCEN, 2015.
[47] French Society for Design and Construction Rules for Nuclear Island Components, *RCC-MX: Design and Construction Rules for Mechanical Components of Research Reactors and their experimental devices*. AFCEN, 2008.
[48] French Society for Design and Construction Rules for Nuclear Island Components, *RCC-MR: Design and Construction Rules for Mechanical Components of Nuclear Installations*. AFCEN, 2007.

[49] Y. Lejeail, P. Lamagnère, C. Petesch, T. Lebarbé, P. Matheron, and A. Martin, "Application case of RCC-MRx 2012 code in significant creep," in *Proceedings of the 2014 ASME Pressure Vessels and Piping Conference*, 2014, p. V001T01A042-V001T01A042.
[50] P. Lamagnère *et al.*, "Design rules for ratcheting damage in AFCEN RCC-MRX 2012 code," in *Proceedings of the 2014 ASME Pressure Vessels and Piping Conference*, 2014, p. V001T01A061-V001T01A061.
[51] ITER IDoMS, *ITER Structural Design Criteria for In-Vessel Components*. 2012.
[52] British Energy, *R5: Assessment Procedure for the High Temperature Response of Structures*. 2015.
[53] V. K. Sikka, M. G. Cowgill, and B. W. Roberts, "Creep properties of modified 9 Cr-1 Mo steel," in *Proceedings of the Topical Conference on Ferritic alloys for Use in Nuclear Energy Technologies*, 1983.
[54] H. Cracking, "Mechanisms of Corrosion Fatigue," in *Fatigue and Fracture*, vol. 19, 1996, pp. 185–192.
[55] S. Srivatsan and T. S. Sudarshan, "Mechanisms of fatigue crack initiation in metals: role of aqueous environments," *J. Mater. Sci.*, vol. 23, no. 5, pp. 1521–1533, 1988.
[56] R. H. Jones and R. E. Ricker, "Mechanisms of Stress-corrosion Cracking," in *Stress-Corrosion Cracking Materials Performance and Evaluation*, R. H. Jones, Ed. 1992, pp. 1–40.
[57] J. R. Donahue, A. B. Lass, and J. T. Burns, "The interaction of corrosion fatigue and stress-corrosion cracking in a precipitation-hardened martensitic stainless steel," *npj Mater. Degrad.*, vol. 1, no. 1, 2017.
[58] B. Pieraggi, "Effect of creep or low cycle fatigue on the oxidation or hot corrosion behaviour of nickel-base superalloys," *Mater. Sci. Eng.*, vol. 88, no. C, pp. 199–204, 1987.
[59] G. Jianting, D. Ranucci, E. Picco, and P. M. Strocchi, "The Effect of Hot Corrosion on Creep and Fracture Behaviour of Cast Nickel-Based Superalloy IN738LC," in *High Temperature Alloys for Gas Turbines*, 1982, pp. 805–819.
[60] T. L. Lin, Y. H. Zhang, and H. W. Yang, "Influence of hot corrosion on the creep strength of the nickel-base superalloy GH37," *Mater. Sci. Eng.*, vol. 62, no. 1, pp. 17–24, 1984.
[61] M. Yoshiba, O. Miyagawa, H. Mizuno, and H. Fujishiro, "Effect of Environmental Factors on the Creep Rupture Properties of a Nickel-Base Superalloy Subjected to Hot Corrosion," *Trans. Japan Inst. Met.*, vol. 29, no. 1, pp. 26–41, 1988.
[62] V. Suryanarayanan, K. J. L. Iyer, and V. M. Radhakrishnan, "Interaction of low temperature hot corrosion and creep," *Mater. Sci. Eng. A*, vol. 112, no. C, pp. 107–116, 1989.
[63] J. Swaminathan and S. Raghavan, "Effect of vanadic corrosion on creep-rupture properties of Superni-600 at 650–750°C," *Mater. High Temp.*, vol. 10, no. 4, 1992.
[64] S. Ahila and S. R. Iyer, "Creep rupture behaviour of 2.25Cr-1Mo steel in sulphate-pyrosulphate mixture," *J. Mater. Sci. Lett.*, vol. 12, no. 24, pp. 1925–1926, 1993.
[65] J. Swaminathan and S. Raghavan, "Vanadic Hot Corrosion – Creep Interaction of Superni – C 276 in the Temperature Range 650 – 750°C," *High Temp. Mater. Process.*, vol. 13, no. 4, pp. 277–298, 1994.
[66] J. G. González-Rodríguez, A. Luna-Ramírez, and A. Martínez-Villafañe, "Effect of hot corrosion on the creep properties of types 321 and 347 stainless steels," *J. Mater. Eng. Perform.*, vol. 8, no. 1, pp. 91–97, 1999.
[67] A. Homaeian and M. Alizadeh, "Interaction of hot corrosion and creep in Alloy 617," *Eng. Fail. Anal.*, vol. 66, pp. 373–384, 2016.
[68] V. Mannava, A. Sambasivarao, N. Paulose, M. Kamaraj, and R. S. Kottada, "An investigation of oxidation/hot corrosion-creep interaction at 800 °C in a Ni-base superalloy coated with salt mixture deposits of Na2SO4-NaCl-NaVO3," *Corros. Sci.*, vol. 147, no. November 2018, pp. 283–298, 2019.
[69] T. C. Totemeier and H. Tian, "Creep-fatigue-environment interactions in INCONEL 617," *Mater. Sci. Eng. A*, vol. 468–470, no. SPEC. ISS., pp. 81–87, 2007.
[70] a. Pineau and J. P. Pédron, "The effect of microstructure and environment on the crack growth behaviour of Inconel 718 alloy at 650 °C under fatigue, creep and combined

loading," *Mater. Sci. Eng.*, vol. 56, no. 2, pp. 143–156, 1982.
[71] B. Fournier *et al.*, "Creep-fatigue interactions in a 9 Pct Cr-1 Pct Mo martensitic steel: Part II. Microstructural evolutions," *Metall. Mater. Trans. A Phys. Metall. Mater. Sci.*, vol. 40, no. 2, pp. 330–341, 2009.
[72] R. J. M. Konings, *Comprehensive Nuclear Materials, Volume 4*. Oxford, U.K.: Elsevier, 2012.
[73] F. A. Garner, M. L. Hamilton, N. F. Panayotou, and G. D. Johnson, "The microstructural origins of yield strength changes in AISI 316 during fission or fusion irradiation," *J. Nucl. Mater.*, vol. 103–104, pp. 803–807, 1981.
[74] F. A. Garner, *Radiation damage in austenitic steels*, vol. 4. Elsevier Inc., 2012.
[75] S. Nogami, K. Abe, A. Hasegawa, K. Imasaki, and T. Tanno, "High-Temperature Helium Embrittlement of 316FR Steel," *J. Nucl. Sci. Technol.*, vol. 48, no. 1, pp. 130–134, 2012.
[76] M. L. Grossbeck, K. Ehrlich, and C. Wassilew, "An assessment of tensile, irradiation creep, creep rupture, and fatigue behavior in austenitic stainless steels with emphasis on spectral effects," *J. Nucl. Mater.*, vol. 174, no. 2–3, pp. 264–281, 1990.
[77] H. Trinkaus, "On the modeling of the high-temperature embrittlement of metals containing helium," *J. Nucl. Mater.*, vol. 118, no. 1, pp. 39–49, 1983.
[78] C. Wassilew, W. Schneider, and K. Ehrlich, "Creep and creep-rupture properties of type 1.4970 stainless steel during and after irradiation," *Radiat. Eff.*, vol. 101, no. 1–4, pp. 201–219, 2007.
[79] K. Anderko, L. Schaefer, C. Wassilew, L. Ehrlich, and H. J. Bergmann, "Mechanical properties of irradiated austenitic stainless steel 1.4970," in *Radiation Effects in Breeder Reactor Structural Materials*, 1977.
[80] S. Ukai, S. Mizuta, T. Kaito, and H. Okada, "In-reactor creep rupture properties of 20% CW modified 316 stainless steel," *J. Nucl. Mater.*, vol. 278, no. 2, pp. 320–327, 2000.
[81] J. R. Lindgren, "Irradiation Effects on High-Temperature Gas-Cooled Reactor Structural Materials," *Nucl. Technol.*, vol. 66, no. 3, pp. 607–618, 2017.
[82] K. Watanabe, T. Kondo, and Y. Ogawa, "Postirradiation Tensile and Creep Properties of Heat-Resistant Alloys," *Nucl. Technol.*, vol. 66, no. 3, pp. 630–638, 2017.
[83] F. Garzarolli, K. P. Francke, and J. Fischer, "Influence of Neutron Irradiation on Tensile and Stress Rupture Properties of Inconel 625," *J. Nucl. Mater.*, vol. 30, pp. 242–246, 1969.
[84] S. Xu, W. Zheng, and L. Yang, "A review of irradiation effects on mechanical properties of candidate SCWR fuel cladding alloys for design considerations," *CNL Nucl. Rev.*, vol. 5, no. 2, pp. 309–331, 2016.
[85] D. F. Kharitonov, "Effect of Neutron Irradiation on Low-Cycle Fatigue of Structural Materials (Review)," *Strength Mater.*, vol. 16, no. 11, pp. 1594–1602, 1984.
[86] N. V. Luzginova, J. W. Rensman, M. Jong, P. Ten Pierick, T. Bakker, and H. Nolles, "Overview of 10 years of irradiation projects on Eurofer97 steel at High Flux Reactor in Petten," *J. Nucl. Mater.*, vol. 455, no. 1–3, pp. 21–25, 2014.
[87] W. Vandermeulen, W. Hendrix, V. Massaut, and J. Van de Velde, "Influence of neutron irradiation at 430°C on the fatigue properties of SA 316L steel," *J. Nucl. Mater.*, vol. 155–157, pp. 953–956, 1988.
[88] P. Marmy and B. M. Oliver, "High strain fatigue properties of F82H ferritic-martensitic steel under proton irradiation," *J. Nucl. Mater.*, vol. 318, no. SUPPL, pp. 132–142, 2003.
[89] R. Lindau and A. Moslang, "Fatigue Tests on a Ferritic-Martensitic Steel At 420-Degrees-C - Comparison Between in-Situ and Postirradiation Properties," *J. Nucl. Mater.*, vol. 212, no. A, pp. 599–603, 1994.
[90] R. Scholz and R. Mueller, "The effect of hold-times on the fatigue behavior of type AISI 316L stainless steel under deuteron irradiation," *J. Nucl. Mater.*, vol. 258–263, pp. 1600–1605, 1998.
[91] R. Scholz and R. Mueller, "The effect of hold-times on the fatigue life of 20% cold-worked Type 316L stainless steel under deutron irradiation," *J. Nucl. Mater.*, vol. 224, pp. 311–313, 1995.
[92] C. R. Brinkman, G. E. Korth, and R. R. Hobbins, "Estimates of Creep-Fatigue Interaction

in Irradiated and Unirradiated Austenitic Stainless Steels," *Nucl. Technol.*, vol. 16, no. 1, pp. 297–307, 1972.
[93] C. R. Brinkman, J. M. Beeston, and G. E. Korth, "Fatigue and Creep-fatigue Behavior of Irradiated Stainless Steels -- Available Data, Simple Correlations, and Reccomendations for Additional Work in Support of LMFBR Design," 1973.
[94] M. J. Norgett, M. T. Robinson, and I. M. Torrens, "A proposed method of calculating displacement dose rates," *Nucl. Eng. Des.*, vol. 33, no. 1, pp. 50–54, 1975.
[95] "Irradiation Damage and Material Limit: Illustration of a way to Codify Rules with RCC-MRX." .
[96] M. C. Messner, V.-T. Phan, R. I. Jetter, and T.-L. Sham, "Assessment of Passively Actuated In-Situ Cyclic Sureillance Test Specimens for Advanced Non-Light Water Reactors," in *Proceedings of the ASME 2018 Pressure Vessels and Piping Conference*, 2018.
[97] M. C. Messner, V.-T. Phan, R. I. Jetter, and T.-L. Sham, "The Mechanical Interaction of Clad and Base Metal for Molten Salt Reactor Structural Components," in *Proceedings of the 2018 ASME Pressure Vessels and Piping Conference*, 2018.
[98] J. A. Francis, H. K. D. H. Bhadeshia, and P. J. Withers, "Welding residual stresses in ferritic power plant steels," *Mater. Sci. Technol.*, vol. 23, no. 9, pp. 1009–1020, 2007.
[99] D. E. McCabe, "Initial Evaluation of the Heat-Affected Zone, Local Embrittlement Phenomenon as it Applies to Nuclear Reactor Vessels," 1999.
[100] D. J. Abson and J. S. Rothwell, "Review of type IV cracking of weldments in 9–12%Cr creep strength enhanced ferritic steels," *Int. Mater. Rev.*, vol. 58, no. 8, pp. 437–473, 2013.
[101] I. A. Shibli and N. Le Mat Hamata, "Creep crack growth in P22 and P91 welds - Overview from SOTA and HIDA projects," *Int. J. Press. Vessel. Pip.*, vol. 78, no. 11–12, pp. 785–793, 2001.
[102] C. Chovet, E. Galand, and B. Leduey, "Effect of various factors on toughness in P92 SAW weld metal," *Weld. World*, vol. 52, no. 7–8, pp. 18–26, 2008.
[103] D. Richardot, J. C. Vaillant, A. Arbab, and W. Bendick, *The T92/P92 Book*. Vallourec & Mannesmann Tubes, 2000.
[104] N. G. Peng, B. Ahmad, M. R. Muhamad, and M. Ahadlin, "Phase Transformation of P91 Steels upon Cooling after Short Term Overheating above AC1 and AC3 Temperature," *Adv. Mater. Res.*, vol. 634–638, pp. 1756–1765, 2013.
[105] British Standards Institute, *British Standard 7910*. 2013.
[106] K. Wasmer, K. M. Nikbin, and I. W. Goodall, "Progress to the steady cyclic state," 2000.

Applied Materials Division
Argonne National Laboratory
9700 South Cass Avenue, Bldg. 212
Argonne, IL 60439

www.anl.gov